Using Hysteresis Analysis to Explore the Sources of Ammonia During Storm Events in the River Lark, UK

A Thesis
Presented in Partial Fulfillment of the Requirements for the
Degree of Master of Science
with a
Major in Environmental Science
in the
College of Graduate Studies
University of Idaho
by
Mariana T. Sandifer

Approved by:
Major Professor: Frank Wilhelm, Ph.D.
Committee Members: Karen Humes, Ph.D.; Timothy Link, Ph.D.
Department Administrator: Jaap Vos, Ph.D.

December 2022

Abstract

Goals of this thesis were to determine if rainfall is a predictor of episodic changes in ammonia concentration in the River Lark downstream of Fornham St. Martin, UK; if there is a relationship between the ammonia concentration-discharge (C-Q) hysteresis patterns observed for storm events and the range of discharge per storm, total event rainfall, or antecedent catchment wetness; and to make inferences about the relative importance of different catchment ammonia sources for storm-related nutrient export during the growing season. Ammonia concentration in the River Lark was sampled at 30-minute intervals for several months during the 2021 growing season by the UK Environment Agency. These data and discharge were used for C-Q hysteresis analyses. An existing hysteresis index was adapted to quantify the total amount of C-Q hysteresis exhibited by storms with complex, figure-of-eight hysteresis patterns. Predominantly clockwise ammonia C-Q hysteresis was observed in the upper River Lark, indicating dilution from stormflow as the primary predictor of ammonia concentration. The constant input of effluent discharged from Sewage Treatment Works (STWs) appeared to be the most important source of ammonia in this part of the catchment during the growing season. However, some anti-clockwise hysteresis was observed during the two storm events with the heaviest rainfall, indicating that the dominant sources of ammonia in the catchment may vary seasonally.

Acknowledgments

First, I would like to thank my major professor, Dr. Frank Wilhelm, for his mentorship throughout the past year. Without his encouragement, I would have never considered turning my graduate project into a thesis. He constantly challenged me to think critically and provided invaluable feedback and support at every step in the process. I am also grateful to my committee members, Dr. Tim Link and Dr. Karen Humes for providing their expertise and time, and for their support in transitioning my project to a thesis.

I thank the River Lark Catchment Partnership (RLCP) for sparking the idea for this thesis, sharing their citizen science data and local knowledge of the River Lark, and providing opportunities to grow through volunteering. RLCP welcomed my involvement, despite Suffolk only being my temporary home, and fostered my understanding of environmental issues and governance in a new country. I especially thank Chairperson Andrew Hinchley for connecting me with local partners for data inquiries, and for helping interpret the intricacies of catchment management in the UK, including a review of my introduction chapter. For a full description of my involvement with RLCP, see Appendix C.

I thank the EA Anglian Region office, who were always willing to answer my inquiries and provided data for this analysis, sometimes at short notice.

I thank the Lawes Agricultural Trust and Rothamsted Research for data from the e-RA database. The Rothamsted Long-term Experiments National Capability (LTE-NCG) is supported by the UK Biotechnology and Biological Sciences Research Council (BBS/E/C/000J0300) and the Lawes Agricultural Trust.

Dedication

My Master's was made possible by the support of my incredible husband Kris, who kept the house from falling apart, was a sounding board for far too many "science" ideas, and financed the whole endeavor while I took two years off work. He loved me even when the combined stress of grad school and chronic pain occasionally made me an irritable jerk. I am grateful to my family for their constant prayers and encouragement, and especially to my sister Melissa for listening to all my complaints with a sympathetic ear. My cat Lina deserves a bit of credit for providing company through many late nights, even if she was asleep for most of it. Finally, and most importantly, I must acknowledge that I truly only completed this by the grace of God. *Phil. 4:13*

Table of contents

Abstract ii
Acknowledgments iii
Dedication iv
Table of contents v
List of tables vii
List of figures ix
List of equations xiv
Chapter 1: Introduction 1
The River Lark 3
Management framework of the River Lark catchment 5
Monitoring STW pollution in the River Lark 7
Nutrient-discharge hysteresis 9
Research questions 11
Chapter 2: Methods 12
Data sources and quality control 12
Deployment and quality checks of the EA datasonde 13
Deployment and quality checks of the RLCP datasonde 15
Validation of discharge data from the EA Fornham St. Martin gauge station 15
Validation of rainfall measured by EA rain gauge E22322 16
Nutrient concentration-discharge analysis 18
Identification of storm events 18
Characterization of hysteresis 19
Contextualizing storm event concentration-discharge hysteresis 21
Statistical analyses 24
Chapter 3: Results 26

Storm event identification 26
Ammonia concentration-discharge hysteresis analysis 28
Storm event 1 28
Storm event 2 32
Storm event 3 37
Storm event 4 41
Storm event 5 45
Contextualization of ammonia C-Q hysteresis 49
Stepwise regression of event-scale context metrics 49
Chapter 4: Discussion 52
Implications of ammonia C-Q patterns observed in the River Lark 52
Lessons learned for future studies 54
Conclusion 56
References 58
Appendix A: Additional data quality control and outlier analysis 68
Quality-checked datasets excluded from C-Q analysis 68
RLCP datasonde deployment and data quality issues 68
Additional sources of rainfall data excluded from analysis 69
Air temperature data validation and exclusion from analysis 69
Systematic outliers in the EA datasonde dataset 71
Appendix B: Additional storm event concentration-discharge plots 73
Appendix C: Description of volunteer role at RLCP 76

List of tables

Table 2.1 Quality checks outlined by Blenkinsop et al. (2017) which were applied to both the EA and Rothamsted Research rainfall data. 17

Table 2.2 Potential storm event metrics considered for providing seasonal and temporal context to HI_{area} via multiple regression, similar to Table 4 in Liu et al. 2021. Metrics were grouped into four broad categories of interest in the left-most column and references to the studies from which these metrics are derived are in the right-most column. 22

Table 3.1 Dates of storm events in June and July 2021 in the River Lark at Fornham St. Martin, UK and their identifiers or reasons for exclusion from hysteresis analysis. 27

Table 3.2 Hysteresis index (HI_{Qi}) values, with instrument error, calculated using the difference in normalized concentration on the rising (C_{RL_Qi}) and falling (C_{FL_Qi}) hydrograph limbs at every 10th percentile of normalized discharge (Q_i) of the River Lark at Fornham St. Martin, UK during storm event 1, 04 June 2021 to 06 June 2021. 31

Table 3.3 Hysteresis index (HI_{Qi}) values, with instrument error (SI), calculated using the difference in normalized concentration on the rising (C_{RL_Qi}) and falling (C_{FL_Qi}) hydrograph limbs at every 10th percentile of normalized discharge (Q_i) of the River Lark at Fornham St. Martin, UK during storm event 2, 18 June 2021 to 21 June 2021. 36

Table 3.4 Hysteresis index (HI_{Qi}) values, with instrument error, calculated using the difference in normalized concentration on the rising (C_{RL_Qi}) and falling (C_{FL_Qi}) hydrograph limbs at every 10th percentile of normalized discharge (Q_i) of the River Lark at Fornham St. Martin, UK during storm event 3, 28 June 2021. 40

Table 3.5 Hysteresis index (HI_{Qi}) values, with instrument error, calculated using the difference in normalized concentration on the rising (C_{RL_Qi}) and falling (C_{FL_Qi}) hydrograph limbs at every 10th percentile of normalized discharge (Q_i) of the River Lark at Fornham St. Martin, UK during storm event 4, 04 to 05 July 2021. 44

Table 3.6 Hysteresis index (HI_{Qi}) values, with instrument error, calculated using the difference in normalized concentration on the rising (C_{RL_Qi}) and falling (C_{FL_Qi})

hydrograph limbs at every 10th percentile of normalized discharge (Q_i) of the River Lark at Fornham St. Martin, UK during storm event 5, 05 to 07 July 2021. 48
Table A.1 Occurrence of outliers in the ammonia and DO data produced by the EA datasonde deployed in the River Lark at Fornham All Saints, UK, May to October 2021.....72
Table A.2 Occurrence of outliers in the temperature data produced by the EA datasonde deployed in the River Lark at Fornham All Saints, UK, May to October 2021.....72
Table C.1 Reverse chronological log of interactions with RLCP and tasks completed in a volunteer capacity. 77

List of figures

Figure 1.1 The chalk aquifer and chalk streams of Southern and Eastern England. Contains © EA copyright and/or database right 2015. All rights reserved. Contains Ordnance Survey data © Crown copyright and database right 2004 (EA and OS 2021). Contains NERC materials © NERC 2008 (BGS 2008). Contains map tiles by Stamen Design, under CC BY 3.0. Data by OpenStreetMap, under ODbL (SD and OSM c2022). Contains map tiles © Esri (2013)..... 2

Figure 1.2 Map of the River Lark Catchment, in Suffolk, UK. The catchment's location in East Anglia is indicated in orange in the inset. Contains OS data © Crown copyright and database right (OS 2021, c2021, c2022). Contains public sector information licensed under the Open Government Licence v3.0 (EA 2021m). Contains map tiles by Stamen Design, under CC BY 3.0. Data by OpenStreetMap, under ODbL (SD and OSM c2022). Contains map tiles by: Esri, HERE, Garmin, FAO, NOAA, USGS, © OpenStreetMap contributors, and the GIS User Community (Esri 2022).4

Figure 1.3 Map of the upper River Lark Catchment, in Suffolk, UK, showing STW discharges. Contains OS data © Crown copyright and database right 2021, 2022 (OS 2021, c2021, c2022). Contains public sector information licensed under the Open Government Licence v3.0 (EA 2021m)..... 6

Figure 2.1 Location of data sources in the River Lark catchment used for concentration-discharge hysteresis analysis of storms that occurred June to July 2021. Contains OS data © Crown copyright and database right 2021, 2022 (OS 2021, c2021, c2022). Contains public sector information licensed under the Open Government Licence v3.0 (EA 2021m).....13

Figure 3.1 Discharge (m3/s) of the River Lark at Fornham St. Martin, UK and rainfall (mm) at Rushbrooke, Bury St. Edmunds, UK between 24 May and 01 August in 2021. 26

Figure 3.2. Discharge (m^3/s) of the River Lark at Fornham St. Martin, UK and rainfall (mm) at Rushbrooke, Bury St. Edmunds, UK during storm event 1, 04 June 2021 to 06 June 2021.....28

Figure 3.3. Ammonia concentration (mg-N/l, a) and instantaneous loads (mg-N/s, b) in the River Lark at Fornham St. Martin, UK during storm event 1, 04 June 2021 to 06 June 2021. Gray area indicates measurement precision (±10%). Open diamonds

represent times for which discharge measurements were available, but concentration was interpolated. 29
Figure 3.4. Normalized concentration-discharge (C-Q) plot for the River Lark at Fornham St. Martin, UK during storm event 1, 04 June 2021 to 06 June 2021. Time is indicated by line/diamond color, from red (start) to green (end). Open diamonds represent times for which discharge measurements were available, but concentration was interpolated. 30
Figure 3.5 Hysteresis index (HI) values calculated at every 10th discharge percentile, as a function of normalized discharge of the River Lark at Fornham St. Martin, UK during storm event 1, 04 June 2021 to 06 June 2021. The dark shaded ribbon represents instrument error. 31
Figure 3.6. Discharge (m^3/s) of the River Lark at Fornham St. Martin, UK and rainfall (mm) at Rushbrooke, Bury St. Edmunds, UK during storm event 2, 18 June 2021 to 21 June 2021. 32
Figure 3.7. Ammonia concentration (mg-N/l, a) and instantaneous loads (mg-N/s, b) in the River Lark at Fornham St. Martin, UK during storm event 2, 18 June 2021 to 21 June 2021. Gray area indicates measurement precision (±10%). Open diamonds represent times for which discharge measurements were available, but concentration was interpolated. 33
Figure 3.8. Normalized concentration-discharge (C-Q) plot for the River Lark at Fornham St. Martin, UK during storm event 2, 18 June 2021 to 21 June 2021. Time is indicated by line/diamond color, from red (start) to green (end). Open diamonds represent times for which discharge measurements were available, but concentration was interpolated. 34
Figure 3.9 Hysteresis index (HI) values calculated at every 10th discharge percentile, as a function of normalized discharge of the River Lark at Fornham St. Martin, UK during storm event 2, 18 June 2021 to 21 June 2021. The dark shaded ribbon represents instrument error. 35
Figure 3.10. Discharge (m^3/s) of the River Lark at Fornham St. Martin, UK and rainfall (mm) at Rushbrooke, Bury St. Edmunds, UK during storm event 3, 28 June 2021. 37
Figure 3.11. Ammonia concentration (mg-N/l, a) and instantaneous loads (mg-N/s, b) in the River Lark at Fornham St. Martin, UK during storm event 3, 28 June 2021. Gray

area indicates measurement precision (±10%). Open diamonds represent times for which discharge measurements were available, but concentration was interpolated. 38
Figure 3.12. Normalized concentration-discharge (C-Q) plot for the River Lark at Fornham St. Martin, UK during storm event 3, 28 June 2021. Time is indicated by line/diamond color, from red (start) to green (end). Open diamonds represent times for which discharge measurements were available, but concentration was interpolated. 39
Figure 3.13 Hysteresis index (HI) values calculated at every 10th discharge percentile, as a function of normalized discharge of the River Lark at Fornham St. Martin, UK during storm event 3, 28 June 2021. The dark shaded ribbon represents instrument error. 40
Figure 3.14. Discharge (m^3/s) of the River Lark at Fornham St. Martin, UK and rainfall (mm) at Rushbrooke, Bury St. Edmunds, UK during storm event 4, 04 to 05 July 2021. 41
Figure 3.15. Ammonia concentration (mg-N/l, a) and instantaneous loads (mg-N/s, b) in the River Lark at Fornham St. Martin, UK during storm event 4, 04 to 05 July 2021. Gray area indicates measurement precision (±10%). Open diamonds represent times for which discharge measurements were available, but concentration was interpolated. 42
Figure 3.16. Normalized concentration-discharge (C-Q) plot for the River Lark at Fornham St. Martin, UK during storm event 4, 04 to 05 July 2021. Time is indicated by line/diamond color, from red (start) to green (end). Open diamonds represent times for which discharge measurements were available, but concentration was interpolated. 43
Figure 3.17 Hysteresis index (HI) values calculated at every 10th discharge percentile, as a function of normalized discharge of the River Lark at Fornham St. Martin, UK during storm event 4, 04 to 05 July 2021. The dark shaded ribbon represents instrument error. 44
Figure 3.18. Discharge (m^3/s) of the River Lark at Fornham St. Martin, UK and rainfall (mm) at Rushbrooke, Bury St. Edmunds, UK during storm event 5, 05 to 07 July 2021. 45

Figure 3.19. Ammonia concentration (mg-N/l, a) and instantaneous loads (mg-N/s, b) in the River Lark at Fornham St. Martin, UK during storm event 5, 05 to 07 July 2021. Gray area indicates measurement precision (±10%). Open diamonds represent times for which discharge measurements were available, but concentration was interpolated. 46

Figure 3.20. Normalized concentration-discharge (C-Q) plot for the River Lark at Fornham St. Martin, UK during storm event 5, to 05 to 07 July 2021. Time is indicated by line/diamond color, from red (start) to green (end). Open diamonds represent times for which discharge measurements were available, but concentration was interpolated. 47

Figure 3.21 Hysteresis index (HI) values calculated at every 10^{th} discharge percentile, as a function of normalized discharge of the River Lark at Fornham St. Martin, UK during storm event 5, 05 to 07 July 2021. The dark shaded ribbon represents instrument error. 48

Figure 3.22 Distributions of event-scale ammonia C-Q hysteresis index values calculated for five storm discharge events in the River Lark at Fornham St. Martin, UK, June to July 2021. From top left are HI_{mean} (a), HI_{abs} (b), HI_{abs+} (c), and HI_{abs-} (d), with bars indicating instrument measurement accuracy.....50

Figure 3.23 Event-scale ammonia C-Q hysteresis index values calculated for five storm discharge events in the River Lark at Fornham St. Martin, UK, June to July 2021, plotted as functions of select hydrological metrics with significant relationship. From top left are HI_{mean} as a function of total event rainfall (a), (b), HI_{mean} as a function of event discharge range, HI_{abs-} as a function of antecedent precipitation index (API) (c), and HI_{abs+} as a function of event discharge range (d). The grey area represents the 95% confidence interval of the linear regression. 51

Figure B.1 Normalized concentration-discharge (C-Q) plots for each discharge peak (a-c) in the River Lark at Fornham St. Martin, UK during storm event 1, 04 June 2021 to 06 June 2021. Plots (a-c) show discharge peaks one to three, respectively, and the extent of each is shown in (d). Time is indicated by line/diamond color, from red (start) to green (end). Open diamonds represent times for which discharge measurements were available, but concentration was interpolated. Vertical bars on points in plots (a-c) show measurement error.....73

Figure B.2 Normalized concentration-discharge (C-Q) plots for each discharge peak (a-e) in the River Lark at Fornham St. Martin, UK during storm event 2, 18 June 2021 to 21 June 2021. Plots (a-e) show discharge peaks one to five, respectively, and the extent of each is shown in (f). Time is indicated by line/diamond color, from red (start) to green (end). Open diamonds represent times for which discharge measurements were available, but concentration was interpolated. Vertical bars on points in plots (a-e) show measurement error. 74

Figure B.3 Normalized concentration-discharge (C-Q) plots for each discharge peak (a-e) in the River Lark at Fornham St. Martin, UK during storm event 5, 05 to 07 July 2021. Plots (a-b) show discharge peaks one and two, respectively, and the extent of each is shown in (c). Time is indicated by line/diamond color, from red (start) to green (end). Open diamonds represent times for which discharge measurements were available, but concentration was interpolated. Vertical bars on points in plots (a-b) show measurement error. 75

List of equations

Equation 2.1.....19
Equation 2.2.....20
Equation 2.3.....20
Equation 2.4.....20
Equation 2.5.....21
Equation 2.6.....24

Chapter 1: Introduction

Earth is known as the blue planet, capable of supporting life due to vast quantities of water. Human survival depends specifically on fresh water, which accounts for just 2.53% of Earth's water (Shiklomanov 1993). Though only 0.006% of fresh water is found in rivers (Shiklomanov 1993), the world's greatest civilizations grew along their banks in ancient times and rivers remain a central part of daily life in modern towns and cities. Today, we consider the benefits provided by rivers to society to be ecosystem services, encompassing not only fresh water supply but critical functions such as biofiltration of water and carbon sequestration (Hanna et al. 2018).

Among rivers, chalk streams are considered especially rare, numbering just over 300 worldwide, and occur only within England, France, and Denmark along shallow Cretaceous chalk deposits (Rangeley-Wilson et al. 2021). Chalk streams are concentrated in southern England (Figure 1.1) with 85% of the global total located in this region (Rangeley-Wilson et al. 2021). Chalk aquifers are composed of "very pure" limestone with high porosity, around 40%, and the typical residence time for water is 20 years or more due to the thickness of the unsaturated zone and slow percolation rate (Berrie 1992). The chalk aquifer discharges from springs along a shallow river valley, emerging at around 11°C, which generally restricts the annual temperature of the receiving stream to 5 to 17°C (Berrie 1992).

Due to their groundwater dependency, chalk streams are characterized by naturally low-nutrient, cool, and clear water which flows year-round in at least the lowest elevations of the river valley (Berrie 1992). The portions of chalk streams fed by higher-elevation springs are often "winterbourne" and run dry during the growing season due to plant-water demand outpacing precipitation, driving the water table downward (Berrie 1992). Chalk streams are typically low-order because the springs feed the main river (Berrie 1992). As a result, there is a strong linear relationship between air and water temperature in chalk streams (Mackey and Berrie 1991).

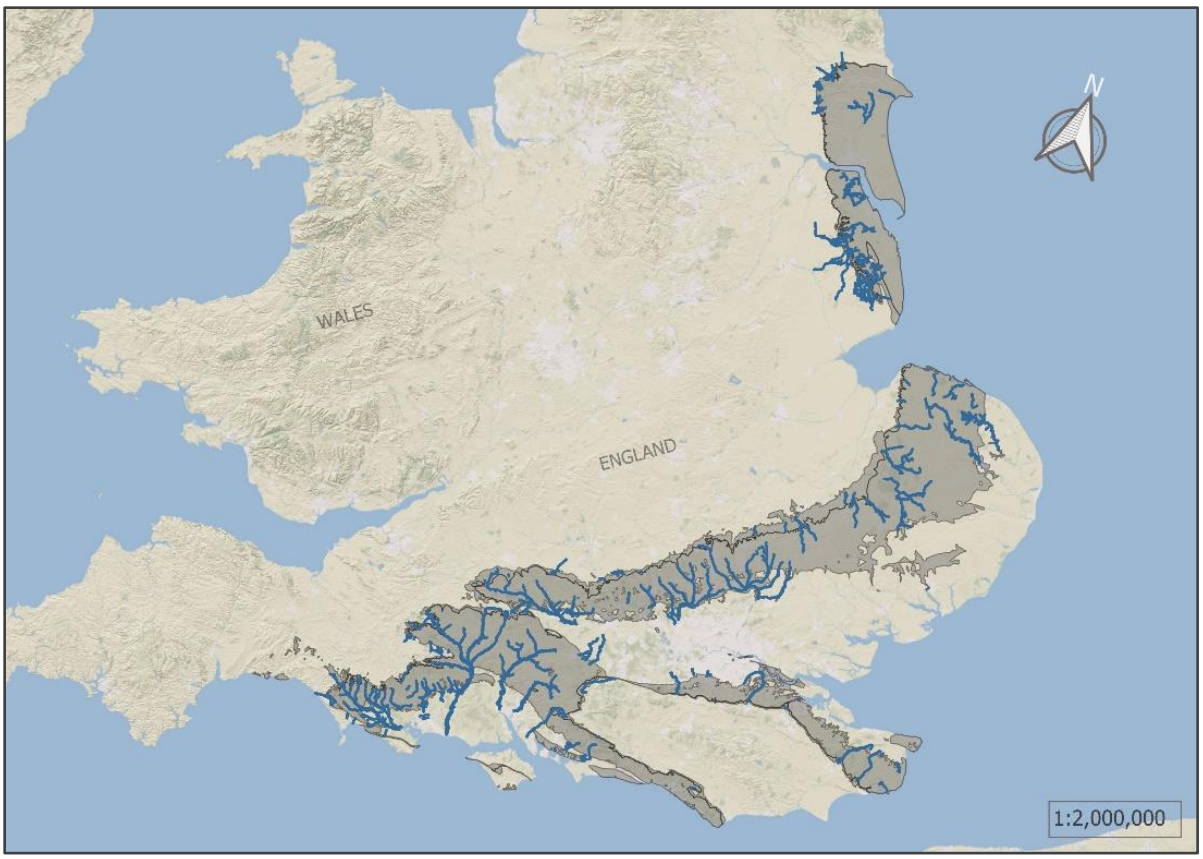

Figure 1.1 The chalk aquifer and chalk streams of Southern and Eastern England. Contains © EA copyright and/or database right 2015. All rights reserved. Contains Ordnance Survey data © Crown copyright and database right 2004 (EA and OS 2021). Contains NERC materials © NERC 2008 (BGS 2008). Contains map tiles by Stamen Design, under CC BY 3.0. Data by OpenStreetMap, under ODbL (SD and OSM c2022). Contains map tiles © Esri (2013).

Chemical composition of chalk streams is typically constant throughout the reach in unmodified streams, with little annual variability due to the predominant groundwater component (Berrie 1992). Chalk stream oxygen content exhibits seasonal and diurnal changes that generally correspond to changes in photosynthesis and respiration activity (Butcher et al. 1927a, 1927b, 1928a, 1928b, 1930). The calcareous stream water is slightly alkaline, with pH generally between 7.4-8.0 (Berrie 1992). The pH exhibits diurnal variation generally corresponding to changes in dissolved oxygen, though distinct seasonal variations may be observed independent of oxygen content (Butcher et al. 1927a, 1927b, 1928a, 1928b, 1930).

Chalk streams are often referred to as "England's rainforests" due to their rich biodiversity of plant and animal life (Rangeley-Wilson et al. 2021). The clean gravel substrate provides excellent spawning habitat for salmonids and the clear flowing water supports the highest

plant species richness of any stream habitat in the country (Rangeley-Wilson et al. 2021). Many wet-dry adapted macroinvertebrates occur within the winterbourne portions of chalk streams, including the rare species *Metacnephia amphora* (winterbourne black fly) and *Ironongquia dubia* (scarce brown sedge) which have only been recorded in southern England (Rangeley-Wilson et al. 2021).

The River Lark

The River Lark (Figure 1.2) is a Pleistocene glacial-impacted chalk stream (Rangeley-Wilson et al. 2021) located in East Anglia, flowing northwest from its headwaters on the eastern edge of the Newmarket Ridge to its confluence with the river Great Ouse northeast of Ely (Hurst 2021). East Anglia has a temperate climate with mean annual temperature (1991-2020) of 10.53°C and mean annual rainfall (1991-2020) totaling 626.91 mm (MO c2022). The upper Lark catchment (Figure 1.3) is 110.2 km^2 (NRFA c2022e) of primarily agricultural land (62.5%) with little (11.6%) urbanized area (NRFA c2022a), draining to the Fornham St. Martin gauge station located just downstream of the town of Bury St. Edmunds, population 41,700 (WSC c2022). Land elevation ranges from 25.50 to 125.70 m above Ordnance Datum (mean sea level measured at Newlyn, UK; NRFA c2022) and much of the chalk aquifer is overlain by loamy and clayey soil (Barker 1992; CU c2022), particularly along the tributaries and headwaters. Many chalk streams have a baseflow index greater than 0.9 (NFRA c2022d), while the Lark at Fornham St. Martin is only 0.5 (NRFA c2022c), reflecting the reduced permeability of the upper catchment.

Like many English chalk streams, the Lark fails to meet UK Environment Agency (EA) Water Framework Directive (WFD) ecological health standards due to over-abstraction, channel modification, and pollution (primarily nutrients, urban runoff, and sediments) (Brighty et al. 2021). Eutrophication of the River Lark is driven by past and present land use practices throughout the catchment (Brighty et al. 2021). After World War II, overapplication of nitrogen and phosphorus fertilizers was common across England in response to the pressure of feeding the booming postwar population (Rangeley-Wilson et al. 2021). This inadvertently loaded chalk aquifers with large amounts of nitrate over a half century of leaching (Rangeley-Wilson et al. 2021). The chalk bedrock underlying the River Lark catchment consists predominantly of fissured limestone with flint banding (Barker 1992),

and therefore also receives contemporary agriculture-derived nitrogen and phosphorus via rapid flow through the fractures (Hurst 2021).

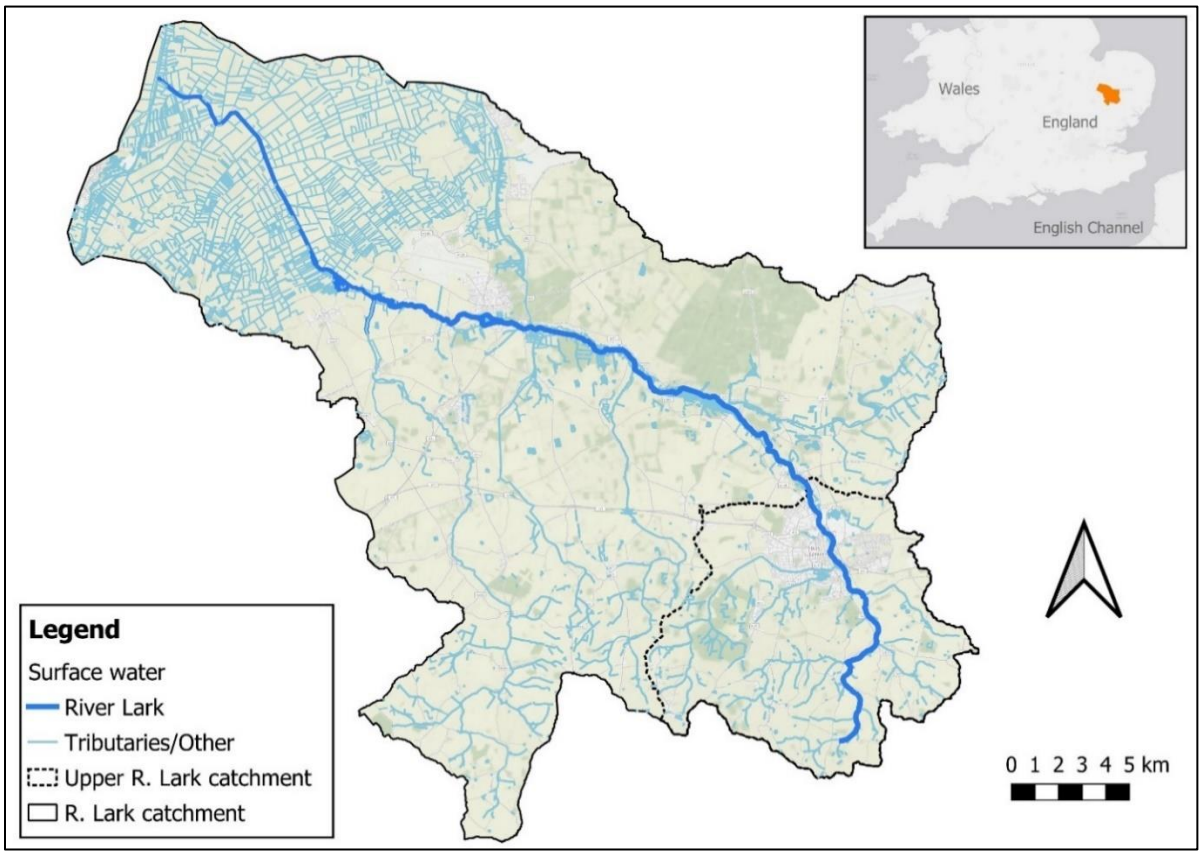

Figure 1.2 Map of the River Lark Catchment, in Suffolk, UK. The catchment's location in East Anglia is indicated in orange in the inset. Contains OS data © Crown copyright and database right (OS 2021, c2021, c2022). Contains public sector information licensed under the Open Government Licence v3.0 (EA 2021m). Contains map tiles by Stamen Design, under CC BY 3.0. Data by OpenStreetMap, under ODbL (SD and OSM c2022). Contains map tiles by: Esri, HERE, Garmin, FAO, NOAA, USGS, © OpenStreetMap contributors, and the GIS User Community (Esri 2022).

Significant point sources of nutrient pollution on the upper River Lark (Figure 1.3) are treated final effluent discharges from sewage treatment works (STW) located in Fornham All Saints and farther upstream (EA 2022f). As with most riverine systems, phosphorus is the limiting nutrient for photosynthetic organisms (Birkby 2020), and the soluble reactive phosphorus (SRP) concentration in the main river and tributaries of the upper catchment remains too high to achieve WFD "good ecological status" (For determination of ecological status with respect to SRP, see p.18 in SS and WM 2015). (EA 2022a, 2022b, 2022c, 2022d, 2022e). Downstream of Bury St. Edmunds, dissolved oxygen also fails to meet the WFD target (EA 2022b) of greater than 60% saturation 90% of the time (SS and WM 2015),

indicating the cumulative nutrient enrichment from upstream drives excessive algal growth and bacterial decomposition that stresses fish and other organisms.

Due to the long history of human settlement and industrial activity in the Lark valley, the natural oxygen balance of the River Lark has long been altered by nutrient pollution. Significant incidents were documented in the 1920s, resulting from industrial process waste discharged by the sugar beet factory in Bury St. Edmunds (Butcher et al. 1927a, 1927b, 1928a, 1928b). During October and November, the River Lark's oxygen saturation was less than 50% (Butcher et al. 1927a, 1927b, 1928a, 1928b). However, the river recovered after the addition of high-oxygen demand waste ceased. Maximum annual dissolved oxygen saturation occurred in March to May, as expected, coinciding with the typical period of maximum diatom and macrophyte growth (Butcher et al. 1927a, 1927b, 1928a, 1928b, 1930).

Management framework of the River Lark catchment

Integrated catchment management (ICM) is the official approach used in the UK for combined management of land and water resources (Klaar et al. 2020). ICM respects ecosystem services alongside ecological, social, and cultural values. Fifty-eight percent of waterbodies which do not meet WFD "good ecological status" fail the standards due to provisioning services, agriculture, and rural land management (Klaar et al. 2020). Recent legislation, including measures proposed post-Brexit, have moved towards environmental management to meet multiple objectives and support ecosystem functioning, which aligns more closely with ICM (Klaar et al. 2020).

Anglian Water operates the municipal drinking water treatment plants and STWs in the River Lark catchment (Figure 1.3), so is mandated by EA to invest in conservation measures and water quality improvements within the catchment (Clifforde et al. 1995). Water supply is a monopoly and UK consumers are protected from predatory pricing by the Office of Water Services (OFWAT) (Glynn et al. 1992). Unlike in the US, where firms negotiate with regulators to set prices which yield a specified rate of return on investment capital, in the UK pricing is not dependent upon the firm's assets but on inflation (Glynn et al. 1992). The OFWAT reviews the water companies' 5-year asset management plans (AMPs), which must tie investments to specific service targets (Glynn et al. 1992) or fulfillment of statutory obligations (Brighty et al. 2021).

The Water Industry National Programme (WINEP) outlines the required improvements to environmental assets' health and resiliency which must be addressed by firms in the AMP (AW 2018). The WINEP is currently under revision to shift from end-of-pipe solutions favored in the past to a more holistic approach that could change OFWAT's economic-environmental calculus and allow greater natural capital investments (UUWL 2020).

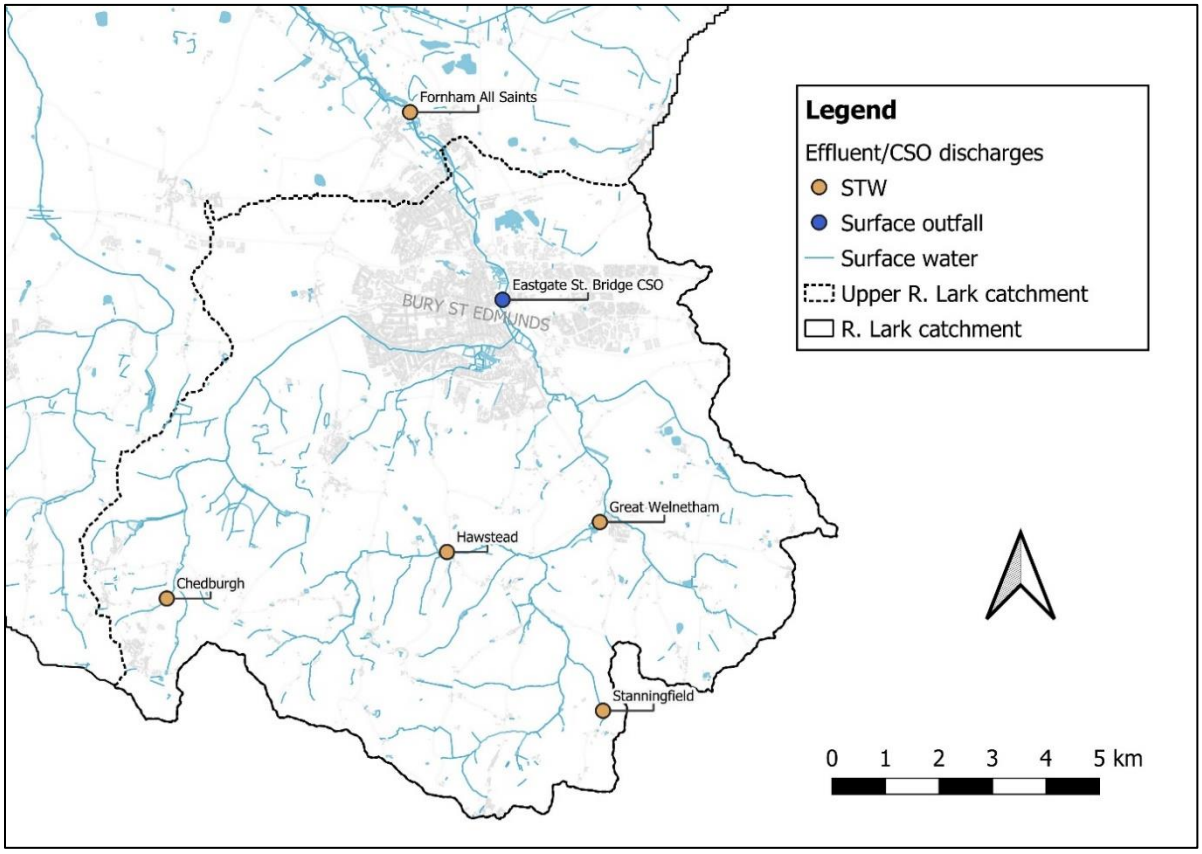

Figure 1.3 Map of the upper River Lark Catchment, in Suffolk, UK, showing STW discharges. Contains OS data © Crown copyright and database right 2021, 2022 (OS 2021, c2021, c2022). Contains public sector information licensed under the Open Government Licence v3.0 (EA 2021m).

Environmental conservation measures for the current Anglian Water AMP cycle ending in 2025 include restoration of several tributaries of the Lark (AW 2018). However, treatment technology upgrades are not a major focus at the largest STW in Fornham All Saints because phosphate concentrations in the effluent are currently as low as technically feasible given the economic constraints of the current regulatory framework (Brighty et al. 2021). Phosphate removal using iron sulfate is being expanded to most STWs in the Lark catchment during this AMP cycle (Brighty et al. 2021), but the cost to invest in more advanced removal technology is not justifiable for the current permitted effluent phosphate concentrations (AW 2018; WW 2018).

The River Lark Catchment Partnership (RLCP) also operates in the Lark catchment and is invested in achieving WFD goals to restore the chalk stream ecosystem. The RLCP represents a diverse range of stakeholders including the EA and local volunteer groups (RLCP c2022). It pursues citizen science projects which build upon EA's monitoring work in the catchment. The River Lark has been designated as a flagship stream for restoration efforts by Anglian Water and the RLCP has committed to scaling up citizen science efforts in the catchment through participation in Catchment Systems Thinking Cooperative (CaSTCo) (A. Hinchley, RLCP Chairperson, personal communication with the author, August 26, 2022). To monitor the Lark's rehabilitation at the catchment scale, the RLCP has begun to establish a volunteer-run water quality observatory on the River Lark. The overall aim of this is to augment EA nutrient and invertebrate sampling and flow monitoring by expanding the number of sites and frequency of monitoring throughout the catchment using citizen science.

Monitoring STW pollution in the River Lark

As part of the effort to establish the River Lark observatory, the RLCP deployed a datasonde approximately 1.5 km downstream of the Fornham All Saints STW for a six-month trial in 2020 (See p.15 in Methods for specific parameters measured). Shortly after the RLCP datasonde was installed, volunteers noticed elevated biological oxygen demand (BOD) and conductivity in real-time that indicated extended combined sewer overflow (CSO) activity (Hurst 2021). Anglian Water investigated the incident and confirmed the occurrence of multiple CSO discharges across several days within the time period the datasonde registered elevated responses in the parameters being recorded (Brighty et al. 2021).

Combined sewer overflows are a relatively common phenomenon in England due to the age of the country's combined sewer systems and the high rate of misconnections between sewer pipes and surface water drains in newer systems (CIWEM 2014). The town of Bury St. Edmunds has separate surface drainage and sewer systems for new development, but misconnections between the two systems are suspected to contribute to overloading of the STW during intense rainfall events (Brighty et al. 2021). Additionally, many buildings in the town date to the medieval period and may have combined systems which can deliver high volumes of runoff along with sewage during heavy rainfall events (Brighty et al. 2021). When the capacity of the STW and storm tanks is exceeded due to exceptionally high flow

volumes, a CSO is triggered to prevent sewage backups in buildings, releasing a mixture of untreated sewage and stormwater to the river (CIWEM 2014).

The Urban Pollution Management (UPM) research program sets the framework for management of wet weather discharges from CSOs in the UK (Clifforde et al. 1995). The UPM incorporates a holistic approach by the industry and regulators to find economically viable solutions (Clifforde et al. 1995). Standards are set by the EA to reduce the negative impacts of CSO intermittent discharges on river aquatic life, bathing, and general amenities (Clifforde et al. 1995). The duration of CSO discharge events is automatically recorded by Event Duration Monitoring (EDM) systems located within many STWs (EA 2018). In 2020, conductivity-based EDM sensors at the Fornham All Saints STW detected 16 CSO events, lasting a total of 199 hours (AW 2021). No CSO events were recorded by the EDM system at the Fornham All Saints STW in 2021, though other STWs in the upper Lark catchment recorded CSO events (AW 2022).

In April 2021, EA deployed its own datasonde for six months to measure temperature, conductivity, pH, ammonia, turbidity, and dissolved oxygen at 30-minute intervals, to determine if CSO events occurred during dry periods (BART 2021). The EA did not find any abnormalities in the data and removed the datasonde in October 2021 (BART 2021). The EA typically monitors nutrient enrichment of the River Lark via regular snapshot sampling at several locations upstream and downstream of Fornham All Saints. However, the datasonde deployment provided an unprecedented opportunity to examine sub-daily nutrient loading due to the high data resolution, with measurements every 30 minutes. Such analysis was outside the scope of the EA investigation, but this dataset would be expected to more accurately capture the potential effects of short-duration, high nutrient content, STW discharges on in-stream water chemistry (Birkby 2020; Hurst 2021) than typical EA modeling using the Source Apportionment Geographic Information System (SAGIS). The SAGIS model uses EA snapshot sampling data and STW monitoring data to determine the overall contributions of various sources within the catchment to eutrophication (Comber et al. 2013). It does not model daily or sub-daily fluctuations in nutrient concentration which may be needed to accurately determine responses in lotic ecosystems due to the transient nature imposed by the flowing water.

To accurately calculate nutrient loads in a chalk stream, sampling intervals should be frequent enough to capture short-duration, high-concentration input events. Bowes et al. (2009) measured nitrate, phosphorus, and silica concentrations in a chalk stream at sub-daily frequency for one year to accurately calculate annual loads (Bowes et al. 2009). Simulated sampling intervals of daily and twice daily applied to the original data set introduced very little error to the annual load calculation (Bowes et al. 2009). However, simulated monthly sampling resulted in increased deviation from loads calculated with the high-resolution data, meaning this sampling interval was too infrequent to accurately capture nutrient load dynamics (Bowes et al. 2009).

Bowes et al. (2012) studied the impact of storm events on phosphorus concentration of final effluent discharged to a chalk stream as well as of the river itself using data collected at 30 min. intervals. Single measurement peaks in nutrient concentration observed at 30-minute intervals were attributed to sensor noise rather than the discharge of temporarily decreased effluent quality from the STW, because such temporary events were expected to last longer than an hour (Bowes et al. 2012). Short-duration storm events had no significant effect on effluent phosphorus concentration, but long-duration storm events were correlated to increased concentration (Bowes et al. 2012). This indicates that long periods of sustained rainfall can result in decreased effluent quality, which may or may not be due to CSO activity.

Nutrient-discharge hysteresis

Hysteresis occurs when the concentration of a stream water constituent differs on the rising and falling hydrograph limbs, creating a loop-shaped concentration-discharge (C-Q) plot (Williams 1989). Loop direction and shape can provide information about nutrient sources and patterns of mobilization during storm events and several classification systems have been developed to assist with this characterization (Butturini et al. 2006; Evans and Davies 1998; Williams 1989; Zuecco et al. 2016). "Clockwise" hysteresis describes a C-Q plot with a higher concentration of solute on the rising limb than on the falling limb of the hydrograph, suggesting early-event flushing (Williams 1989). In contrast, a C-Q plot exhibiting "anti-clockwise" hysteresis is characterized by a loop shape with higher solute concentration on the falling limb of the hydrograph (Williams 1989). This lag in peak solute concentration indicates catchment sources are only mobilized later in the storm event and are likely

runoff-related (Bowes et al. 2005a). "Figure-of-eight" C-Q loops combine both clockwise and anti-clockwise loops, meaning the dominant solute source changes during the storm event (Williams 1989). Concentration-discharge relationships marked by dilution generate linear plots, exhibiting no hysteresis because no additional solute sources are mobilized by the storm as compared to pre-storm conditions (Williams 1989).

Bowes et al. (2005a, 2005b, 2009, 2012, 2015) studied nutrient C-Q hysteresis patterns in STW discharge-impacted chalk streams to infer dominant nutrient sources. Clockwise nutrient hysteresis indicates a rapidly mobilized nutrient source, which may already be in the stream or is likely to originate at a single point near the monitoring location, such as a CSO or effluent discharge (Bowes et al. 2009, 2012). Conversely, anti-clockwise hysteresis indicates the nutrient input arises from diffuse sources throughout the catchment, farther from the monitoring location (Bowes et al. 2009, 2012).

Previous studies by Lawler et al. (2006), Rose et al. (2018), and Mihiranga et al. (2021) noted ammonia C-Q hysteresis in catchments with diverse geology and land use characteristics. Lawler et al. (2006) studied the dynamics of five water quality parameters, including ammonia, during stormflow events in the headwaters of a highly urbanized UK river heavily affected by industrial pollution and STW discharges. They concluded that the decreased prevalence of ammonia concentration peaks during the final storm events in multiple-succession sequences was likely caused by decreased event total rainfall which was not sufficient to trigger CSO events (Lawler et al. 2006). Rose et al. (2018) studied storm event C-Q hysteresis patterns in a third-order Pennsylvania, USA stream with catchment land use dominated by agriculture and forestry. Of the 12 biogenic and geogenic solutes examined, they found ammonia C-Q hysteresis was the most variable in relation to discharge (Rose et al. 2018). In China, Mihiranga et al. (2021) conducted total phosphorus and nitrogen C-Q hysteresis analysis in a semi-arid mountainous watershed with heavy agricultural land use. Ammonia exhibited clockwise C-Q hysteresis in all four storms studied, and surface runoff drove storm event ammonia fluxes to increase to four times the pre-event baseline (Mihiranga et al. 2021).

Ammonia is an important form of nitrogen in the River Lark and other UK rivers as it is the dominant form of nitrogen in animal waste sources, including human wastewater effluent. Most large STWs in the UK, including the Fornham All Saints STW, discharge treated

effluent continuously, so ammonia is also constantly added to the receiving waters. The maximum ammonia concentration reported by Anglian Water in treated effluent samples from the Fornham All Saints STW on the Lark in 2021 was 0.303 mg-N/l (EA c2021), but the STW is permitted to discharge up to 8 mg-N/l, with the 95th percentile limited to 2 mg-N/l (EA 2019). Lawler et al. (2006) suggested that high ammonia concentration occurring in response to storm events can be used to index low-quality, nutrient-rich STW discharges or storm drain misconnections. However, the upper River Lark catchment has numerous diffuse sources of ammonia that could also be mobilized by rainfall events, such as livestock operations and septic systems. Characterization of ammonia concentration-discharge hysteresis could be leveraged to determine the relative importance of these pollution sources to inform future catchment nutrient management improvements. As most chalk stream nitrogen C-Q hysteresis studies have focused primarily on nitrate-N (Bowes et al. 2005b, 2009, 2015; Lloyd et al. 2016a, 2016b), rather than ammonia-N, describing ammonia C-Q hysteresis in the River Lark would also increase understanding of nutrient sources and transport pathways in a rare freshwater ecosystem.

Research questions

The availability of the high-resolution EA datasonde data, my involvement with the RLCP, and curiosity about hysteresis analysis led me to formulate the following research questions: i) Are there rainfall-driven episodic changes in ammonia concentration during the growing season in the River Lark downstream of Fornham St. Martin? ii) Is there a relationship between the ammonia concentration-discharge hysteresis patterns observed for storm events and the range of discharge per storm, total event rainfall, or antecedent catchment wetness? and iii) What can be inferred, based on the observed hysteresis patterns, about the relative importance of different catchment ammonia sources for storm-related nutrient export during the growing season?

Chapter 2: Methods

Data sources and quality control

The data for the analyses in this thesis were originally collected for other purposes, and thus come from various sources. Consequently, each required processing and validation prior to incorporation to address the above questions. The primary data are derived from measurements taken by the EA multimeter datasonde deployment on the River Lark downstream of Fornham All Saints in 2021 and from the EA gauge station on the River Lark at Fornham St. Martin (Figure 2.1). Rainfall data were also checked for errors before inclusion in storm event analyses. Several additional datasets were checked and excluded from analysis; these are mentioned below as relevant, with further details provided in Appendix A. All data quality control was conducted using Microsoft Excel and RStudio (RCT 2022). The R packages used for specific analyses are referenced in the subsequent sections below, but nearly all time-series data were formatted using lubridate (Grolemund and Wickham 2011).

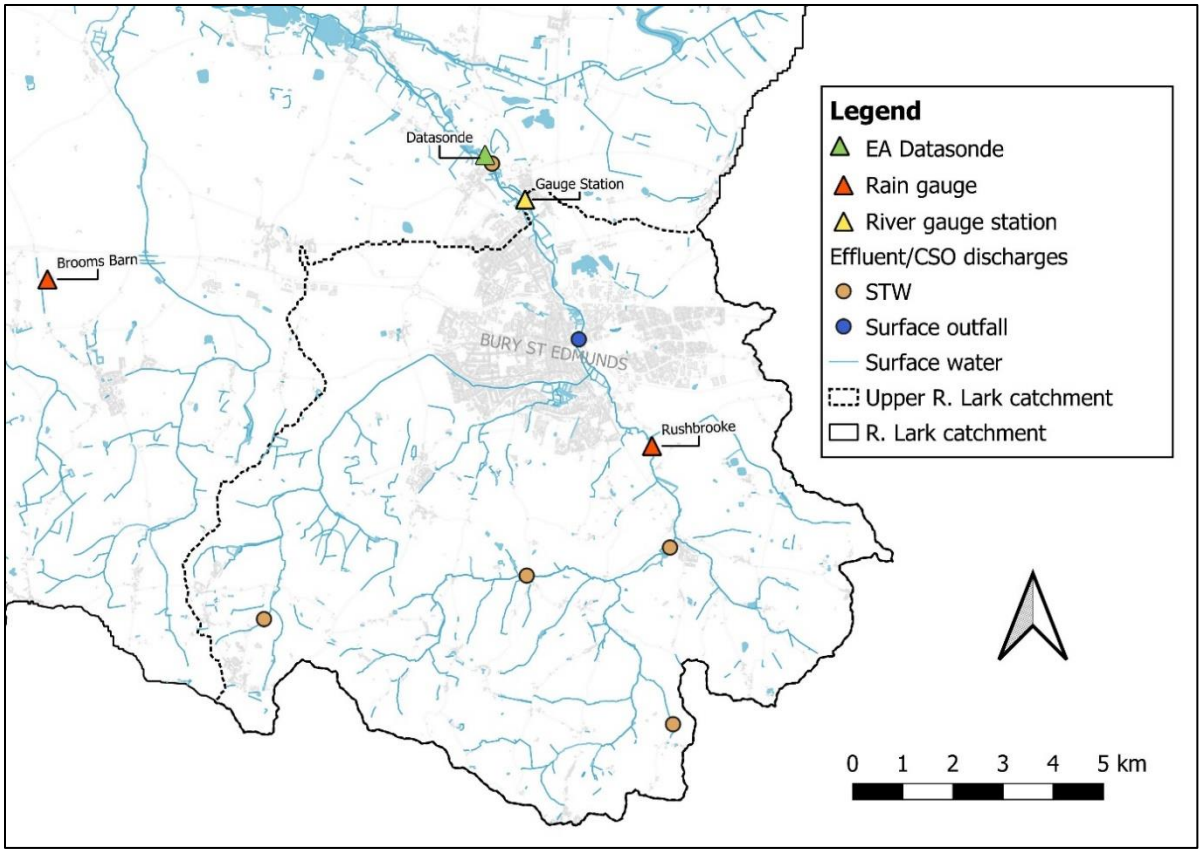

Figure 2.1 Location of data sources in the River Lark catchment used for concentration-discharge hysteresis analysis of storms that occurred June to July 2021. Contains OS data © Crown copyright and database right 2021, 2022 (OS 2021, c2021, c2022). Contains public sector information licensed under the Open Government Licence v3.0 (EA 2021m).

Deployment and quality checks of the EA datasonde

Dissolved oxygen (DO), ammonia concentration, and temperature were measured by an EA datasonde (YSI EXO-2, Yellow Springs Instrument Inc., Yellow Springs Ohio, USA) deployed downstream of the Fornham All Saints STW (Figure 2.1) on the River Lark between May and October 2021. This dataset (EA 2021l) was provided by the EA Anglian Region office via the RLCP. It is Crown copyright and the data were used under the terms of the Open Government Licence v3.0. The EA replaced the datasonde with a freshly calibrated instrument of the same model every 4-6 weeks throughout the deployment period (Burgess et al. 2021). The EA datasonde measured ammonia with an ion-selective electrode (ISE) accurate to ±10% over the range of values measured in the River Lark (YSI 2020). It measured DO using a combined optical and luminescence lifetime sensor accurate to ±1% of reading or ±0.1 mg/L, whichever is greater (YSI 2020). The thermistor is factory-calibrated to be accurate within ±0.01 °C (YSI 2020). Water samples were collected during

datasonde maintenance for laboratory analysis to generate an ammonia correction factor (BART 2021), which was provided with the dataset. This correction factor was necessary due to inflation of ammonia measurements, caused by high conductivity, which was noted during a trial datasonde deployment period in April 2021 (BART 2021).

The EA did not validate individual datasonde measurements, only analyzed general data trends (BART 2021), so the data were checked for outliers. To determine if the data were normally distributed, Q-Q plots were created in RStudio (RCT 2022) and visually examined for deviation from a straight line. The R package bestNormalize (Peterson 2021) was used to determine the best transformations to normalize DO and ammonia; the ordered quantile normalization method (Peterson and Cavanaugh 2020) was applied. Five-point moving window medians and standard deviations of the raw and normalized DO and ammonia, and raw temperature measurements were calculated using the R package caTools (Tuszynski 2021). Values greater than two standard deviations from the 5-point median were flagged for manual review to ensure true inflection points were not erroneously discarded from the dataset. Ammonia and DO measurements were considered paired, and detection of an outlier in either dataset triggered removal of both measurements for the given point in time. All outliers and missing measurements were replaced by linear interpolation from neighboring values using R package zoo (Zeileis and Grothendieck 2005) after all quality checks were completed.

The EA datasonde experienced prolonged fouling (BART 2021), as indicated by constant near-zero DO percent saturation measurements which were primarily resolved with maintenance (Burgess et al. 2021). Dissolved oxygen and ammonia measurements during fouling periods were removed and not considered for analysis. Extended fouling occurred from 00:00 01 August 2021 to 08:30 17 August 2021 and 20:00 10 September 2021 to 03 October 2021. Temperature data were not discarded because diurnal fluctuations remained as expected and sediment temperature was assumed to be similar to that of the water column. Temperature data quality was considered independent of other measurements due to the high reliability of the factory-calibrated sensor (YSI 2020), but was checked using the same methods described for ammonia and DO. However, 86% of paired ammonia/DO outliers and 64% of temperature outliers removed occurred at 4-hour intervals beginning at 00:30, indicating influence of an underlying factor not related to storm discharge. Due to the regularity with which these outliers occurred, they may have been caused by

anthropogenic discharges to the river. All measurements of ammonia, DO, and temperature taken at these times were removed from the dataset and replaced by linear interpolation from neighboring measurements using R package zoo (Zeileis and Grothendieck 2005). See Appendix A for details.

Deployment and quality checks of the RLCP datasonde

The RLCP (2021) provided data collected by their datasonde (Proteus Water Quality Probe, Proteus Instruments Ltd., Stoke Prior, UK) which was deployed in the River Lark approximately 1.5 km downstream of Fornham All Saints, at Mill Farm, between December 2020 and March 2021. The RLCP datasonde measured temperature (°C), ammonium concentration (mg/l), pH, oxidation-reduction potential (mV), turbidity (NTU), conductivity (µS/cm), and tryptophan-like fluorescence (ppb) at 15-minute intervals; dissolved oxygen was not measured. The RLCP datasonde was dislodged by flooding 23 days after deployment and stopped logging data at 11:30 GMT 27 December 2020 (A. Hinchley, RLCP Chairperson, personal communication, October 3, 2022). Therefore, only the initial measurement period, 13:10 GMT 03 December 2020 to 11:30 GMT 27 December 2020 was considered suitable for analysis and checked for outliers and instrument noise. However, the dataset was excluded from this C-Q hysteresis analysis because the ammonium ISE on the RLCP datasonde was not sensitive enough, at ±5% or 2 mg/l per measurement. The relatively low accuracy of the datasonde ISE in this freshwater application caused 99% of ammonium (mg/l) measurements to be insignificant, as they were less than 2.0 mg/l. The quality checks conducted to validate the RLCP datasonde dataset are detailed in Appendix A.

Validation of discharge data from the EA Fornham St. Martin gauge station

The EA Anglian Region provided 15-minute river discharge measurements from EA gauge station 033070, located on the Lark at Fornham St. Martin (Figure 2.1) as a partially validated data set (2021k). These data (EA 2021k) are Crown copyright and were used under the terms of the Open Government Licence v3.0. The data validation procedures outlined by Crochemore et al.'s (2020) analysis of global river flow data were used to check the dataset for outliers. The time series was standardized using modified z-scores (Crochemore et al. 2020) and scores with an absolute value greater than 3 were considered outliers. No outlier flow measurements which occurred outside of the EA validated

timeframe were detected using these criteria. However, there were EA-validated abnormally high values identified in Dec 2020 – Feb 2021 which exceeded the 95th percentile of gauged daily flow measured at Fornham St. Martin from 1985 – 2021 by 136-466% (NRFA c2022c). River flows in the East of England between December 2020 and February 2021 were notably higher than average (EA 2021a, 2021b), which supports the observation of exceptionally high flows in the Lark during this time.

Validation of rainfall measured by EA rain gauge E22322

The EA Anglian Region provided 15-minute rainfall totals from rain gauge E22322, located along the perennial reach of the Lark at Rushbrooke (Figure 2.1). These data (EA 2022g, 2022h) are Crown copyright and were used under the terms of the Open Government Licence v3.0. This rain gauge, hereafter referred to as "the EA rain gauge", is located within the Upper Lark sub-catchment and is considered representative of the average rainfall over this portion of the chalk aquifer. The EA rain gauge is part of a UK-wide network which collects quality-assured data for real-time flood forecasting (Everitt 2017). The gauge at Rushbrooke is a Lambrecht meteo rain[e] weighing precipitation sensor registered to the UK Met Office and is calibrated approximately every eight weeks (EA, email message, July 15, 2022). The total rainfall collected is compared to a standard storage check gauge to determine if the weighing sensor has over- or under-recorded rainfall (EA, email message, July 15, 2022). The weighing sensor eight-week totals were within 10% of the check gauge amounts for Dec 2020 – Oct 2021 (EA 2022g, 2022h), indicating quality data.

The EA rain gauge measurements were aggregated to hourly, daily, and monthly values and subjected to six quality checks (Table 2.1) following Blenkinsop et al.'s (2017) methods, to ensure they did not contain errant values and agreed with EA descriptions of local monthly precipitation patterns and totals (EA 2021a, 2021b, 2021c, 2021d, 2021e, 2021f, 2021g, 2021h, 2021i, 2021j). Monthly rainfall accumulations were also compared to the East Anglia long-term average calculated using areal rainfall values from the HadUK-Grid 1 km gridded climate dataset (NCIC 2022). Two additional sources of rainfall data, from personal weather stations, were also quality checked, but were found to be unreliable and excluded from analyses. Further details are provided in Appendix A.

Table 2.1 Quality checks outlined by Blenkinsop et al. (2017) which were applied to both the EA and Rothamsted Research rainfall data.

Check Number	Description
1	Do any of the values equal/exceed the British record hourly rainfall? (92 mm)
2	Is 80% of the hourly British record met/exceeded during Apr-Oct? (73.6 mm)
3	Are there suspect "daily accumulations" at 0900 or 1200?
4	Does daily rainfall equal/exceed 24 h England record? (279 mm)
5	Is monthly rainfall within 20% of East Anglia 30-year mean (1990-2019)?
6	Is monthly rainfall within 20% of the Met Office or EA East Anglia amount for that month?

The aggregated hourly EA rain gauge measurements were also checked against hourly rainfall measurements collected by Rothamsted Research's Brooms Barn Meteorological Station (RR 2022) using linear regression. The Brooms Barn station (Figure 2.1) uses an Environmental Measurements Ltd SBS500 TBR, which is calibrated by Campbell Scientific, and the rainfall data are validated by Rothamsted Research (RR c2022a, c2022b). For consistency, the Brooms Barn TBR data were subjected to the same quality checks (Table 2.1) as the EA rain gauge data prior to analyses. Both gauges passed all checks except numbers 5 and 6, but anomalous monthly values agreed with EA (2021a, 2021b, 2021c, 2021d, 2021e, 2021f, 2021g, 2021h, 2021i, 2021j) descriptions of regional monthly precipitation patterns and amounts.

At the rainfall rates observed during the study period, the EA rain gauge is accurate to ±0.1 mm or 1% (LM 2022) and the Brooms Barn rain gauge is 98% accurate (RR c2022b). The acceptable threshold to determine agreement between sites via linear regression was set at $p < 0.01$ and $R^2 > 0.70$. Regression of the rain gauge hourly time series revealed poor correlation between values for the two sites ($p < 0.001$, $R^2 = 0.39$), which may be due to geographic variation in precipitation rates across storm cells. Linear regression of the same data, aggregated to daily rainfall values for each rain gauge showed better agreement ($p < 0.001$, $R^2 = 0.83$). Therefore, the EA rain gauge was considered suitable for contextualization of storm event C-Q hysteresis.

Nutrient concentration-discharge analysis

Ammonia concentration-discharge (C-Q) hysteresis analysis was conducted to characterize the relationship between abnormally high or low water quality values observed on the River Lark downstream of Fornham St. Martin and rainfall events during the growing season. This analysis was conducted using RStudio (RCT 2022) and Microsoft Excel. Time series data were formatted for analysis using the R package lubridate (Grolemund and Wickham 2011) and all included plots were created using the R package ggplot2 (Wickham 2016).

Identification of storm events

Discharge values for the River Lark at Fornham St. Martin were plotted in R using ggplot2 (Wickham 2016) and Plotly (Sievert 2020) over the period for which validated EA datasonde ammonia measurements were available, to first visually identify discharge peaks suspected to be the results of storms. Storm hydrographs were then refined to include those with maximum discharge at or above 140% of base flow (Bowes et al. 2015), with base flow defined as the lowest discharge measurement that occurred before multiple increasing discharge measurements with positive slope (Lloyd et al. 2016a, 2016b).

The rising limb of the hydrograph included all measurements from the final antecedent base flow measurement to peak discharge (Lloyd et al. 2016b). Multi-peak storms were considered as having discontinuous rising and falling limbs, with the maximum discharge treated as the overall event peak (Lloyd et al. 2016a). The falling limb of the storm hydrographs was considered to begin at the first measurement after peak discharge (D'Amario et al. 2021). The falling limb was considered to end at the point at which the rate of change in discharge dropped below 10% per day (Butturini and Sabater 2002; Butturini et al. 2006), or at the lowest discharge measurement before a subsequent storm event (Lloyd et al. 2016b). To characterize event concentration-discharge hysteresis, the final storm discharge measurement should be similar to the initial event discharge (Baker and Showers 2018). Storm events for which discharge did not fall to at least 20% of the rising limb were excluded from hysteresis characterization due to falling limb insufficiency (cf Baker and Showers 2018, who used 50%).

Characterization of hysteresis

Concentration-discharge (C-Q) plots were created using normalized values, such that all plots used the same dimensionless axes, with x and y values scaled from zero to one (Lloyd et al. 2016a). Discharge and concentration were normalized per storm event by subtracting, respectively, the minimum event value from individual measurements, then dividing by the range of the values per event (Lloyd et al. 2016a). Event hysteresis was first classified by visual C-Q loop shape and direction approximation. Storm hydrographs were excluded from analysis if at least 2 concentration measurements were not available on each limb and one at peak discharge (Evans and Davies 1998).

For discharge, normalized measurements represent the ratio of deviation from baseflow to the maximum amount of deviation from base flow per storm event. As the lowest event concentration does not necessarily occur at baseflow, this interpretation is not true for normalized concentration values. Rather, using normalized concentration values enables comparison of hysteresis indices between-storms, without index values for high-concentration events being higher than those of low-concentration storms by default (Lloyd 2016a). A dimensionless hysteresis index (*HI*) value was calculated for every 10% of discharge of each storm event, using the Lloyd et al. (2016a) equation (Equation 2.1), where HI_{Qi} is the value of *HI* at a given percentile of normalized discharge Q_i. This is defined by the difference between the normalized values of concentration on the rising (C_{RL_Qi}) and falling (C_{FL_Qi}) limbs of the hydrograph at normalized discharge percentile Q_i.

$$HI_{Qi} = C_{RL_{Qi}} - C_{FL_{Qi}} \quad \text{Equation 2.1}$$

Linear interpolation of normalized concentration was used to obtain values at each discharge percentile for which real measurements were not available (cf Lawler et al. 2006). Concentration data were available for the 10th to 90th discharge percentile for all events, except storm three, which ended at Q_{82}. Discharge percentiles where the difference between rising and falling limb concentration was less than datasonde measurement uncertainty were considered to not exhibit hysteresis (Baker and Showers 2018).

Lloyd et al. (2016a) used the mean event hysteresis index HI_{mean} to compare storm events but acknowledge that negative and positive HI_{Qi} values within the same storm event can result in HI_{mean} near zero, which may not reflect the actual hysteresis pattern. In these

cases, a positive loop area is used to indicate the presence of complex hysteresis and Lloyd et al. (2016a) recommended examining the distribution of HI_{Qi} values alongside the storm HI_{mean} value to improve the description of complex loop shapes. Integration of *HI* plotted as a function of normalized discharge describes the predominant direction of this hysteresis, via the sign of the integral being positive or negative (Lloyd et al. 2016a).

Lloyd et al.'s (2016a) methods were adapted to improve description of figure-of-eight C-Q hysteresis patterns to enable comparison of hysteresis magnitude per directional component across multiple storm events. Complex hysteresis was observed in the storms included in this analysis, so quantifying the magnitude of each directional component was necessary to adequately understand storm nutrient delivery dynamics because of the different underlying mechanisms associated with each component. The contribution of each directional component to the overall magnitude of storm hysteresis was quantitatively described by calculating the absolute value of the weighted average of HI_{Qi} per directional component separately, as HI_{abs+} (Equation 2.2) for positive (clockwise) HI_{Qi} values, and HI_{abs-} (Equation 2.3) for negative (anti-clockwise) HI_{Qi} values. The weight of each directional component was achieved by dividing the sum of the absolute values of each group of like-direction HI_{Qi} values by the total number of HI_{Qi} values calculated, n_{total}. The overall magnitude of hysteresis per storm was then quantified by HI_{abs} (Equation 2.4), which is the sum of the two directional components, HI_{abs+} and HI_{abs-} If $HI_{abs+} > HI_{abs-}$, the event was considered to exhibit majority clockwise hysteresis, and if $HI_{abs+} < HI_{abs-}$, the event was considered to exhibit majority anti-clockwise hysteresis. In the unlikely event that $HI_{abs+} = HI_{abs-}$, the event would be considered to display equal parts clockwise and anti-clockwise hysteresis (Lloyd et al. 2016a).

$$HI_{abs+} = \sum_{i=1}^{n_{positive}} \frac{\left|HI_{Qi,positive}\right|}{n_{total}} \qquad \text{Equation 2.2}$$

$$HI_{abs-} = \sum_{i=1}^{n_{negative}} \frac{\left|HI_{Qi,negative}\right|}{n_{total}} \qquad \text{Equation 2.3}$$

$$HI_{abs} = HI_{abs+} + HI_{abs-} \qquad \text{Equation 2.4}$$

The flushing index (*FI*) was calculated for each storm following Vaughan et al. (2017) to compare the degree of ammonia flushing per event. The flushing index (Equation 2.5) is defined as "the slope of the line that intersects the normalized solute concentration at the beginning and at the point of peak discharge of the storm" (Vaughan et al. 2017). It ranges from -1 to 1, with the magnitude indicating the degree, and the sign characterizing the pattern, of event flushing behavior (Vaughan et al. 2017). A negative slope indicates dilution behavior, while a positive slope indicates flushing behavior (Vaughan et al. 2017).

$$\mathrm{FI} = C_{Qpeak,norm} - C_{Qinitial,norm} \quad \text{Equation 2.5}$$

Contextualizing storm event concentration-discharge hysteresis

Normalization enables between-storm comparison of hysteresis patterns (Lloyd et al. 2016a) but does not indicate storm magnitude or any influences related to seasonality. Therefore, 18 metrics (Table 2.2) were identified, via review of the current concentration-discharge hysteresis literature, to contextualize storms and determine if changes in metrics were associated with a particular hysteresis pattern. These metrics were broadly classed into four categories of interest: discharge, rainfall, concentration, and load. Discharge metric candidates (Table 2.2) were chosen to encompass the range of discharge variability across all storms studied (Butturini et al. 2006; Lloyd et al. 2016b; Mihiranga et al. 2021), as well as explore the potential influence of the previous storm's magnitude on nutrient hysteresis (Evans and Davies 1998). Because rainfall drives delivery of nutrients via direct runoff, storm drains, and increased effluent discharge during storms, rainfall metric candidates (Table 2.2) were selected to describe the antecedent, average, maximum, and cumulative event rainfall conditions (Lawler et al. 2006; Lloyd et al. 2016b; Mihiranga et al. 2021; Vaughan et al. 2017). Concentration metric candidates (Table 2.2) were selected to capture the between-storm differences that were lost due to normalization of these values in the HI calculations (Aguilera and Melack 2018; Lloyd et al. 2016b). Load metric candidates (Table 2.2) were selected to compare total nutrient export per storm and differences in export rates between storms (Bowes et al. 2005a, 2015).

Table 2.2 Potential storm event metrics considered for providing seasonal and temporal context to HI_{area} via multiple regression, similar to Table 4 in Liu et al. 2021. Metrics were grouped into four broad categories of interest in the left-most column and references to the studies from which these metrics are derived are in the right-most column.

Category	Metric	Units	Reference
Discharge	Peak	m^3/s	Butturini et al. 2006; Lloyd et al. 2016b; Wymore et al. 2019
Discharge	Pre-Event Baseflow	m^3/s	Butturini et al. 2006; Lloyd et al. 2016b; Wymore et al. 2019
Discharge	Range	m^3/s	Butturini et al. 2008; Lloyd et al. 2016b; Mihiranga et al. 2021
Discharge	Previous Storm Maximum	m^3/s	Evans and Davies 1998
Discharge	Event Duration	days	Lloyd et al. 2016b; Mihiranga et al. 2021
Rainfall	Event Total	mm	Lawler et al. 2006; Lloyd et al. 2016b; Mihiranga et al. 2021
Rainfall	Antecedent Precipitation Index	dimensionless	Lloyd et al. 2016b; Mihiranga et al. 2021
Rainfall	Maximum Intensity	mm/h	Lawler et al. 2006; Mihiranga et al. 2021
Rainfall	Antecedent 24hr Total	mm	Lloyd et al. 2016b
Rainfall	Mean Intensity	mm/h	Lawler et al. 2006
Rainfall	Duration	h	Lawler et al. 2006; Mihiranga et al. 2021
Concentration	Pre-Event Baseline	mg-N/l	Aguilera and Melack 2018; Lloyd et al. 2016b
Concentration	At Peak Discharge	mg-N/l	Aguilera and Melack 2018; Lloyd et al. 2016b
Concentration	Maximum	mg-N/l	Aguilera and Melack 2018; Lloyd et al. 2016b
Concentration	Minimum	mg-N/l	Lloyd et al. 2016b

Table 2.2 Continued

Category	Metric	Units	Reference
Load	Maximum Instantaneous	mg-N/s	Bowes et al. 2005a, 2015
Load	Minimum Instantaneous	mg-N/s	Bowes et al. 2005a, 2015
Load	Event Total	kg-N	Bowes et al. 2005a, 2015

Liu et al. (2021) compiled a similar list of potential explanatory metrics for C-Q hysteresis and concluded that analysis of the large number of variables lends itself to machine learning. Such extensive investigation was beyond the scope of this thesis and not warranted given the limited ammonia concentration dataset available, which provided only a small sample of the full range of intra- and inter-annual variation in hysteresis patterns. Furthermore, the concentration and load metric categories were considered better suited to describe C-Q hysteresis characteristics than to explain mechanisms of causation. Therefore, four key metrics were chosen from the list of 18 candidates to gain insight into potential hydrological controls of storm-driven nutrient delivery in the River Lark. The range of discharge (m^3/s) per storm, defined as the difference between maximum and baseline discharge per event, was chosen to explore if there was an association between the magnitude of discharge peaks and the C-Q hysteresis patterns observed. Previous studies focused on C-Q hysteresis in chalk streams (Bowes et al. 2015; Lloyd et al. 2016b) found that the magnitude of the storm discharge peak influenced hysteretic behavior of several nutrients. Total rainfall (mm) per storm was selected for regression analysis because Lawler et al.'s (2006) analysis of four rainfall metrics found this was most strongly correlated to ammonia peaks in the headwaters of a British river with dry weather flow dominated by effluent input, similar to the River Lark. Rainfall which occurred during the five hours before an increase in discharge began was considered event rainfall, in addition to rain that fell while discharge was elevated, to account for transit time of event water.

The Antecedent Precipitation Index (API) was selected for regression, as an estimate of pre-storm catchment wetness, which can influence the amount of runoff or infiltration that occurs in response to storm rainfall (Brocca et al. 2008; Lloyd et al. 2016b). Dominance of runoff-driven, rather than subsurface, nutrient flow paths can alter hysteresis patterns

(Aguilera and Melack 2018). A 30-day API was calculated for each storm using rainfall data from the EA TBR and the function "getApi" from R package HydroBE (Bühlmann et al. 2019). This uses Kohler and Linsley's (1951) equation (Equation 2.6), where *n* is the day for which API_n is calculated and *k* is a decay constant less than 1. Precipitation on days before day *n*, P_{n-1} to P_{n-30} is weighted using *k*, which was kept at the default function value $k = 0.9$.

$$API_n = P_{n-1} + k * P_{n-2} + k^2 * P_{n-3} + \cdots + k^{29} * P_{n-30} \quad \text{Equation 2.6}$$

Statistical analyses

The distributions of HI_{Qi} values for each storm were tested for normality prior to analysis using RStudio (RCT 2022). First, the Shapiro-Wilk test was used, then HI_{Qi} distributions of all five storms were also visually examined via histograms, geometric density plots, and box plots, to determine if the storms could be compared via analysis of variance (ANOVA). Storms 1 and 2 were grouped for Kruskal-Wallis testing of the distribution of HI_{Qi} values, while storms 3 to 5 were grouped for ANOVA testing. See section titled "Stepwise Regression of Event-Scale Context Metrics" in Results chapter for further detail. To determine if the shape of the figure-of-eight ammonia C-Q hysteresis loops significantly differed from one another, the HI_{Qi} data for storms 1 and 2 were analyzed in RStudio (RCT 2022) using the Kruskal-Wallis rank sum test with 8 degrees of freedom and α of 0.05.

Stepwise linear regression of the ammonia C-Q hysteresis index values, HI_{mean}, HI_{abs}, HI_{abs+}, and HI_{abs-}, and flushing index, *FI,* for the five storms was conducted in RStudio (RCT 2022), using the three storm context metrics as the independent value in a pairing. The relationship between pairings was considered significant at $\alpha = 0.05$ and $R^2 \geq 0.70$. Metrics meeting these criteria were then combined for multiple regression and those results were evaluated with the same significance threshold. Polynomial, log, or other linear transformations were not applied to the data to improve regression fit at any step, due to the low predictive power of regression using a small sample of storms. The purpose of regression analysis was not to develop a quantitative predictive model for the River Lark, but to inform future research in the Lark catchment regarding factors that affect storm nutrient export.

While only three storm context metrics were chosen for regression analysis of the hysteresis index, total ammonia loads (kg-N) per storm were calculated to describe inter-event differences in the magnitude of nutrient export. Because excess nutrient loading of the Lark is a significant management concern, changes in instantaneous ammonia loads (mg-N/s) were examined over the course of each storm event (Bowes et al. 2005a, 2015). Then, total ammonia export per storm was estimated using the "timeIntegration" function from R package Smisc (Sego 2016) to calculate the area under the instantaneous load curves.

Chapter 3: Results

Storm event identification

A total of eleven storm events with peak discharge at least 140% of baseflow occurred in the River Lark during the period for which the EA datasonde ammonia concentration values were available (Figure 3.1). Due to extended sensor fouling starting 01 August 2021, and ammonia concentration data being unavailable for the rising limb of the storm which began before datasonde deployment, events before June or after August could not be analyzed. After the suitability of each storm for concentration-discharge analysis was considered (Table 3.1), six storms were excluded. Hysteresis analysis of the remaining five storms is detailed in the next section.

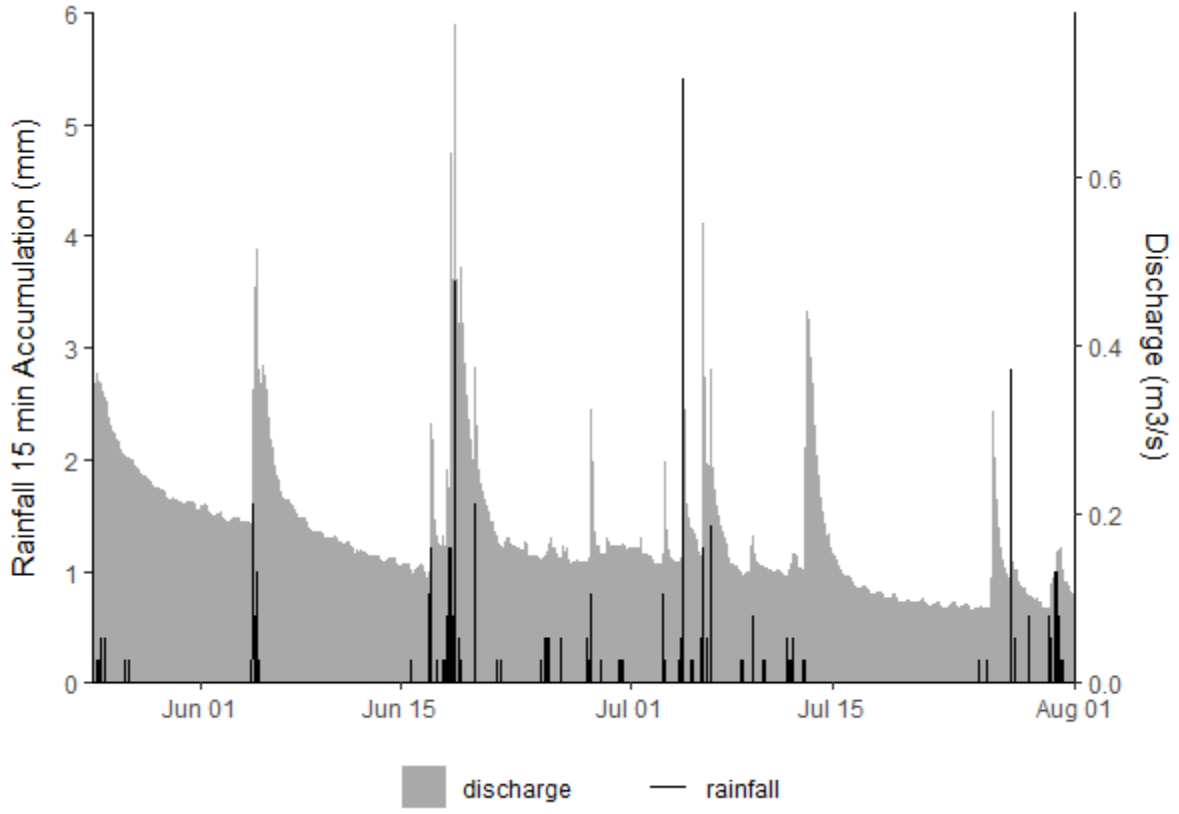

Figure 3.1 Discharge (m3/s) of the River Lark at Fornham St. Martin, UK and rainfall (mm) at Rushbrooke, Bury St. Edmunds, UK between 24 May and 01 August in 2021.

Table 3.1 Dates of storm events in June and July 2021 in the River Lark at Fornham St. Martin, UK and their identifiers or reasons for exclusion from hysteresis analysis.

Event Dates	**Storm Identifier or Reason for Exclusion**
04 to 06 June	Storm 1
16 to 17 June	Discharge did not fall below 20% of peak
18 to 21 June	Storm 2
28 Jun	Storm 3
03 Jul	Discharge did not fall below 20% of peak
04 to 05 July	Storm 4
05 to 07 July	Storm 5
13 to 15 July	No rainfall measured at Rushbrooke or Brooms Barn gauges
26 to 27 July	No rainfall measured at Rushbrooke or Brooms Barn gauges

Ammonia concentration-discharge hysteresis analysis

Storm event 1

Storm 1 began at 13:30 GMT, 04 June 2021 and ended at 15:15 GMT 06 June 2021, lasting 2.07 days (Figure 3.2). Discharge rose quickly in response to periods of heavier rainfall, with little lag time before the first two peaks, indicating there may have been a large runoff component. The third peak was the least flashy, occurring several hours after rain cessation. This could have been groundwater-driven or reflective of increased STW effluent discharge volume, with the lag time due to stormwater influent transit time to and through the STW. The maximum event discharge of 0.57 m^3/s was between the 50^{th} and 90^{th} percentiles of gauged daily flow measured at Fornham St. Martin from 1985 – 2021 (NRFA c2022c).

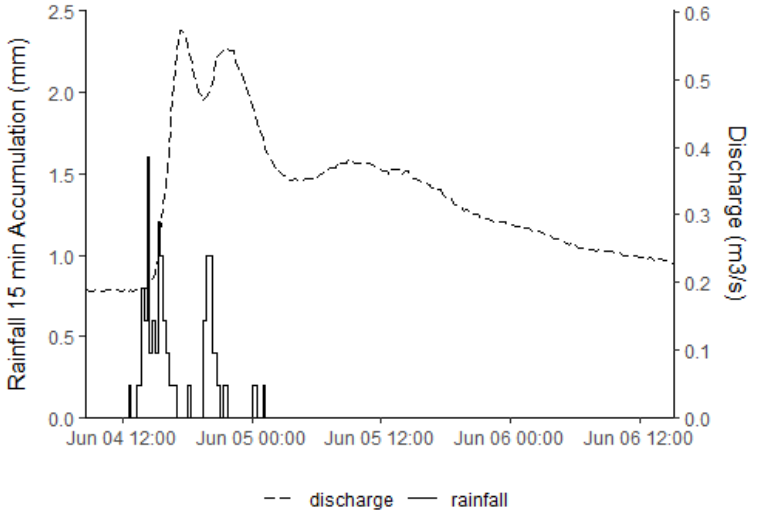

Figure 3.2. Discharge (m^3/s) of the River Lark at Fornham St. Martin, UK and rainfall (mm) at Rushbrooke, Bury St. Edmunds, UK during storm event 1, 04 June 2021 to 06 June 2021.

Ammonia concentration (Figure 3.3a) and instantaneous loads (Figure 3.3b) fluctuated over the course of Storm 1. The ammonia concentration in the River Lark displayed few sustained spikes that would indicate flushing, which agreed with the overall storm *FI* = -0.49. The first discharge peak's rising limb (ending 17:15 04 Jun 2021) followed a clear dilution curve, but examination of instantaneous ammonia loads (Figure 3.3b) indicated that the event exhibited a degree of flushing behavior which was not easily described by *FI*. Ammonia export peaked during the beginning of the storm event, and the maximum

instantaneous load of 101.68 mg-N/s occurred before the sustained decline in discharge. Total ammonia export during storm 1 was 11.3 kg-N.

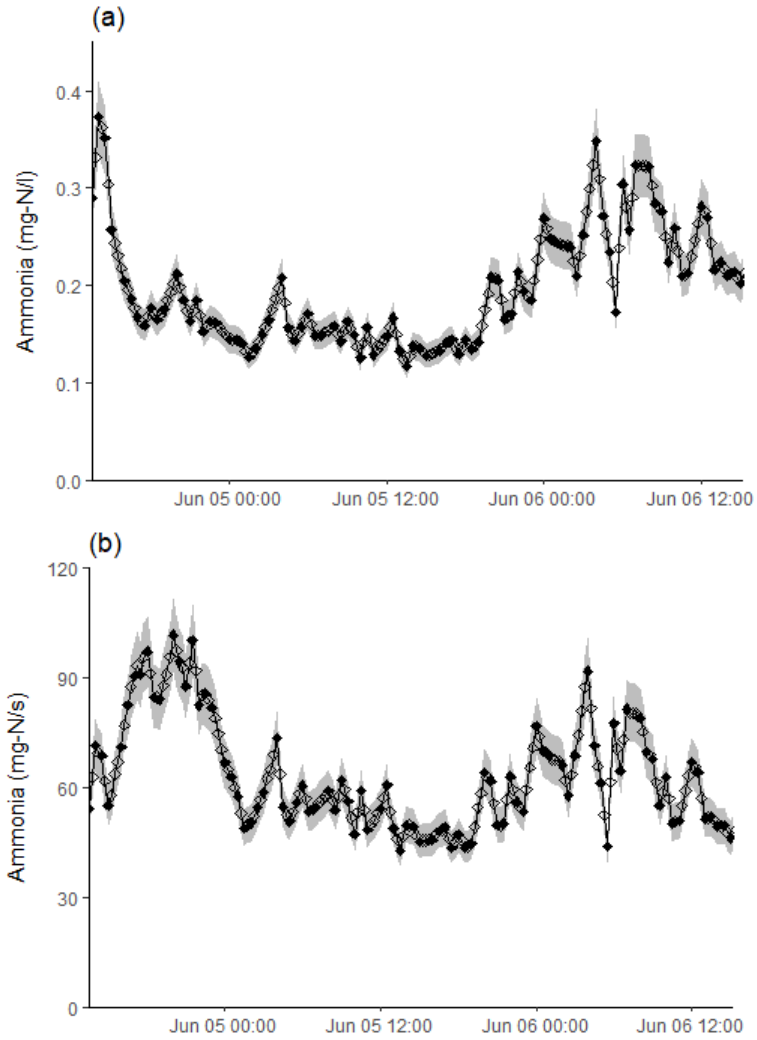

Figure 3.3. Ammonia concentration (mg-N/l, a) and instantaneous loads (mg-N/s, b) in the River Lark at Fornham St. Martin, UK during storm event 1, 04 June 2021 to 06 June 2021. Gray area indicates measurement precision (±10%). Open diamonds represent times for which discharge measurements were available, but concentration was interpolated.

Storm 1 had three distinct discharge peaks and the normalized ammonia C-Q plot (Figure 3.4) showed that storm 1 clearly exhibited complex (figure-of-eight) hysteresis, as there were several points of intersection as discharge rose and fell. However, the majority of the storm exhibited clockwise hysteresis. The first, and highest, discharge peak's rising limb followed a clear dilution curve. The second peak exhibited some flushing on the rising limb, followed by clockwise hysteresis due to the falling limb concentration being distinctly lower than the rising limb of the first event peak. The third peak appeared to be chiefly a dilution

curve in its overall trend, though concentration fluctuated on the falling limb late in the storm event, with two distinct multi-point spikes.

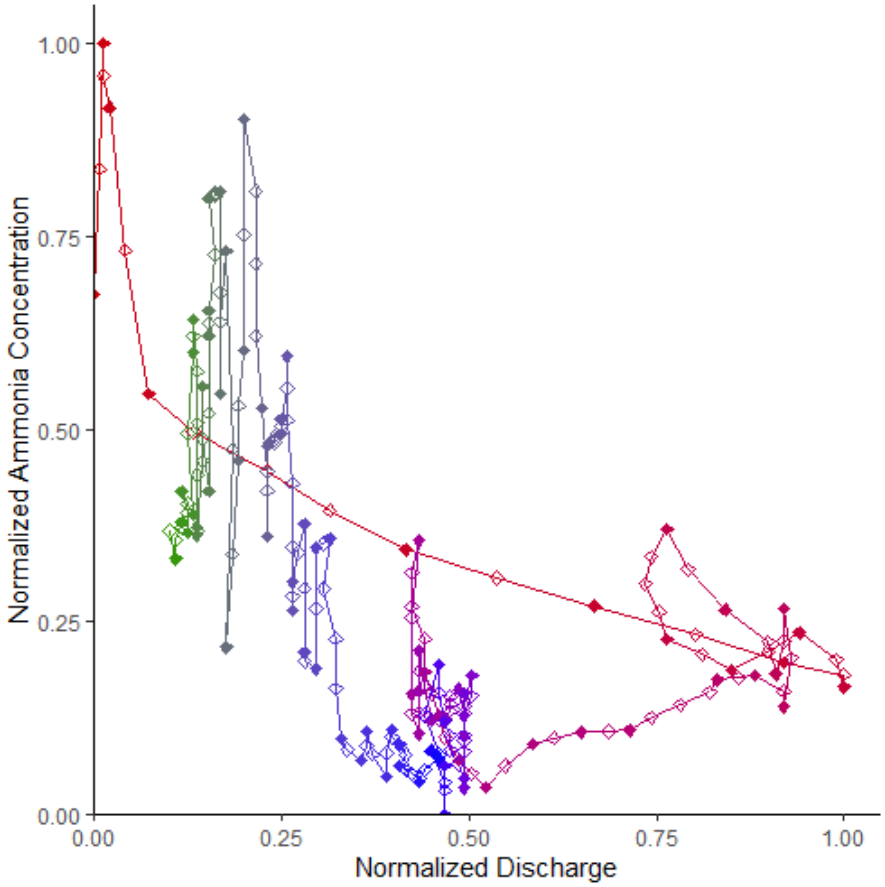

Figure 3.4. Normalized concentration-discharge (C-Q) plot for the River Lark at Fornham St. Martin, UK during storm event 1, 04 June 2021 to 06 June 2021. Time is indicated by line/diamond color, from red (start) to green (end). Open diamonds represent times for which discharge measurements were available, but concentration was interpolated.

The HI_{Qi} values (Figure 3.5; Table 3.2) were positive for nearly all discharge percentiles and the overall storm event HI_{mean} was 0.094, indicating very weak C-Q clockwise hysteresis. Positive HI_{Qi} values ranged from HI_{20} equal to 0.092, to HI_{60} equal to 0.252. However, HI_{80} was -0.298, indicating there was a significant component of weak anti-clockwise hysteresis. This was clearly indicated in the HI_{Qi}-Q_i plot, but not the HI_{mean}. Calculation of the absolute value hysteresis index for each direction component yielded HI_{abs} equal to 0.161, with HI_{abs+} equal to 0.128 and HI_{abs-} equal to 0.033, signifying that storm 1 exhibited weak figure-of-eight hysteresis with a majority clockwise direction.

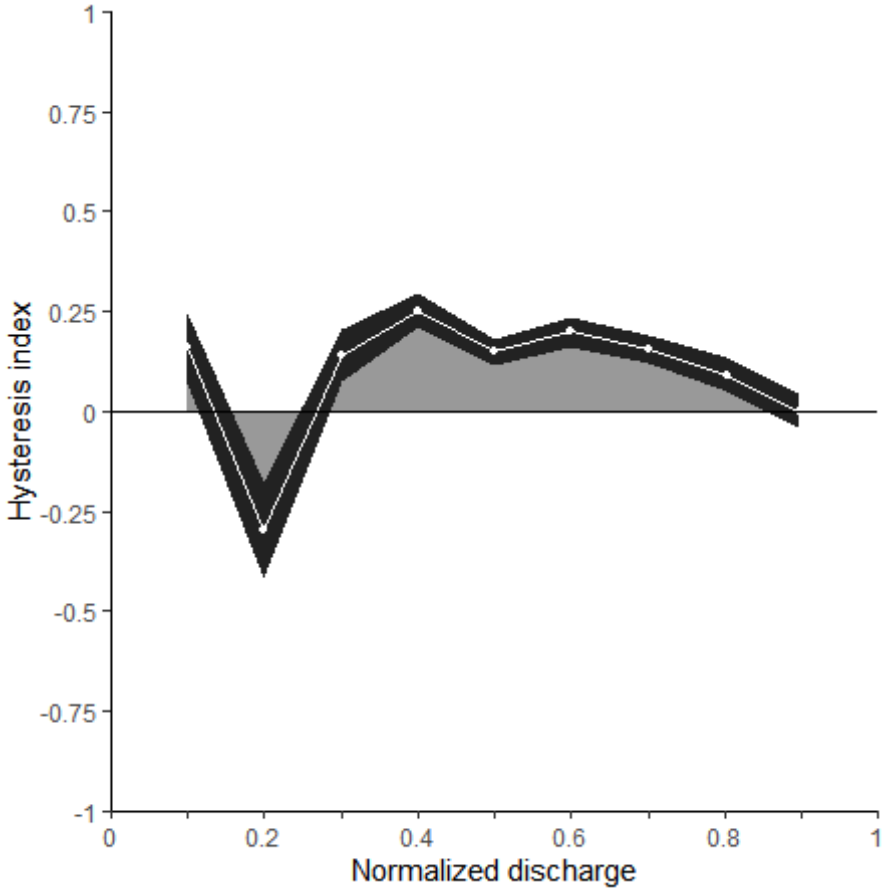

Figure 3.5 Hysteresis index (HI) values calculated at every 10th discharge percentile, as a function of normalized discharge of the River Lark at Fornham St. Martin, UK during storm event 1, 04 June 2021 to 06 June 2021. The dark shaded ribbon represents instrument error.

Table 3.2 Hysteresis index (HI_{Qi}) values, with instrument error, calculated using the difference in normalized concentration on the rising (C_{RL_Qi}) and falling (C_{FL_Qi}) hydrograph limbs at every 10th percentile of normalized discharge (Q_i) of the River Lark at Fornham St. Martin, UK during storm event 1, 04 June 2021 to 06 June 2021.

Q_i	C_{RL_Qi}	C_{FL_Qi}	HI_{Qi}	±SI
0.10	0.522	0.363	0.159	±0.089
0.20	0.459	0.910	-0.298	±0.122
0.30	0.399	0.340	0.139	±0.076
0.40	0.346	0.089	0.252	±0.044
0.50	0.312	0.041	0.149	±0.033
0.60	0.283	0.084	0.198	±0.037
0.70	0.254	0.097	0.157	±0.035
0.80	0.301	0.202	0.092	±0.043
0.90	0.216	0.203	0.002	±0.046

Storm event 2

Storm event 2 began at 02:30 GMT 18 June 2021 and ended at 07:30 GMT 21 June 2021 (Figure 3.6). It was the longest storm examined, lasting 3.2 days. It had five distinct discharge peaks. Similar to storm 1, discharge rose quickly in response to rainfall and there were multiple hydrograph peaks in response to the intermittent rainfall pattern throughout the storm. The third discharge peak had the maximum event discharge and occurred 45 minutes after the end of a brief, but intense, period of rainfall (Figure 3.6). The maximum event discharge of 0.80 m^3/s was between the 90th and 95th percentiles of gauged daily flow measured at Fornham St. Martin from 1985 – 2021 (NRFA c2022c).

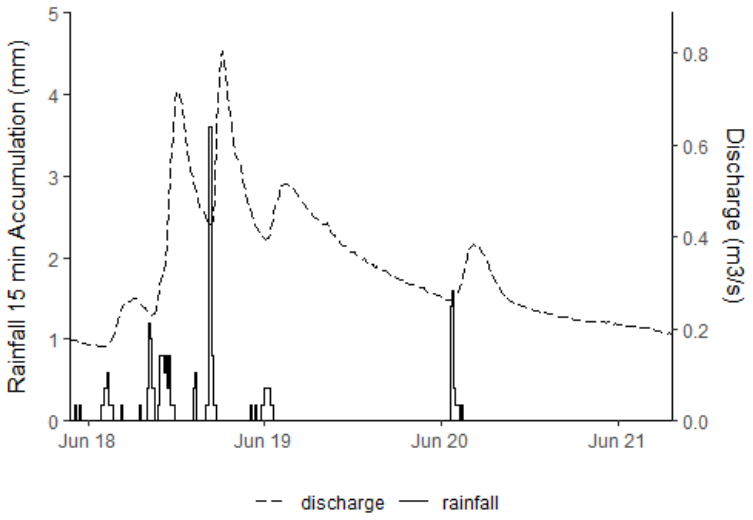

Figure 3.6. Discharge (m^3/s) of the River Lark at Fornham St. Martin, UK and rainfall (mm) at Rushbrooke, Bury St. Edmunds, UK during storm event 2, 18 June 2021 to 21 June 2021.

Ammonia concentration (Figure 3.7a) and instantaneous loads (Figure 3.7b) over the course of storm 2 were generally higher at the beginning and end than during the middle, indicating dilution. However, concentration and instantaneous loads both spiked at the beginning of the storm, which suggests brief flushing behavior. The maximum rate of ammonia export, 122.79 mg-N/s, occurred early in the event, but did not recover to near this level until discharge returned to near baseline indicating that flushing was not sustained, and *FI* was -0.19. Total export of ammonia during this storm was 16.85 kg-N, the largest amount observed across all five storm events studied.

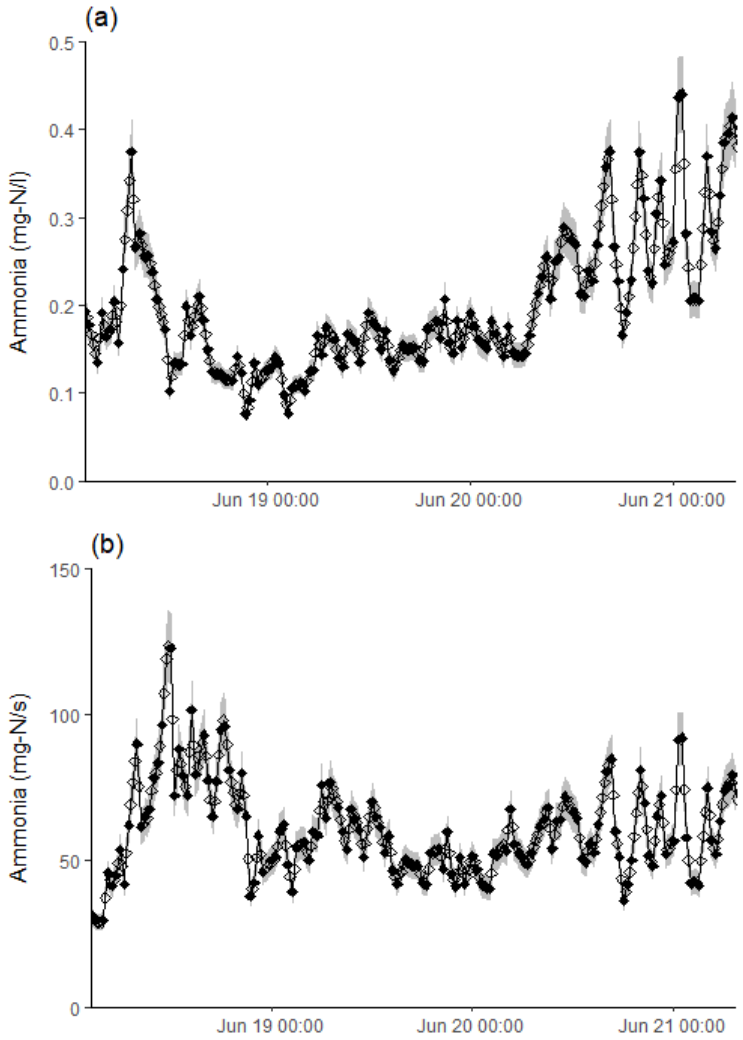

Figure 3.7. Ammonia concentration (mg-N/l, a) and instantaneous loads (mg-N/s, b) in the River Lark at Fornham St. Martin, UK during storm event 2, 18 June 2021 to 21 June 2021. Gray area indicates measurement precision (±10%). Open diamonds represent times for which discharge measurements were available, but concentration was interpolated.

The normalized ammonia C-Q plot (Figure 3.8) showed that storm event 2 clearly exhibited complex (figure-of-eight) hysteresis, as there were numerous points of intersection as discharge rose and fell (see Appendix B for plots of individual peaks). Discharge peak one exhibited incomplete anti-clockwise ammonia C-Q hysteresis, with normalized concentration remaining near 0.25 as discharge rose, then spiking to 0.75 on the first falling limb. Discharge peak two exhibited clockwise ammonia C-Q hysteresis after following a dilution curve along the rising limb, because concentration on the falling limb recovered to the near the midpoint of the rising limb after experiencing a sharp drop at peak discharge. Ammonia concentration followed a dilution curve over the third and largest discharge peak, interrupted by a brief dip on the latter half of the falling limb to the minimum concentration

observed during event 2, which created an anti-clockwise loop shape. Ammonia concentration fluctuated along a dilution curve during subsequent discharge peaks and exhibited no visually obvious hysteresis during the remainder of the storm.

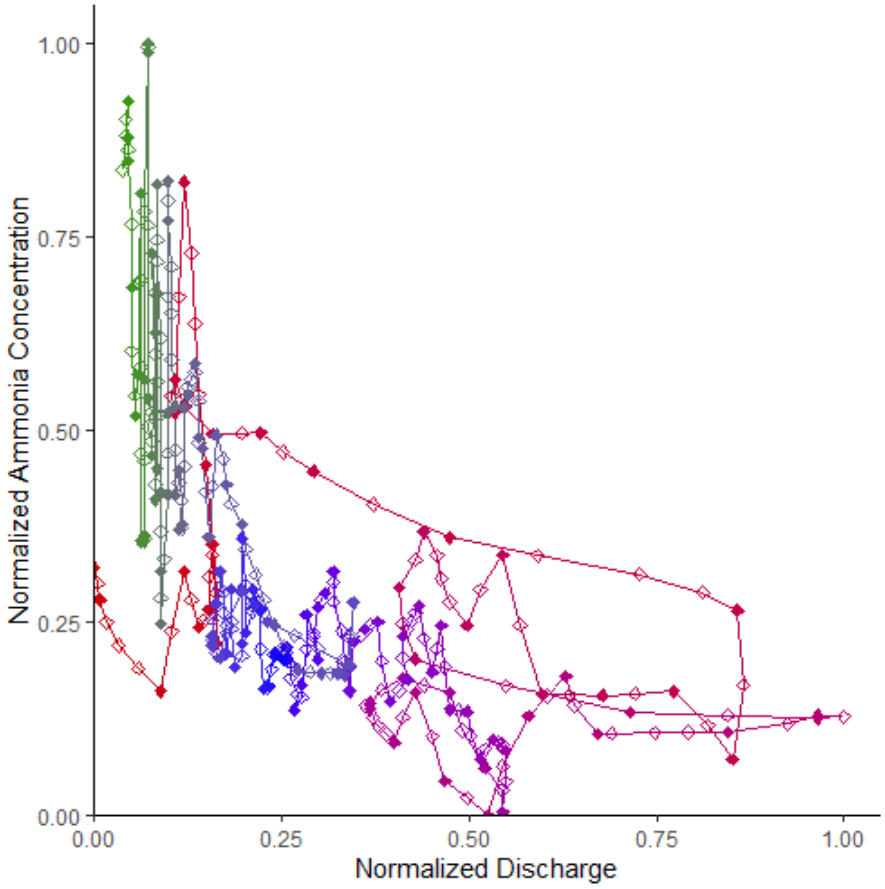

Figure 3.8. Normalized concentration-discharge (C-Q) plot for the River Lark at Fornham St. Martin, UK during storm event 2, 18 June 2021 to 21 June 2021. Time is indicated by line/diamond color, from red (start) to green (end). Open diamonds represent times for which discharge measurements were available, but concentration was interpolated.

The HI_{Qi}-Q_i plot for storm 2 (Figure 3.9) indicated there was a majority clockwise, figure-of-eight ammonia C-Q hysteresis. Moderate anti-clockwise hysteresis occurred at low discharge values, but was outnumbered by the weak clockwise hysteresis occurring at other discharge percentiles, leading to a positive HI_{mean}. The overall storm event two HI_{mean} of 0.051 indicated very weak C-Q clockwise hysteresis was present, as did most HI_{Qi} values (Table 3.3). However, HI_{90} was -0.251, which was the largest magnitude of hysteresis indicated by any value of HI_{Qi} for storm two and the strongest anti-clockwise behavior seen across all five storms. The HI_{abs} was 0.107, while the HI_{abs+} was 0.079, and HI_{abs-} was 0.028, which indicated weak figure-of-eight hysteresis with a majority clockwise direction.

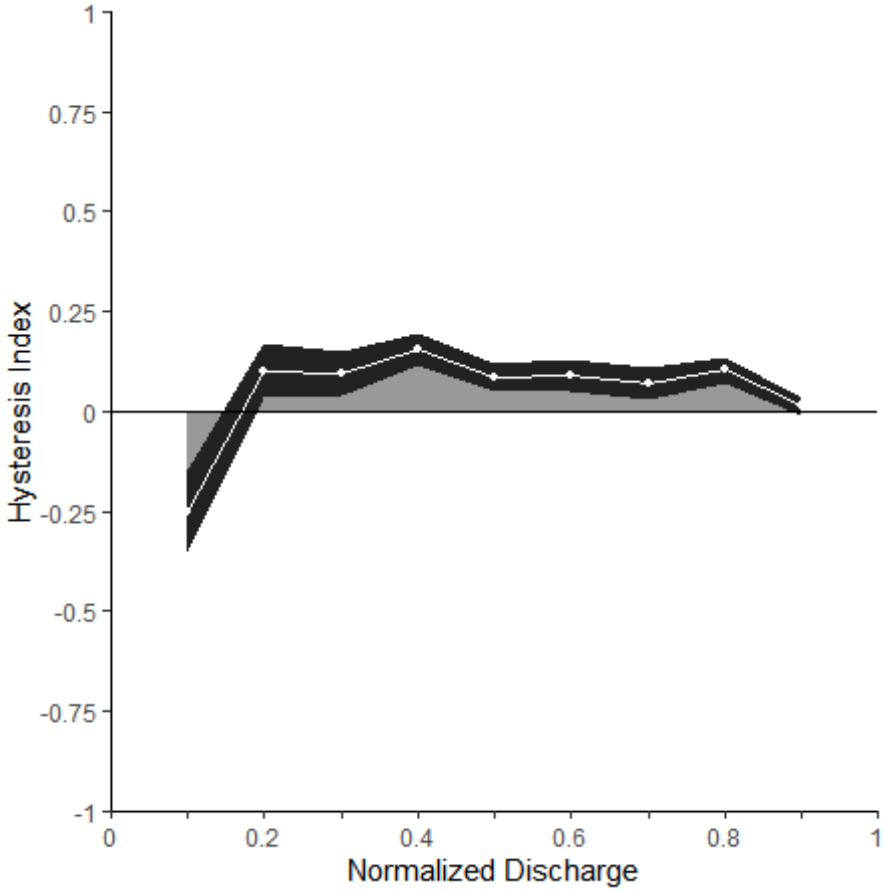

Figure 3.9 Hysteresis index (HI) values calculated at every 10th discharge percentile, as a function of normalized discharge of the River Lark at Fornham St. Martin, UK during storm event 2, 18 June 2021 to 21 June 2021. The dark shaded ribbon represents instrument error.

Table 3.3 Hysteresis index (HI_{Qi}) values, with instrument error (SI), calculated using the difference in normalized concentration on the rising (C_{RL_Qi}) and falling (C_{FL_Qi}) hydrograph limbs at every 10th percentile of normalized discharge (Q_i) of the River Lark at Fornham St. Martin, UK during storm event 2, 18 June 2021 to 21 June 2021.

Q_i	C_{RL_Qi}	C_{FL_Qi}	HI_{Qi}	±SI
0.10	0.391	0.642	-0.251	±0.103
0.20	0.393	0.292	0.101	±0.068
0.30	0.329	0.233	0.096	±0.056
0.40	0.281	0.124	0.157	±0.041
0.50	0.211	0.127	0.084	±0.034
0.60	0.246	0.156	0.090	±0.040
0.70	0.227	0.157	0.070	±0.038
0.80	0.212	0.108	0.104	±0.032
0.90	0.128	0.116	0.012	±0.024

Storm event 3

Storm event 3 began at 01:15 GMT 28 June 2021 and ended at 12:15 GMT 28 June 2021, lasting 0.46 days (11 h). It had one distinct discharge peak (Figure 3.10). Discharge initially increased very gradually, then rose rapidly after a short-duration (1.25 h) rainstorm. The maximum event discharge of 0.36 m^3/s was between the 50th and 90th percentiles of gauged daily flow measured at Fornham St. Martin from 1985 – 2021 (NRFA c2022c). Return to baseflow conditions occurred only slightly slower than rise, likely owing to the relatively small accumulation and duration of rain which produced a subsequently small-magnitude discharge response.

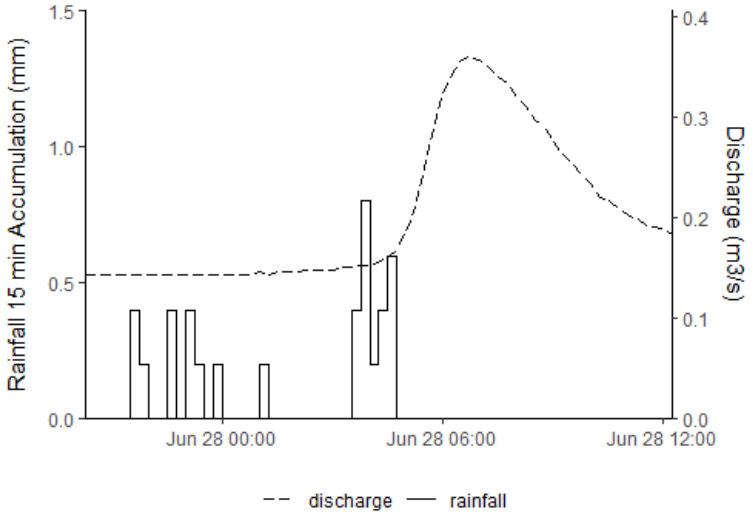

Figure 3.10. Discharge (m^3/s) of the River Lark at Fornham St. Martin, UK and rainfall (mm) at Rushbrooke, Bury St. Edmunds, UK during storm event 3, 28 June 2021.

Ammonia concentration (Figure 3.11a) on the rising limb of the storm event 3 hydrograph initially rose rapidly and remained high until discharge peaked sharply. Instantaneous ammonia loads (Figure 3.11b) spiked at the beginning of the event following the same trajectory as concentration but remained steady over the remainder of the storm, until both concentration and load spiked again at the end of the falling limb. The overall shape of both plots (Figure 3.11a-b) indicates dilution was the dominant mechanism controlling ammonia concentration changes during storm event 3. This general concentration-discharge trend was described well by *FI* = -0.037. The total ammonia exported over the course of storm three was 2.52 kg-N, the lowest of the five storms studied.

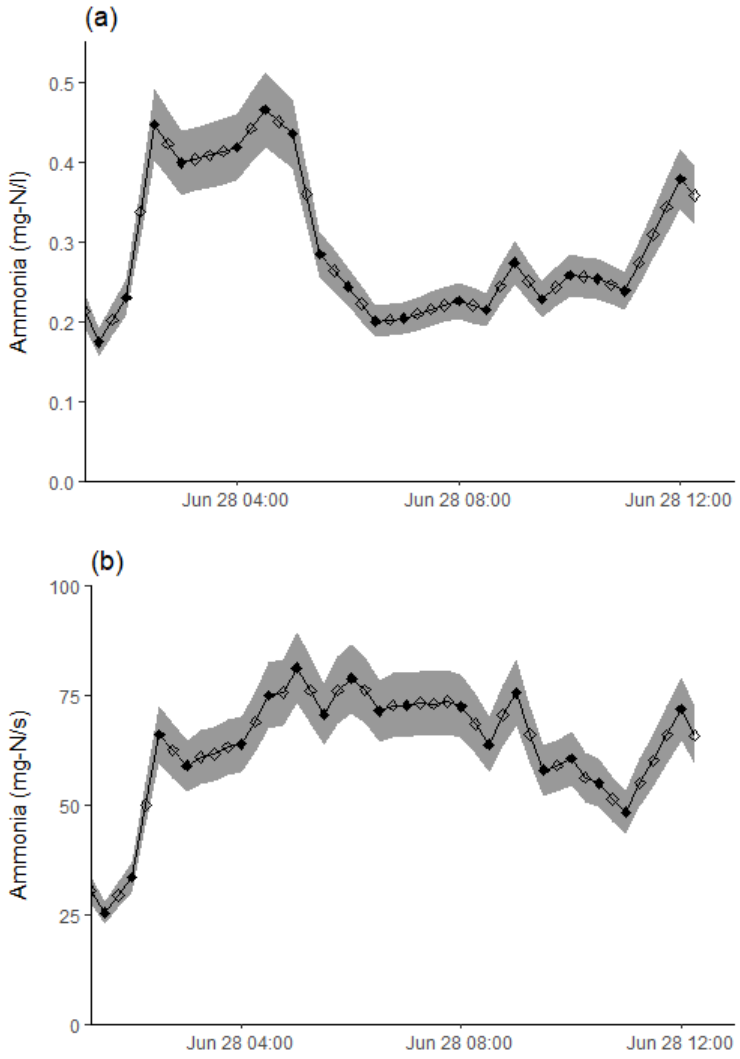

Figure 3.11. Ammonia concentration (mg-N/l, a) and instantaneous loads (mg-N/s, b) in the River Lark at Fornham St. Martin, UK during storm event 3, 28 June 2021. Gray area indicates measurement precision (±10%). Open diamonds represent times for which discharge measurements were available, but concentration was interpolated.

The normalized ammonia C-Q plot (Figure 3.12) showed that storm event 3 exhibited weak clockwise ammonia concentration-discharge hysteresis. The C-Q loop was very thin, with concentration on the rising and falling limbs converging to no significant hysteresis near peak discharge. The overall plot also trended downward, as described by the negative value of *FI* (-0.037). However, the rise in concentration at the end of the falling limb, which occurred without an associated change in discharge volume, could represent mobilization of nutrient sources from upstream which lagged peak discharge.

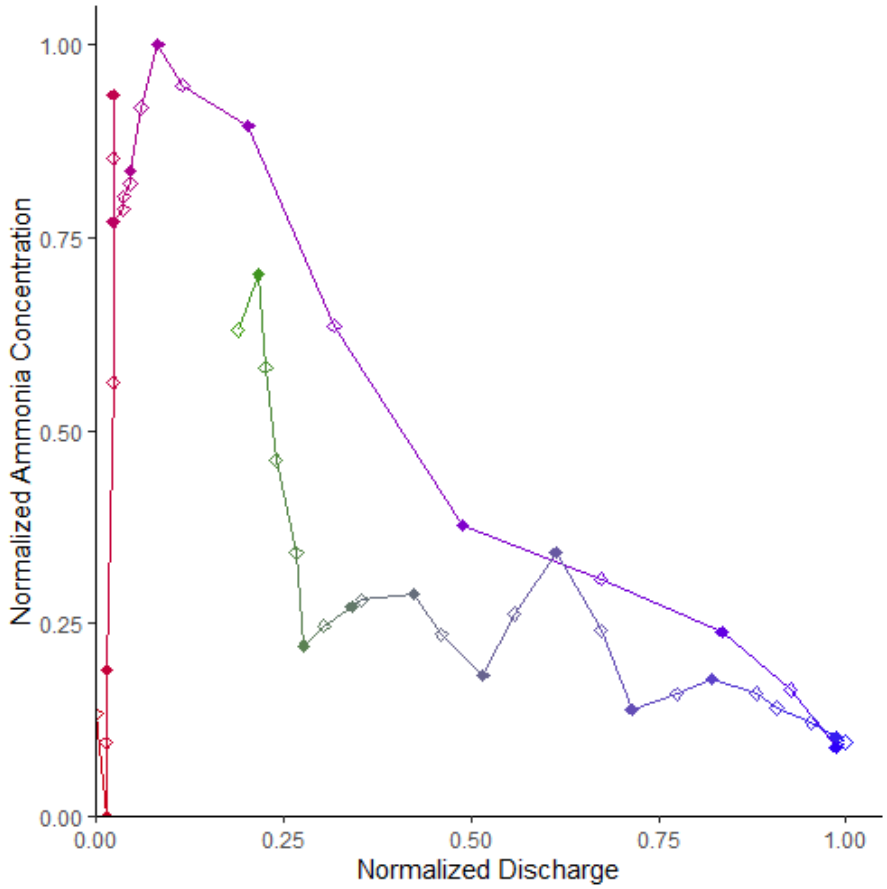

Figure 3.12. Normalized concentration-discharge (C-Q) plot for the River Lark at Fornham St. Martin, UK during storm event 3, 28 June 2021. Time is indicated by line/diamond color, from red (start) to green (end). Open diamonds represent times for which discharge measurements were available, but concentration was interpolated.

The HI_{Qi}-Q_i plot for storm 3 (Figure 3.13) showed that the degree of ammonia C-Q hysteresis was strongest at high discharge percentiles. The plot approached zero at Q_{40} and was also weak near peak discharge. Because there was only one direction of C-Q hysteresis, HI_{mean} and HI_{abs} did not differ, equaling 0.170. The positive value indicates the storm exhibited simple clockwise ammonia C-Q hysteresis. Every HI_{Qi} value (Table 3.4) calculated except HI_{40} was significantly different from zero once datasonde measurement error was considered. The highest value, 0.430, occurred at Q_{70} and signifies that the lower concentration on the falling limb compared to the rising limb resulted in moderate ammonia concentration-discharge hysteresis.

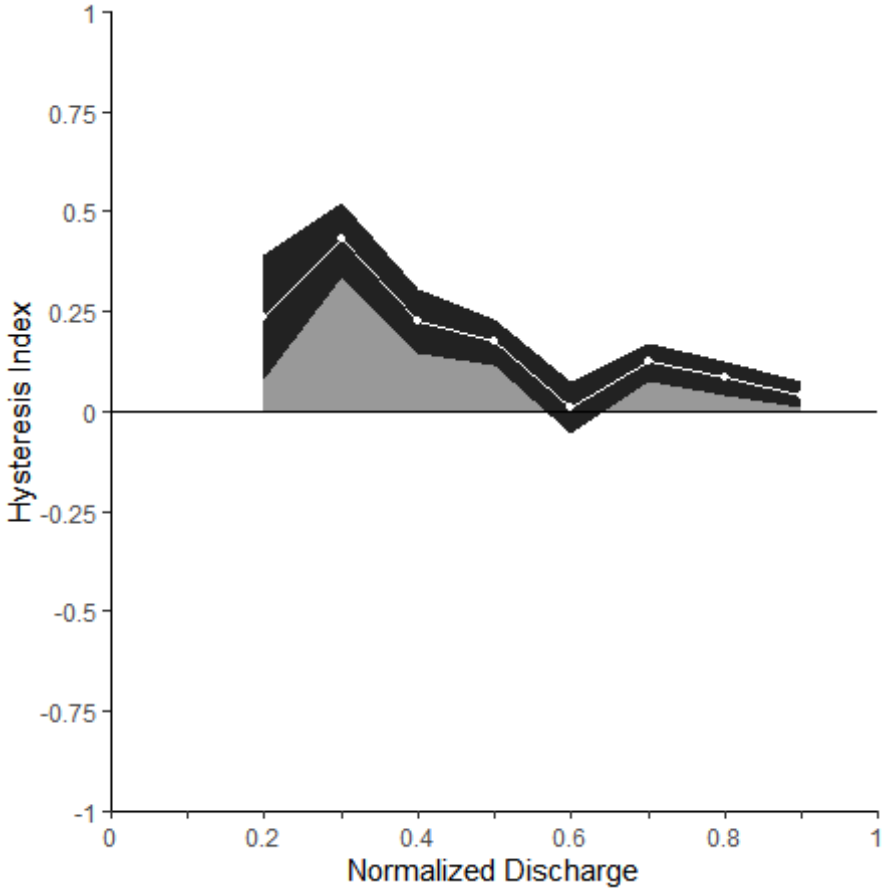

Figure 3.13 Hysteresis index (HI) values calculated at every 10th discharge percentile, as a function of normalized discharge of the River Lark at Fornham St. Martin, UK during storm event 3, 28 June 2021. The dark shaded ribbon represents instrument error.

Table 3.4 Hysteresis index (HI_{Qi}) values, with instrument error, calculated using the difference in normalized concentration on the rising (C_{RL_Qi}) and falling (C_{FL_Qi}) hydrograph limbs at every 10th percentile of normalized discharge (Q_i) of the River Lark at Fornham St. Martin, UK during storm event 3, 28 June 2021.

Qi	C_{RL_Qi}	C_{FL_Qi}	HI_{Qi}	$\pm SI$
0.20	0.895	0.659	0.236	±0.155
0.30	0.676	0.247	0.430	±0.092
0.40	0.511	0.247	0.226	±0.076
0.50	0.373	0.198	0.174	±0.057
0.60	0.335	0.324	0.011	±0.066
0.70	0.296	0.173	0.123	±0.047
0.80	0.253	0.169	0.084	±0.042
0.90	0.185	0.146	0.040	±0.033

Storm event 4

Storm event 4 began at 12:30 GMT 04 July 2021 and ended at 00:45 GMT 05 July 2021. It was the briefest storm studied, lasting 0.51 days (12.25 h). It had one distinct discharge peak (Figure 3.14) which reached 0.68 m^3/s. This was between the 50th and 90th percentiles of gauged daily flow measured at Fornham St. Martin from 1985 – 2021 (NRFA c2022c). Discharge increased rapidly in response to brief, but intense rainfall. Return to baseflow conditions from peak discharge occurred slower than rise and the baseflow was also boosted slightly by the influx of rainwater.

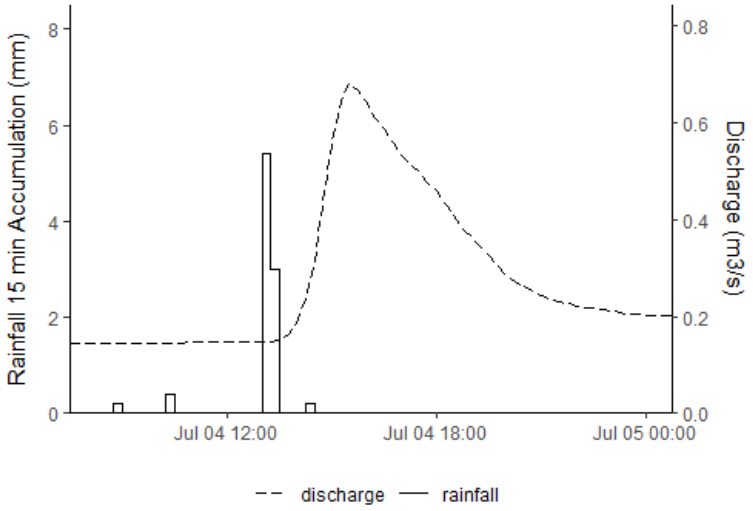

Figure 3.14. Discharge (m^3/s) of the River Lark at Fornham St. Martin, UK and rainfall (mm) at Rushbrooke, Bury St. Edmunds, UK during storm event 4, 04 to 05 July 2021.

Ammonia concentration (Figure 3.15a) was inversely related to discharge during storm event 4, following a dilution curve. Minimum concentration occurred just after peak discharge. Instantaneous ammonia loads (Figure 3.15b) spiked in response to rapidly increasing discharge, then quickly declined, outpacing hydrograph recession. The total ammonia exported was 3.54 kg-N. There was a minor pulse of ammonia concentration and load on the falling limb, which may represent delayed delivery of nutrients from diffuse upstream sources. However, the general shape of both plots (Figure 3.15a-b) was well-described by the *FI* of -0.669, indicating dilution was a dominant mechanism contributing to changes in ammonia concentration during the storm.

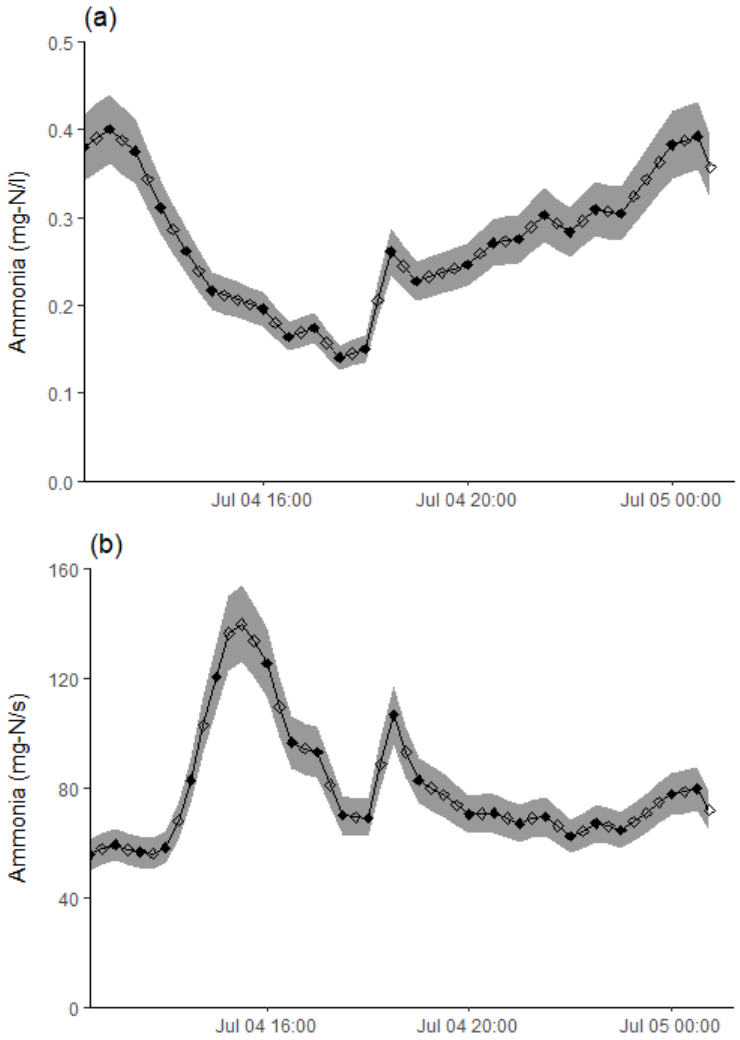

Figure 3.15. Ammonia concentration (mg-N/l, a) and instantaneous loads (mg-N/s, b) in the River Lark at Fornham St. Martin, UK during storm event 4, 04 to 05 July 2021. Gray area indicates measurement precision (±10%). Open diamonds represent times for which discharge measurements were available, but concentration was interpolated.

The normalized ammonia C-Q plot (Figure 3.16) showed that storm event four exhibited weak clockwise ammonia concentration-discharge hysteresis. Concentration trended downward as discharge rose, as indicated by the strongly negative event *FI* value. As storm discharge receded, ammonia concentration did not rebound until an abrupt rise in concentration occurred mid-falling limb. This concentration spike closed the small clockwise hysteresis loop above Q_{50} and could represent mobilization of nutrient sources from upstream which lagged peak discharge due to transit time. The downward slope of the C-Q loop signified that concentration changes until this point were primarily dilution-driven. Combined with the clockwise loop direction, this suggested that close-proximity or in-channel ammonia sources were becoming depleted by storm discharge.

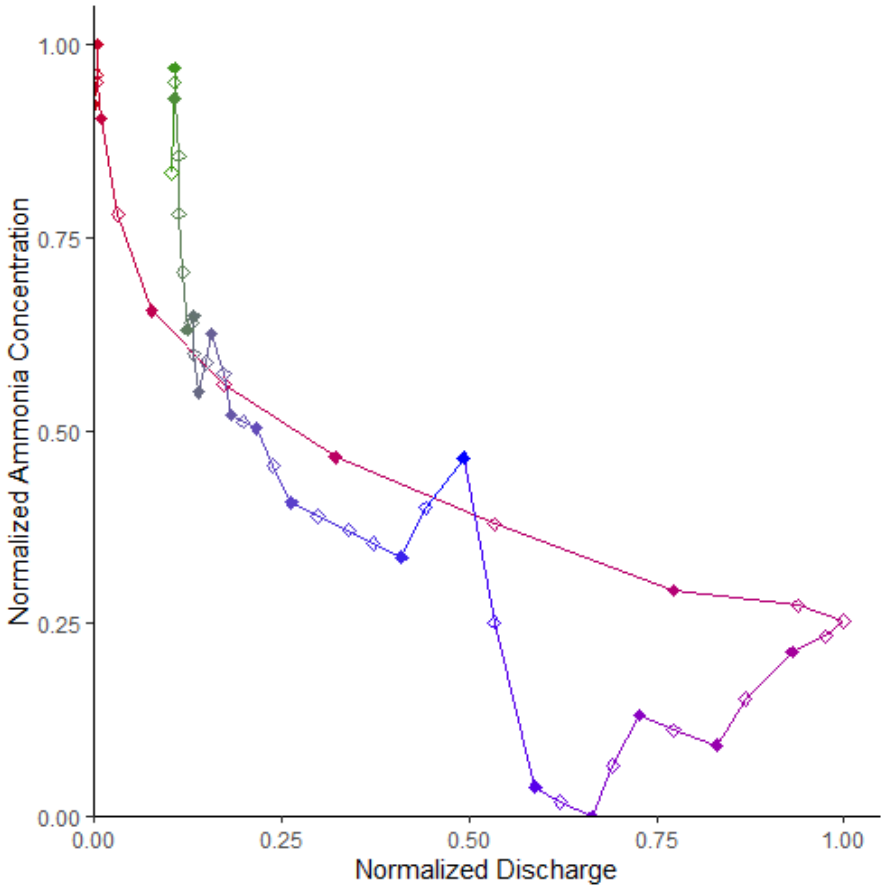

Figure 3.16. Normalized concentration-discharge (C-Q) plot for the River Lark at Fornham St. Martin, UK during storm event 4, 04 to 05 July 2021. Time is indicated by line/diamond color, from red (start) to green (end). Open diamonds represent times for which discharge measurements were available, but concentration was interpolated.

The HI_{Qi}-Q_i plot (Figure 3.17) indicated that storm 4 exhibited a degree of figure-of-eight ammonia C-Q hysteresis, but once datasonde measurement accuracy was considered, the pattern was determined to be overwhelmingly clockwise with HI_{abs-} near zero. The HI_{Qi} values (Table 3.5) which differed from zero were all positive or less than -0.10. Owing to the large degree of instrument uncertainty present from Q_{50} to Q_{90}, HI_{mean} and HI_{abs} did not significantly differ, equaling 0.091 and 0.113, respectively. The largest degree of hysteresis occurred at the 60th discharge percentile, where HI_{60} equaled 0.324.

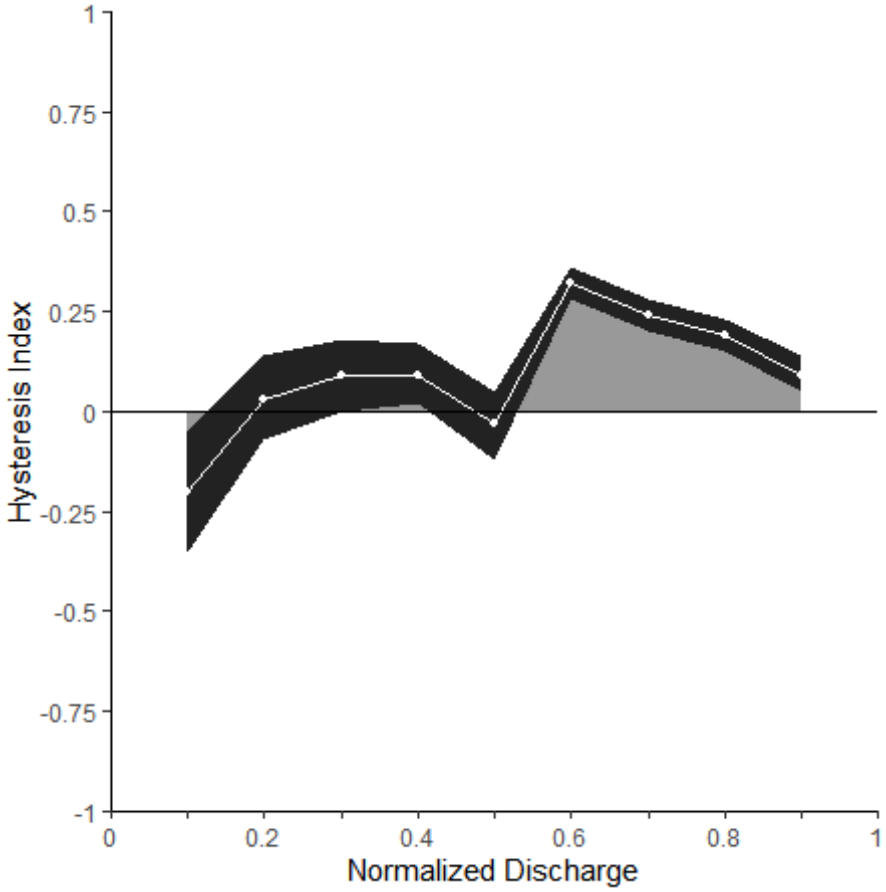

Figure 3.17 Hysteresis index (HI) values calculated at every 10th discharge percentile, as a function of normalized discharge of the River Lark at Fornham St. Martin, UK during storm event 4, 04 to 05 July 2021. The dark shaded ribbon represents instrument error.

Table 3.5 Hysteresis index (HI_{Qi}) values, with instrument error, calculated using the difference in normalized concentration on the rising (C_{RL_Qi}) and falling (C_{FL_Qi}) hydrograph limbs at every 10th percentile of normalized discharge (Q_i) of the River Lark at Fornham St. Martin, UK during storm event 4, 04 to 05 July 2021.

Q_i	C_{RL_Qi}	C_{FL_Qi}	HI_{Qi}	±SI
0.10	0.633	0.834	-0.202	±0.147
0.20	0.543	0.511	0.031	±0.105
0.30	0.479	0.389	0.090	±0.087
0.40	0.433	0.340	0.093	±0.077
0.50	0.393	0.426	-0.033	±0.082
0.60	0.355	0.031	0.324	±0.039
0.70	0.319	0.081	0.238	±0.040
0.80	0.290	0.102	0.187	±0.039
0.90	0.278	0.183	0.094	±0.046

Storm event 5

Storm event 5 began at 23:15 GMT 05 July 2021 and ended at 22:00 GMT 07 July 2021, lasting 1.91 days. It had two distinct discharge peaks (Figure 3.18). The maximum event discharge of 0.61 m^3/s, reached on the first peak, was between the 50th and 90th percentiles of gauged daily flow measured at Fornham St. Martin from 1985 – 2021 (NRFA c2022c). Rainfall was discontinuous over the course of the event, but both discharge peaks showed rapid response to rainfall exceeding one millimeter. A third period of rainfall occurred between both peaks, but discharge was only slightly boosted, forming a gentle crest in the hydrograph that was not large enough to be considered a third peak. Return to baseflow conditions from the second discharge peak occurred much more slowly than the rise.

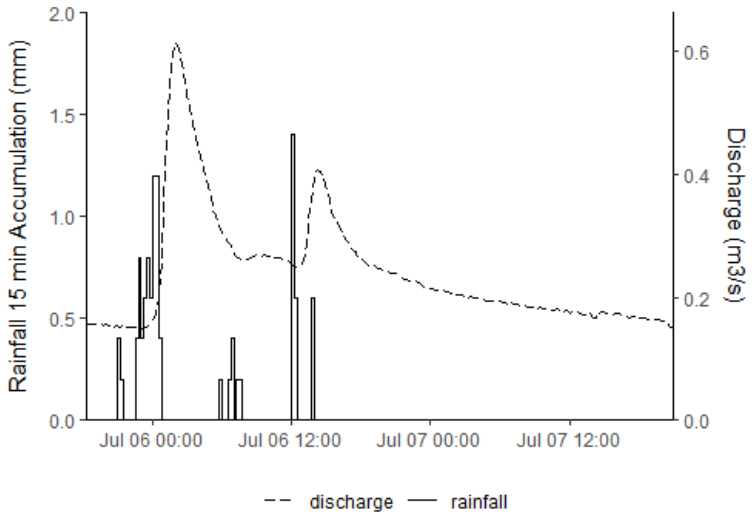

Figure 3.18. Discharge (m^3/s) of the River Lark at Fornham St. Martin, UK and rainfall (mm) at Rushbrooke, Bury St. Edmunds, UK during storm event 5, 05 to 07 July 2021.

Ammonia concentration (Figure 3.19a) and instantaneous loads (Figure 3.19b) were tightly coupled during storm event 5 and exhibited dilution behavior for the majority of the event. The *FI* of -0.683 was calculated using only the first, and largest, discharge peak, and appeared to describe ammonia concentration on the rising limb well. However, as discharge rose a second time, around 12:00 GMT on 06 July, ammonia concentration briefly peaked, though not to a level near as high as at before the storm or on the second receding limb. Concentration and instantaneous loads gradually increased as discharge returned to near the same level as before the second rising limb, then abruptly decreased at 10:30 GMT 07

July to the lowest levels observed during the storm event. The total ammonia exported over the course of storm event 5 was 8.98 kg-N.

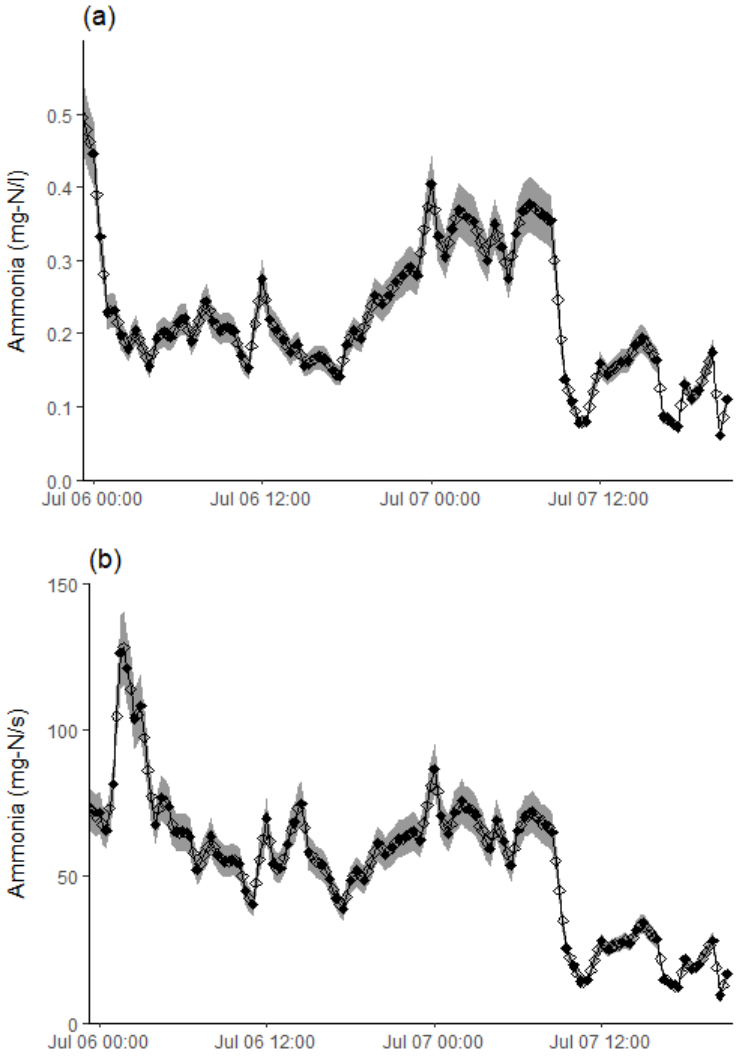

Figure 3.19. Ammonia concentration (mg-N/l, a) and instantaneous loads (mg-N/s, b) in the River Lark at Fornham St. Martin, UK during storm event 5, 05 to 07 July 2021. Gray area indicates measurement precision (±10%). Open diamonds represent times for which discharge measurements were available, but concentration was interpolated.

The normalized ammonia C-Q plot (Figure 3.20) showed that storm event 5 exhibited weak clockwise ammonia concentration-discharge hysteresis. There were two distinct clockwise loops, each associated with a discharge peak. The downward slope of both C-Q loops signifies that concentration changes were primarily dilution-driven. However, there was a brief spike in ammonia concentration on the falling limb near Q_{80}, followed by an abrupt

crash to the lowest levels of the storm event. See Appendix B for C-Q plots of each discharge peak.

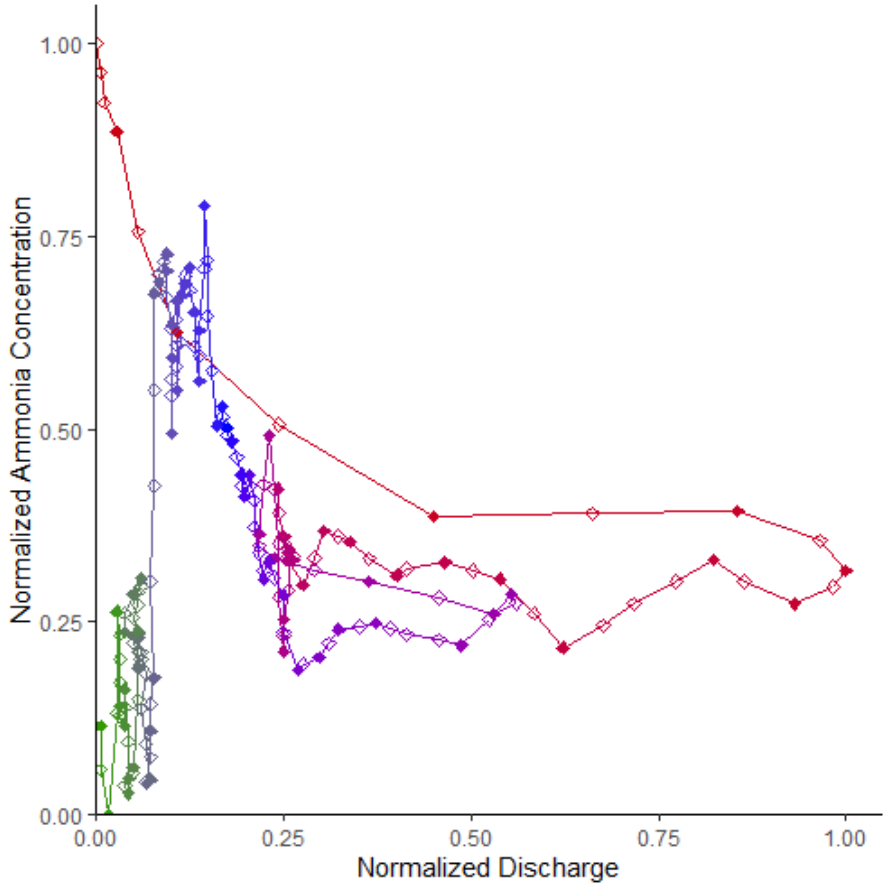

Figure 3.20. Normalized concentration-discharge (C-Q) plot for the River Lark at Fornham St. Martin, UK during storm event 5, to 05 to 07 July 2021. Time is indicated by line/diamond color, from red (start) to green (end). Open diamonds represent times for which discharge measurements were available, but concentration was interpolated.

The HI_{Qi}-Q_i plot for storm 5 (Figure 3.21) showed that HI_{Qi} was positive for the entire range of discharge for which it was calculated, the 10th to 90th percentiles. Therefore, HI_{mean} and HI_{abs} both equaled 0.097, indicating weak clockwise ammonia C-Q hysteresis. The HI_{Qi} values (Table 3.6) varied little, but were highest at Q_{40}, at 0.147, and approached zero at Q_{90} once datasonde measurement error was considered.

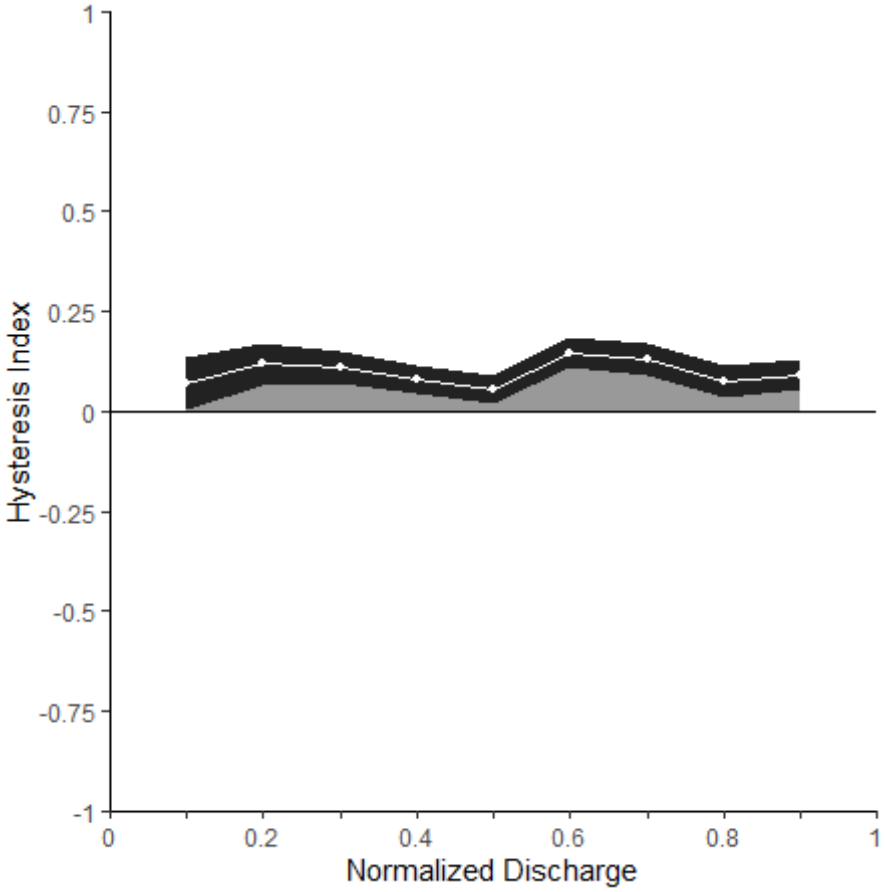

Figure 3.21 Hysteresis index (HI) values calculated at every 10th discharge percentile, as a function of normalized discharge of the River Lark at Fornham St. Martin, UK during storm event 5, 05 to 07 July 2021. The dark shaded ribbon represents instrument error.

Table 3.6 Hysteresis index (HI_{Qi}) values, with instrument error, calculated using the difference in normalized concentration on the rising (C_{RL_Qi}) and falling (C_{FL_Qi}) hydrograph limbs at every 10th percentile of normalized discharge (Q_i) of the River Lark at Fornham St. Martin, UK during storm event 5, 05 to 07 July 2021.

Q_i	C_{RL_Qi}	C_{FL_Qi}	HI_{Qi}	±SI
0.10	0.645	0.577	0.069	±0.065
0.20	0.545	0.426	0.118	±0.054
0.30	0.395	0.286	0.109	±0.039
0.40	0.355	0.274	0.081	±0.036
0.50	0.328	0.274	0.055	±0.033
0.60	0.389	0.243	0.147	±0.039
0.70	0.391	0.261	0.130	±0.039
0.80	0.393	0.317	0.076	±0.039
0.90	0.378	0.286	0.092	±0.038

Contextualization of ammonia C-Q hysteresis

The Shapiro-Wilk p-values of storms 1 and 2 were less than 0.05, while the remaining storms exceeded this alpha-value (α) threshold and were considered approximately normal distributions. The distributions of HI_{Qi} values for storms 1 and 2 did not appear approximately normal, unlike storms 3 to 5. Because storms 1 and 2 were the only storms which had an $HI_{Qi} < -0.100$, their distinctly different HI_{Qi} distributions compared to the other storms was considered confirmation that storms 1 and 2 exhibited significant figure-of-eight C-Q hysteresis. Therefore, storms 1 and 2 were grouped for Kruskal-Wallis testing of the distribution of HI_{Qi} values, while storms 3 to 5 were grouped for ANOVA testing. The Kruskal-Wallis p-value of 0.4335 indicated there was no significant difference in hysteretic C-Q behavior between storms 1 and 2. ANOVA of the HI_{Qi} distributions for storms 3 to 5 produced similar results, a p-value of 0.38, which indicated there was no significant difference among the clockwise C-Q hysteresis patterns observed.

Stepwise regression of event-scale context metrics

Because the HI_{Qi} distributions of all five storms could not be compared simultaneously, the overall event ammonia C-Q hysteresis index values and flushing index values were plotted (Figure 3.22). Based on instrument sensitivity, there was no difference amongst the four event-scale hysteresis index values. However, there was an apparent difference in the C-Q loop directional components between storm events.

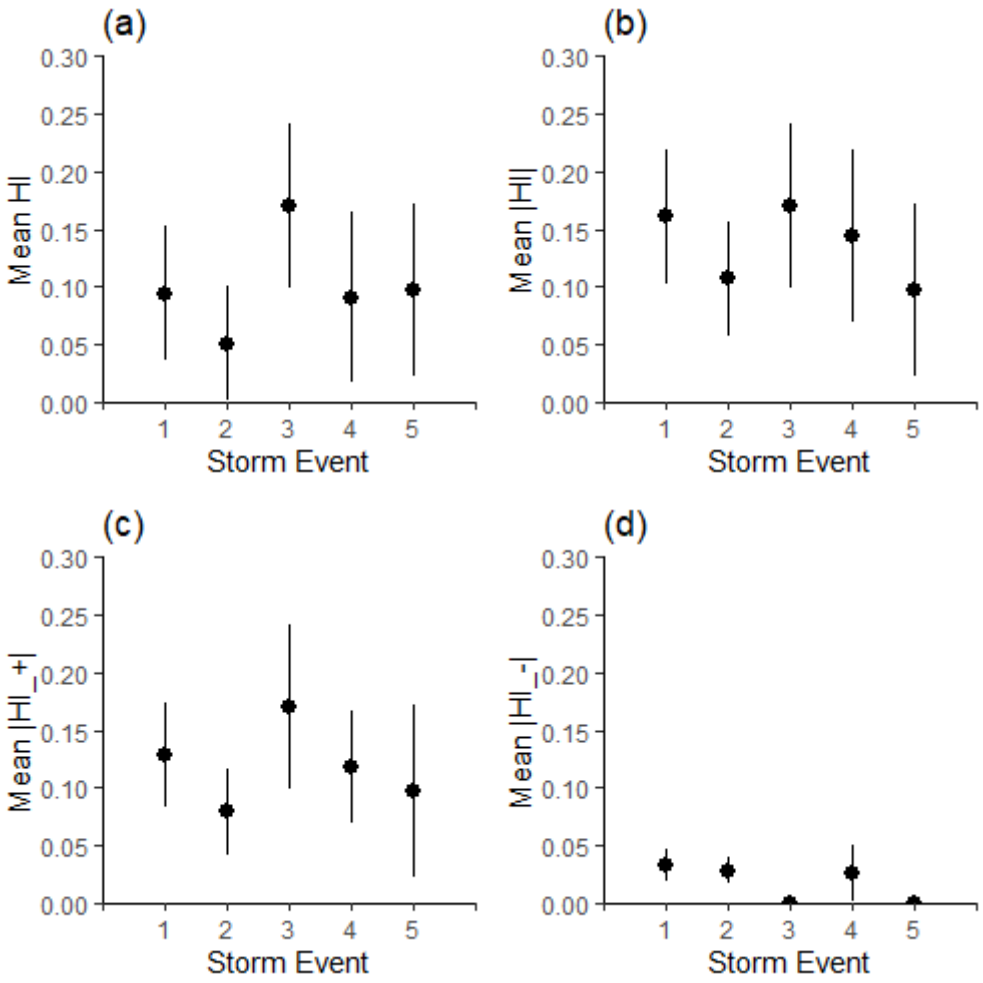

Figure 3.22 Distributions of event-scale ammonia C-Q hysteresis index values calculated for five storm discharge events in the River Lark at Fornham St. Martin, UK, June to July 2021. From top left are HI_{mean} (a), HI_{abs} (b), HI_{abs+} (c), and HI_{abs-} (d), with bars indicating instrument measurement accuracy.

Significant inverse relationships were found between total event rainfall and HI_{mean} (p = 0.047; R^2 = 0.707) and between event discharge range and HI_{mean} (p = 0.015; R^2 = 0.862) via linear model fits, so these metrics were combined for multiple regression. This marginally improved the model fit (R^2 = 0.880), but the p-value (p = 0.060) exceeded the significance threshold. A possible interfering relationship between event discharge range and total event rainfall was also explored via linear regression but was not detected (p = 0.103; R^2 = 0.523). Storms 1 and 2 had the highest rainfall and also the lowest HI_{mean} values (Figure 3.23a).

No significant relationships were found for *FI* or HI_{abs} with any of the three hydrological context metrics. However, the directional components of HI_{abs} did have significant relationships with context metrics. The absolute value mean negative hysteresis index, HI_{abs-}, was the only index for which a significant relationship was found with API (p = 0.020; R^2 = 0.830). For HI_{abs+}, the only significant relationship was with the event discharge range (p = 0.021; R^2 = 0.823).

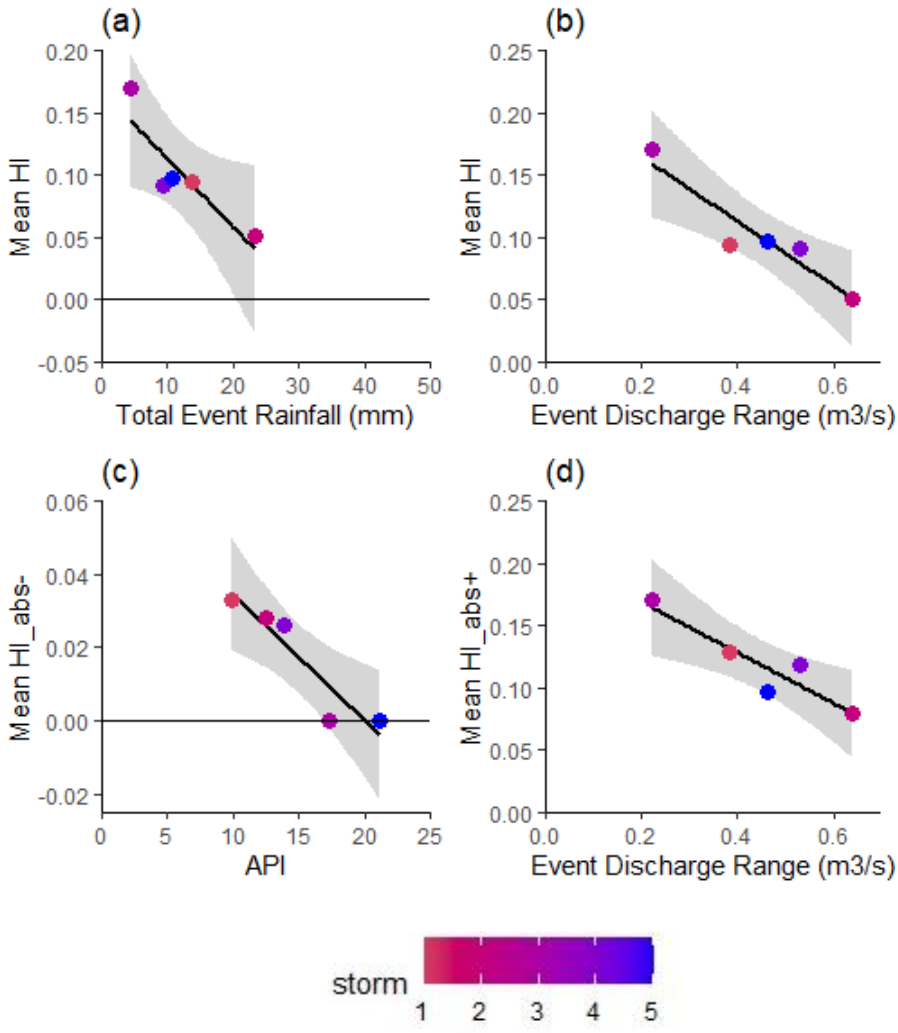

Figure 3.23 Event-scale ammonia C-Q hysteresis index values calculated for five storm discharge events in the River Lark at Fornham St. Martin, UK, June to July 2021, plotted as functions of select hydrological metrics with significant relationship. From top left are HI_{mean} as a function of total event rainfall (a), (b), HI_{mean} as a function of event discharge range, HI_{abs-} as a function of antecedent precipitation index (API) (c), and HI_{abs+} as a function of event discharge range (d). The grey area represents the 95% confidence interval of the linear regression.

Chapter 4: Discussion

Implications of ammonia C-Q patterns observed in the River Lark

The hysteresis index values indicate that changes in ammonia concentration were chiefly driven by dilution of close-proximity sources during growing-season stormflow events in the River Lark. While concentration-discharge hysteresis was not strongly pronounced, the predominant pattern observed was higher concentration on the rising limb than on the falling limb of the storm hydrograph. This indicates the dominant source of ammonia in the stormflow was located close to the monitoring point at Fornham All Saints (Bowes et al. 2015). Three of the five storms studied exhibited this clockwise ammonia C-Q hysteresis pattern exclusively. The remaining two storms exhibited significant anti-clockwise behavior at higher storm discharge percentiles, but majority clockwise hysteresis which resulted in $HI_{abs+} > HI_{abs-}$ and positive HI_{mean}. Mihiranga et al. (2021) found the same dominance of clockwise hysteresis for ammonia concentration but also noted that storms with large discharge peaks had the largest HI_{mean} values. This contrasts with the inverse relationship that was determined for the storms in this study. However, the storm with the most prominent discharge peak had the smallest HI_{mean} due in part to displaying significant anti-clockwise C-Q hysteresis, which pulled down the average of the HI_{Qi} values. Flushing index values were negative for all events, indicating dilution strongly influenced the overall trends in ammonia concentration as discharge rose (Vaughan et al. 2017).

The low discharge volumes of the Lark during the growing season likely contributed to the dilution-dominant, clockwise ammonia C-Q hysteresis patterns observed. During summer, evapotranspiration exceeds rainfall, and irrigation abstraction increases, lowering the baseflow contribution from the chalk aquifer (Barker 1992). Overland flow contributions of ammonia during the study period may have been limited by a strong negative soil water potential gradient driven by increased vegetation cover in agricultural areas of the upper catchment. Ammonia-containing runoff could have also been intercepted by macrophyte growth along the channel (Aich et al. 2014), which becomes seasonally very dense. However, effluent discharges from the Fornham All Saints STW and other treatment plants in the upper Lark catchment delivered near-constant ammonia, which is likely to have driven the C-Q relationships observed in June and July (Bowes et al. 2015). Bowes et al. (2015) described the dominance of clockwise nutrient C-Q hysteresis in the River Enborne at a

point with similar baseflow index (0.54) to the Lark at Fornham St. Martin and where the upper portion of the chalk aquifer is also overlain by clay. The decrease in concentration in response to rainfall was considered a strong indicator that the major nutrient source was a constant input and likely to be a STW upstream of the monitoring point (Bowes et al. 2015).

The short-lived spikes in ammonia concentration observed at the beginning of storms 1 through 3 were not large enough to produce positive *FI* values but also may have been sewage related. The relatively short duration and total amount of rain that fell during storm event 3 may have been sufficient to only mobilize very proximate sources, resulting in the initial spike in ammonia concentration that was exhausted as discharge rose. Holzer (1998) described the "wash-out effect" of sewers, which mobilizes concentrated sewage at the start of a stormflow event, rapidly delivering a wave of high ammonia content water to the river. Wash-out of misconnected surface outfalls upstream of Fornham All Saints could therefore have caused these brief jolts of ammonia concentration seen shortly after the storms began. Alternatively, near-channel septic systems could have caused a similar change in concentration (e.g., Bowes et al. 2015), but this pathway would not be expected to deliver ammonia quite as rapidly because of the slower rate of flow through the soil as compared to the surface.

Storms 1 and 2 had the highest rainfall and the lowest HI_{mean} values. However, the HI_{mean} values of these storms were depressed by the significant negative HI_{Qi} values that were calculated near the storm hydrograph tails, as indicated by the increased HI_{abs} values. While the sample size was too small to develop a definitive relationship, these results indicated that large amounts of event rainfall could drive increased late-storm nutrient delivery. Anti-clockwise C-Q hysteresis indicates the nutrient source was not close to the study site (Bowes et al. 2015), but it is unclear whether this pattern resulted from the accumulation of diffuse nutrient sources throughout the catchment, or from a more concentrated source upstream, such as a CSO event in the headwaters of the Lark. Storms 1 and 2 both occurred in June, not long after spring fertilizer application in East Anglia, so there may have been excess nutrients built up on the ground surface that were mobilized by runoff. However, Lawler et al. (2006) found that high total event rainfall was associated with anti-clockwise ammonia C-Q hysteresis and used the increased concentration on the falling limb to index CSO events. While CSOs are not likely to occur in June due to rainfall typically not being intense enough to cause STWs to be overwhelmed by surface drainage, Great

Whelnetham STW spilled 13 times in 2021 (AW 2022), and a spill could have occurred during storm 1 or 2.

Both storms which exhibited partial anti-clockwise hysteresis were multi-peak storm discharge events. Aich et al. (2014) found that higher concentrations on later peaks of multi-peak storms occurred due to increased connectivity of more distant nutrient sources resulting from increased runoff in response to intense rainfall. However, storm event 5 also had multiple discharge peaks, with a burst of intense rain before the second peak, and it did not exhibit anti-clockwise ammonia C-Q hysteresis. The relationship between event discharge range and HI_{mean} did not show a clear division between the overall storm C-Q hysteresis patterns but demonstrated that ammonia concentration is likely to be much higher on the rising limb than on the falling limb of small magnitude discharge peaks. This underscored the importance of dilution as a controlling factor for ammonia concentration on the rising limb. The inverse relationship observed between HI_{abs+} and event discharge range was considered to reflect the same underlying mechanisms as that between HI_{mean} and the same variable, as the predominantly clockwise C-Q hysteresis observed across all storm events made these index values very similar.

While the inverse relationship observed between HI_{abs-} and API was significant, the small sample size means these results should be viewed with caution. Biron et al. (1999) noted that dry antecedent conditions increased the likelihood of anti-clockwise C-Q hysteresis for some nutrients, notably sulfate. This pattern was hypothesized as being caused by hydrophobic organic coatings on soil particles preventing infiltration, leading to runoff even without the soils reaching saturation (Biron et al. 1999). The regression of HI_{abs-} as a function of API revealed that there could be a threshold of antecedent catchment wetness for the Lark above which anti-clockwise hysteresis does not occur, as the storms which exhibited only clockwise hysteresis had API scores above 15. Storm event 4 exhibited a degree of anti-clockwise hysteresis which was not considered significant due to instrument error, so its API of 13.9 could be near a "tipping point" where infiltration is uninhibited.

Lessons learned for future studies

Separation of the rising and falling limbs of each multi-peak storm and averaging of the HI_{Qi} was indicated by Lloyd (2016a), to produce a single event-level hysteresis index value. However, averaging multiple hydrograph limbs dampens the hysteresis signal of individual

peaks if they do not all follow the same pattern. Thus, for this analysis, clockwise and anti-clockwise components of individual storms were separated and the overall magnitude of hysteresis was calculated. This aligned with this study's goal of relative ammonia source attribution for the upper Lark catchment, and these methods could be applied to future C-Q hysteresis studies which include a full year's worth, or multiple years, of data. The intensity of rainstorms in winter is often greater than during the growing season, and the resulting increased likelihood of CSO events at STWs in the upper Lark catchment would be expected to deliver late-storm nutrient pulses that would be observed as complex, figure-of-eight C-Q hysteresis. However, to quantify the total C-Q hysteresis of multi-peak storm events, a loop area-based hysteresis index like that used by Zuecco (2016) may be better suited because peaks could be separately considered, rather than averaged. The hydrograph separation methods used in this analysis would seem to work well for this approach.

To improve understanding of nutrient dynamics in the River Lark, year-round, high-frequency, quality-checked monitoring data are required. The data used in this study were collected during the summer, when the River Lark experiences very low flows and there is a rainfall deficit. The majority of stormflow-associated nutrient loading would be expected to occur during the wetter winter months, so there is a gap in understanding that needs to be filled. The RLCP datasonde could have been used for this purpose but suffered from data quality issues due to lack of calibration and maintenance. The EA datasonde experienced extensive fouling over a long period of time, which caused the loss of about one month's worth of data. To avoid wasting resources and ensure data quality in the future, it is imperative that datasondes and other in-situ sampling equipment are checked regularly, and any abnormalities noted by telemetry are rectified quickly.

Nutrient export from tributaries of the River Lark is under-studied in comparison to the main river, though the tributaries have more treated STW effluent and CSO discharge points combined than the main river. Given that base flow index of the Lark remains lower than most chalk streams near mid-reach, at only 0.77 (NRFA c2022b), runoff from the extensive agricultural operations along the tributaries could also constitute a significant contribution to the overall nutrient budget, particularly in response to intense rainstorms. While the STWs along the tributaries receive smaller volumes of sewage than the largest STW at Fornham All Saints, the tributaries also have lower flows than the Lark and therefore could deliver nutrient loads to the main river which are disproportionate to discharge volume. However,

there is not enough data to understand the effects of eutrophication along the tributaries or the quantity of nutrients exported to the main river because water quality data are scarce and flow is only quantified for one of the six tributaries. Increased monitoring of discharge and water quality along all tributaries of the River Lark would enable robust characterization of the relative importance of point- and nonpoint-sources of nutrients throughout the catchment and downstream of each confluence on the main river.

Rainfall monitoring in the upper Lark catchment could be improved by installation of additional rain gauges, as high-resolution, quality-assured rainfall data are currently collected at only one location in the upper Lark catchment. The EA rain gauge at Rushbrooke is located near the town of Bury St. Edmunds, an area with relatively high population density within the floodplain. The town also has a large amount of impermeable surface cover, which increases the amount of runoff delivered to the river during rainstorms. These characteristics make the gauge's location advantageous for flood monitoring purposes, but reliance on a single point increases the risk of storms not being detected due to operational failure. Furthermore, rainstorms are not spatially homogenous, so one measurement point cannot capture all rainfall in the catchment. One or both of these issues was illustrated in this analysis, as the EA rain gauge did not register rainfall in the hours before or during two separate stormflow events in the River Lark.

Conclusion

This study identified that rainfall drives changes in ammonia concentration in the River Lark downstream of Fornham St. Martin, described those changes using hysteresis analysis, and attempted to infer their causes. Predominantly clockwise ammonia C-Q hysteresis was observed in the upper River Lark during the growing season, chiefly driven by dilution from stormflow. Therefore, the constant input of effluent discharged from STWs appeared to be the most important source of ammonia in this part of the catchment during June and July. However, a degree of anti-clockwise hysteresis was observed during the two storm events with the heaviest rainfall, at the beginning of the study period. This indicates that the dominant sources of ammonia may change in the catchment, depending on season. Total storm loads of ammonia increased alongside storm duration during summer, when proximate sources dominated, but this trend may not be expected in winter because distant or diffuse sources could be mobilized over shorter timespans. Given that much of the net

annual rainfall in East Anglia occurs after fall harvest, there may be increased ammonia concentration in runoff from bare agricultural soils that could cause a shift to predominantly anti-clockwise ammonia C-Q hysteresis over winter. Heavy winter rainfall also increases the likelihood of CSO events, which would be expected to deliver high ammonia loads to the Lark, causing the same result. Such seasonal variations cannot be understood without high-frequency monitoring throughout the entire year, so a year-long datasonde deployment is recommended for further research. Increased monitoring of phosphorus and nitrate concentrations would also be beneficial because it could enhance understanding of changes to nutrient ratios which can alter primary production. Furthermore, storm C-Q hysteresis patterns are often dissimilar for different solutes.

References

Aguilera R, Melack JM. 2018. Concentration-discharge responses to storm events in coastal California watersheds. Water Resour Res. 54:18.

Aich V, Zimmermann A, Elsenbeer H. 2014. Quantification and interpretation of suspended-sediment discharge hysteresis patterns: How much data do we need? Catena. 122:120-129.

[AW] Anglian Water Services Limited. 2018. Our plan 2020-2025. Huntingdon (GB): Anglian Water Services Limited.

[AW] Anglian Water Services Limited. 2021. EDM return for Anglian Water annual 2020 [spreadsheet]. Bristol (GB): Environment Agency and Open Government Licence v3.0. [updated Mar 31, 2022; accessed Mar 31, 2022]. https://environment.data.gov.uk/portalstg/home/item.html?id=045af51b3be545b79b0c219811d3d243

[AW] Anglian Water Services Limited. 2022. EDM 2021 storm overflow annual return [spreadsheet]. Bristol (GB): Environment Agency and Open Government Licence v3.0. [updated Mar 31, 2022; accessed Mar 31, 2022]. https://environment.data.gov.uk/portalstg/home/item.html?id=7581f0165e864d7e93c5535d04906932

Auguie B. 2017. Gridextra: miscellaneous functions for "grid" graphics [R package]. Version 2.3. [place unknown]: The Comprehensive R Network. [updated Sep 9, 2017]. https://cran.r-project.org/package=gridExtra

Bühlmann A, Schwanbeck J, Rössler O, Horton P, Schick S. 2019. HydroBE: Miscellaneous functions of the group of hydrology Bern [R package]. Version 0.9. San Francisco (CA): GitHub. [updated Sep 20, 2019]. https://rdrr.io/github/hydro-giub/hydroBE/

Baker EB, Showers WJ. 2018. Hysteresis analysis of nitrate dynamics in the Neuse River, NC. Sci Total Environ. 652:11.

Barker JA. 1992. The management of the water resources of the Lark groundwater unit. Bristol (GB): National Rivers Authority Anglian Region.

Berrie AD. 1992. The chalk-stream environment. Hydrobiol. 248(1):3-9.

Birkby N. 2020. The River Lark and its tributaries: a review of monitoring and mitigation. Bristol (GB): Environment Agency.

Biron PM, Roy AG, Courschesne F, Hendershot WH, Cote B, Fyles J. 1999. The effects of antecedent moisture conditions on the relationship of hydrology to hydrochemistry in a small forested watershed. Hydrol Process. 13(11):1541-1555.

Blenkinsop S, Lewis E, Chan S, Fowler H. 2017. Quality-control of an hourly rainfall dataset and climatology of extremes for the UK. Int J Climatol. 37(2):19.

Bowes MJ, House WA, Hodgkinson RA, Leach DV. 2005a. Phosphorus–discharge hysteresis during storm events along a river catchment: The River Swale, UK. Water Res. 39(5):751-762.

Bowes MJ, Leach DV, House WA. 2005b. Seasonal nutrient dynamics in a chalk stream: The River Frome, Dorset, UK. Sci Total Environ. 336:16.

Bowes MJ, Smith JT, Neal C. 2009. The value of high-resolution nutrient monitoring: A case study of the River Frome, Dorset, UK. J Hydrol. 378(1-2):82-96.

Bowes MJ, Palmer-Felgate EJ, Jarvie HP, Loewenthal M, Wickham HD, Harman SA, Carr E. 2012. High-frequency phosphorus monitoring of the River Kennet, UK: Are ecological problems due to intermittent sewage treatment works failures? J Environ Monit. 14(12):3137-3145.

Bowes MJ, Jarvie HP, Halliday SJ, Skeffington RA, Wade AJ, Loewenthal M, Gozzard E, Newman JR, Palmer-Felgate EJ. 2015. Characterising phosphorus and nitrate inputs to a rural river using high-frequency concentration-flow relationships. Sci Total Environ. 511:608-620.

[BART] Brampton A&R Team. 2021. River Lark sonde review 30th September 2021. Brampton (GB): Environment Agency.

Brighty J, Hurst S, Hawkins I, Hinchley A, Stephens J, Gerrard C, Westwood S, Leach J, Mundy B, Bakewell R et al. 2021. River Lark pollution review and action plan. Brighty J, editor. Norwich (GB): Environmental Sustainability Associates Limited.

[BGS] British Geological Survey. 2008. BGS geology 625k [Esri shapefile]. Nottingham (GB): Natural Environment Research Council and Open Government Licence v3.0. [updated Jan 1, 2008; accessed Mar 27, 2022]. http://data.bgs.ac.uk/id/dataHolding/13480426

Brocca L, Melone F, Moramarco T. 2008. On the estimation of antecedent wetness conditions in rainfall-runoff modelling. Hydrol Process. 22:14.

Burgess A, O'Reilly K, Hood G. 2021. LARK_FORNHAM STW DS_E_202104 calibration sheets. (GB): Environment Agency and Open Government Licence v3.0.

Butcher RW, Pentelow FTK, Woodley JWA. 1927a. The diurnal variation of the gaseous constituents of river waters. Biochem J. 21(4):945-957.

Butcher RW, Pentelow FTK, Woodley JWA. 1927b. The diurnal variation of the gaseous constituents of river waters part II. Biochem J. 21(6):1423-1435.

Butcher RW, Pentelow FTK, Woodley JWA. 1928a. The diurnal variation of the gaseous constituents of river waters part III. Biochem J. 22(4):1035-1047.

Butcher RW, Pentelow FTK, Woodley JWA. 1928b. The diurnal variation of the gaseous constituents of river waters part IV. Biochem J. 22(6):1478-1489.

Butturini A, Sabater F. 2002. Nitrogen concentrations in a small Mediterranean stream: 1. Nitrate 2. Ammonium. Hydrol Earth Syst Sci. 6(3):12.

Butturini A, Gallart F, Latron J, Vazquez E, Sabater F. 2006. Cross-site comparison of variability of DOC and nitrate C-Q hysteresis during the autumn-winter period in three Mediterranean headwater streams: A synthetic approach. Biogeochem. 77(3):327-349.

[CS] Campbell Scientific. 2017. EE181 temperature and relative humidity probe instruction manual. Logan (UT): Campbell Scientific, Inc.

[CW] Challenge Works. c2022. Catchment Systems Thinking Cooperative (CaSTCo) [Internet]. London (GB): Nesta. [accessed Oct 17, 2022]. https://waterinnovation.challenges.org/winners/castco/

[CIWEM] Chartered Institution of Water and Environmental Management. 2014. Policy position statement misconnections. London (GB): Chartered Institution of Water and Environmental Management.

Clark MR, Webb JDC, Kirk PJ. 2018. Fine-scale analysis of a severe hailstorm using crowd-sourced and conventional observations. Meteorol Appl. 25(3):472-492.

Clifforde I, Morris G, Crabtree B. 1995. The UK response to the challenge of urban stormwater management. Water Sci Technol. 32(1):177-183.

Comber SDW, Smith R, Daldorph P, Gardener MJ, Constantino C, Ellor B. 2013. Development of a chemical source apportionment decision support framework for catchment management. Environ Sci Technol. 47(17):9.

Coney J, Pickering B, Dufton D, Lukach M, Brooks B, Neely RR. 2022. How useful are crowdsourced air temperature observations? An assessment of Netatmo stations and quality control schemes over the United Kingdom. Meteorol Appl. 29(3).

[CU] Cranfield Soil and Agrifood Institute. c2022. Soilscapes [Internet]. Wharley End (GB): Cranfield University. [accessed Jul 4, 2022]. https://www.landis.org.uk/soilscapes/index.cfm

Crochemore L, Isberg K, Pimentel R, Pineda L, Hasan A, Arheimer B. 2020. Lessons learnt from checking the quality of openly accessible river flow data worldwide. Hydrol Sci J. 65(5):699-711.

D'Amario SC, Wilson HF, Xenopoulos MA. 2021. Concentration-discharge relationships derived from a larger regional dataset as a tool for watershed management. Ecol Appl. 31(8).

[DI] Davis Instruments. 2021a. Vantage Pro2 wireless stations specification sheet. Hayward (CA): Davis Instruments.

[DI] Davis Instruments. 2021b. Weatherlink station 03 Saxham data Mar to Oct 2021 [spreadsheet]. Hayward (CA): Davis Instruments. [updated Oct 31, 2021]. https://www.weatherlink.com/browse/71d0d2fd-1452-4b33-a81b-e35812c2de25

[EA] Environment Agency. 2018. Storm overflow assessment framework. Version 1.6. Bristol (GB): Environment Agency.

[EA] Environment Agency. 2019. The environmental permitting (England and Wales) regulations 2016 permit number AW1NF545. Bristol (GB): Environment Agency.

[EA] Environment Agency. 2021a. East Anglia monthly water situation report April 2021. Bristol (GB): Environment Agency.

[EA] Environment Agency. 2021b East Anglia monthly water situation report December 2020. Bristol (GB): Environment Agency.

[EA] Environment Agency. 2021c. East Anglia monthly water situation report January 2021. Bristol (GB): Environment Agency.

[EA] Environment Agency. 2021d. East Anglia monthly water situation report June 2021. Bristol (GB): Environment Agency.

[EA] Environment Agency. 2021e. East Anglia monthly water situation report May 2021. Bristol (GB): Environment Agency.

[EA] Environment Agency. 2021f. East of England monthly water situation report August 2021. Bristol (GB): Environment Agency.

[EA] Environment Agency. 2021g. East of England monthly water situation report February 2021. Bristol (GB): Environment Agency.

[EA] Environment Agency. 2021h. East of England monthly water situation report March 2021. Corrected version. Bristol (GB): Environment Agency.

[EA] Environment Agency. 2021i. East of England monthly water situation report October 2021. Bristol (GB): Environment Agency.

[EA] Environment Agency. 2021j. East of England monthly water situation report September 2021. Bristol (GB): Environment Agency.

[EA] Environment Agency. 2021k. Fornham St. Martin River Lark 15 minute flow December 2020 - October 2021 [spreadsheet]. Norwich (GB): Environment Agency and Open Government Licence v3.0. [updated Aug 2, 2022].

[EA] Environment Agency. 2021l. River Lark sonde downstream of Fornham All Saints water recycling center discharge April - October 2021 [spreadsheet]. Brampton (GB): Environment Agency and Open Government Licence v3.0. [updated Jan 21, 2022].

[EA] Environment Agency. 2021m. WFD river water body catchments cycle 2 [Esri shapefile]. Bristol (GB): Environment Agency and Open Government Licence v3.0. [accessed Feb 22, 2022]. https://environment.data.gov.uk/catchment-planning/v/c3-plan/OperationalCatchment/3249

[EA and OS] Environment Agency, Ordnance Survey. 2021. Chalk rivers [Esri shapefile]. Environment Agency and Open Government Licence v3.0. [updated Dec 10, 2021; accessed Oct 25, 2021]. https://environment.data.gov.uk/DefraDataDownload/?mapService=EA/ChalkRivers&Mode=spatial

[EA] Environment Agency. c2021. Sampling point Bury St. Edmunds Stw F/E [Internet]. Bristol (GB): Environment Agency and Open Government Licence v3.0. [accessed July 30, 2022]. https://environment.data.gov.uk/water-quality/view/sampling-point/AN-BURYSTE.

[EA] Environment Agency. 2022a. Hawstead tributary water body [Internet]. Bristol (GB): Environment Agency and Open Government Licence v3.0. [updated Aug 22, 2022; accessed Oct 25, 2022]. https://environment.data.gov.uk/catchment-planning/WaterBody/GB105033042930

[EA] Environment Agency. 2022b. Lark (Abbey Gardens to Mildenhall) water body [Internet]. Bristol (GB): Environment Agency and Open Government Licence v3.0. [updated Aug 22, 2022; accessed Oct 25, 2022]. https://environment.data.gov.uk/catchment-planning/WaterBody/GB105033043051

[EA] Environment Agency. 2022c. Lark (Hawstead to Abbey Gardens) water body [Internet]. Bristol (GB): Environment Agency and Open Government Licence v3.0. [updated Aug 22, 2022; accessed Oct 25, 2022]. https://environment.data.gov.uk/catchment-planning/WaterBody/GB105033042940

[EA] Environment Agency. 2022d. Lark (US Hawstead) water body [Internet]. Bristol (GB): Environment Agency and Open Government Licence v3.0. [updated Aug 22, 2022; accessed Oct 25, 2022]. https://environment.data.gov.uk/catchment-planning/WaterBody/GB105033042920

[EA] Environment Agency. 2022e. Linnet water body [Internet]. Bristol (GB): Environment Agency and Open Government Licence v3.0. [updated Aug 22, 2022; accessed Oct 25, 2022]. https://environment.data.gov.uk/catchment-planning/WaterBody/GB105033042950

[EA] Environment Agency. 2022f. Phosphate RNAG in Lark (Abbey Gardens to Mildenhall) [Internet]. Bristol (GB): Environment Agency and Open Government Licence v3.0. [updated Aug 22, 2022; accessed Oct 25, 2022]. https://environment.data.gov.uk/catchment-planning/WaterBody/GB105033043051/rnag?cycle=3&element=71.

[EA] Environment Agency. 2022g. Rushbrooke WSW 15 minute precipitation, April 2021 - October 2021 [spreadsheet]. Brampton (GB): Environment Agency and Open Government Licence v3.0. [updated Aug 4, 2022].

[EA] Environment Agency. 2022h. Rushbrooke WSW 15 minute precipitation, December 2020 - March 2021 [spreadsheet]. Norwich (GB): Environment Agency and Open Government Licence v3.0. [updated Jul 15, 2022].

Esri. 2013. World shaded relief [map tiles]. Redlands (CA): Esri. [updated Jun 18, 2014; accessed Oct 25, 2022]. https://server.arcgisonline.com/ArcGIS/rest/services/World_Shaded_Relief/MapServer

Esri. 2022. Light gray canvas base [map tiles]. Redlands (CA): Esri. [updated Sep 21, 2022; accessed Oct 25, 2022]. https://basemaps.arcgis.com/arcgis/rest/services/World_Basemap_v2/VectorTileServer

Evans C, Davies TD. 1998. Causes of concentration/discharge hysteresis and its potential as a tool for analysis of episode hydrochemistry. Water Resour Res. 34(1):129-137.

Glynn DR, Baker WR, Jones CA, Liesner JL. 1992. Economic issues in water privatisation and regulation. Water Sci Technol. 26(7-8):1921-1928.

Grolemund G, Wickham H. 2011. Dates and times made easy with lubridate. J Stat Softw. 40(3):25.

Hanna DEL, Tomscha SA, Oullet Dallaire C, Bennett EM. 2018. A review of riverine ecosystem service quantification: research gaps and recommendations. J Appl Ecol. 55:1299-1311.

Holzer P, Krebs P. 1998. Modelling the total ammonia impact of CSO and WWTP effluent on the receiving water. Water Sci Technol. 38(10):31-39.

Hurst S. 2021. River Lark catchment appraisal. Holt (GB): Norfolk Rivers Ecology.

Klaar MJ, Carver S, Kay P. 2020. Land management in a post-Brexit UK: an opportunity for integrated catchment management to deliver multiple benefits?. WIREs Water. [accessed Nov 6, 2021]. 7(5). https://doi.org/10.1002/wat2.1479

Kohler MA, Linsley RK. 1951. Predicting the runoff from storm rainfall. Washington (D.C.): Weather Bureau.

[LM] Lambrecht meteo. 2022. Rain[e] weighing precipitation sensor product-view. Göttingen (DE): Lambrecht meteo.

Lawler DM, Petts GE, Foster IDL, Harper S. 2006. Turbidity dynamics during spring storm events in an urban headwater river system: The Upper Tame, West Midlands, UK. Sci Total Environ. 360(1-3):109-126.

Liu WL, Birgand F, Tian SY, Chen C. 2021. Event-scale hysteresis metrics to reveal processes and mechanisms controlling constituent export from watersheds: A review. Water Res. 200:117254.

Lloyd CEM, Freer JE, Johnes PJ, Collins AL. 2016a. Technical note: testing an improved index for analysing storm discharge-concentration hysteresis. Hydrol Earth Syst Sci. 20(2):625-632.

Lloyd CEM, Freer JE, Johnes PJ, Collins AL. 2016b. Using hysteresis analysis of high-resolution water quality monitoring data, including uncertainty, to infer controls on nutrient and sediment transfer in catchments. Sci Total Environ. 543:388-404.

Mackey AP, Berrie AD. 1991. The prediction of water temperatures in chalk streams from air temperatures. Hydrobiol. 210(3):183-189. Mihiranga HKM, Jiang Y, Li X, Wang W, De Silva K, Kumwimba MN, Bao X, Nissanka SP. 2021. Nitrogen/phosphorus behavior traits and implications during storm events in a semi-arid mountainous watershed. Science of the Total Environment. 791.

[MO] Met Office. 2022. Observation site G0TMX [Internet dataset]. Exeter (GB): Met Office [updated Feb 21, 2022; accessed Aug 27, 2022]. https://wow.metoffice.gov.uk/observations/details/20220221aitfp4wubce63yupyyb96scthc

[MO] Met Office. c2022. UK climate averages Brooms Barn (Suffolk) [Internet]. Exeter (GB): Met Office [accessed Nov 22, 2022]. https://www.metoffice.gov.uk/research/climate/maps-and-data/uk-climate-averages/u123kcwkd

[NCIC] Met Office National Climate Information Center. 2022. Monthly, seasonal and annual total precipitation amount for East Anglia [Internet dataset]. Exeter (GB): Met Office [updated Oct 1, 2022; accessed Oct 16, 2022]. https://www.metoffice.gov.uk/pub/data/weather/uk/climate/datasets/Rainfall/date/East_Anglia.txt

[NRFA] National River Flow Archive. c2022a. Catchment info 33070- Lark at Fornham St. Martin [Internet]. Crowmarsh Gifford (GB): UK Centre for Ecology and Hydrology. [accessed Nov 22, 2022]. https://nrfa.ceh.ac.uk/data/station/spatial/33070

[NRFA] National River Flow Archive. c2022b. Daily flow data 33014- Lark at Temple [Internet]. Crowmarsh Gifford (GB): UK Centre for Ecology and Hydrology. [accessed Nov 23, 2022]. https://nrfa.ceh.ac.uk/data/station/meanflow/33014

[NRFA] National River Flow Archive. c2022c. Daily flow data 33070- Lark at Fornham St. Martin [Internet]. Crowmarsh Gifford (GB): UK Centre for Ecology and Hydrology. [accessed Sep 1, 2022]. https://nrfa.ceh.ac.uk/data/station/meanflow/33070

[NRFA] National River Flow Archive. c2022d. Derived flow statistics [Internet]. Crowmarsh Gifford (GB): UK Centre for Ecology and Hydrology. [accessed Sep 24, 2022]. https://nrfa.ceh.ac.uk/derived-flow-statistics

[NRFA] National River Flow Archive. c2022e. Station info 33070- Lark at Fornham St. Martin [Internet]. Crowmarsh Gifford (GB): UK Centre for Ecology and Hydrology. [accessed Nov 22, 2022]. https://nrfa.ceh.ac.uk/data/station/info/33070

[OS] Ordnance Survey. 2021. OS open rivers [Esri shapefile]. Nursling (GB): Ordnance Survey and Open Government Licence v3.0. [updated Nov 5, 2021; accessed Feb 21, 2021]. https://www.ordnancesurvey.co.uk/business-government/products/open-map-rivers

[OS] Ordnance Survey. c2021. OS vectormap® district TL [Esri shapefile]. Nursling (GB): Ordnance Survey and Open Government Licence v3.0. [accessed Feb 7, 2022]. https://www.os.uk/business-and-government/products/vectormap-district.html

[OS] Ordnance Survey. c2022. Lark at Fornham St. Martin catchment boundary [Esri shapefile]. Crowmarsh Gifford (GB): UK Centre for Ecology and Hydrology. [accessed Feb 22, 2022]. https://nrfa.ceh.ac.uk/data/station/spatial/33070

Overton AK. 2009. A guide to the siting, exposure and calibration of automatic weather stations for synoptic and climatological observations. Version 3.1. [place unknown]: Andrew K. Overton.

Peterson RA, Cavanaugh JE. 2020. Ordered quantile normalization: A semi-parametric transformation built for the cross-validation era. J Appl Stat. 47(1):13.

Peterson RA. 2021. Finding optimal normalizing transformations via bestNormalize. R J. 13(1):20.

[PIL] Proteus Instruments Ltd. 2021. Proteus user manual. Version 2.3. Stoke Prior (GB): Proteus Instruments Ltd.

[PIL] Proteus Instruments Ltd. 2022. Proteus datasheet. Stoke Prior (GB): Proteus Instruments Ltd.

[RCT] R Core Team. 2022. R: A language and environment for statistical computing [software]. Vienna (AT): R Foundation for Statistical Computing. https://www.R-project.org/

Rangeley-Wilson C, Powell S, Broadfield S, Panayiotou A, Dacey A, O'Neill R, Rose C, Benlamkadem F, Styles M, Tickner D, et al. 2021. Chalk stream restoration strategy 2021 main report. (GB): Catchment Based Approach.

[RLCP] River Lark Catchment Partnership. 2021. Proteus Lark raw data [spreadsheet]. Bury St. Edmunds (GB): River Lark Catchment Partnership. [updated Mar 11, 2021].

[RLCP] River Lark Catchment Partnership. c2022. Community [Internet]. Bury St. Edmunds (GB): River Lark Catchment Partnership. [accessed Oct 25, 2022]. https://www.riverlark.org.uk/community.html.

Rose LA, Karwan DL, Godsey SE. 2018. Concentration-discharge relationships describe solute and sediment mobilization, reaction, and transport at event and longer timescales. Hydrol Process. 32:16.

[RR] Rothamsted Research. 2022. Brooms Barn hourly air and rain 20201201 to 20211031 [spreadsheet]. [updated Jul 4, 2022]. Harpenden (GB): Lawes Agricultural Trust and Rothamsted Research.

[RR] Rothamsted Research. c2022a. Data quality in e-RA. Harpenden (GB): Lawes Agricultural Trust and Rothamsted Research. [accessed Jul 27, 2022]. http://www.era.rothamsted.ac.uk/info/dataQuality

[RR] Rothamsted Research. c2022b. Meteorological data available in BROOMET [Internet]. Harpenden (GB): Lawes Agricultural Trust and Rothamsted Research. [accessed Jul 27, 2022]. http://www.era.rothamsted.ac.uk/station/bms#datasets

[SS and WM] The Secretary of State, the Welsh Ministers. 2015. The water framework directive (standards and classification) directions (England and Wales) 2015. London (GB): The Secretary of State and the Welsh Ministers.

Sego LH. 2016. Smisc: Sego miscellaneous. A collection of functions for statistical computing and data manipulation in R. Version 0.4.0. Richland (WA): Pacific Northwest National Laboratory. https://pnnl.github.io/Smisc

Shiklomanov IA. 1993. World fresh water resources. In: Gleick PH, editor. Water in crisis: A guide to the world's fresh water resources. New York (NY): Oxford University Press. p. 13-24.

Sievert C. 2020. Interactive web-based data visualization with R, plotly, and shiny. Boca Raton (FL): Chapman and Hall and CRC Florida.

[SD and OSM] Stamen Design, OpenStreetMap. c2022. Terrain map tiles [map tiles]. San Francisco (CA): http://maps.stamen.com/#terrain/12/37.7706/-122.3782

Tuszynski J. 2021. _caTools: Tools: Moving window statistics, GIF, base64, ROC AUC, etc_ [R package]. Version 1.18.2. [place unknown]: The Comprehensive R Network. [updated Mar 28, 2021]. https://CRAN.R-project.org/package=caTools

[UUWL] United Utilities Water Limited. 2020. Evolving the water industry national programme to deliver greater value. Warrington (GB): United Utilities Water Limited.

Vaughan MCH, Bowden WB, Shanley JB, Vermilyea A, Sleeper R, Gold AJ, Pradhanang SM, Inamdar SP, Levia DF, Andres AS et al. 2017. High-frequency dissolved organic carbon and nitrate measurements reveal differences in storm hysteresis and loading in relation to land cover and seasonality. Water Resour Res. 53:19.

[WW] Wessex Water. 2018. Atkins - phosphorus removal - technology review. Appendix 5.1.C, PR19 Business Plan September 2018. Bath (GB): Wessex Water YTL Group.

[WSC] West Suffolk Council. c2022. About the area [Internet]. Bury St. Edmunds (GB): West Suffolk Council. [accessed Nov 22, 2022]. https://www.westsuffolk.gov.uk/council/data-and-information/abouttheareа.cfm

Wickham H. 2016. ggplot2: Elegant graphics for data analysis. New York (NY): Springer-Verlag.

Williams GP. 1989. Sediment concentration versus water discharge during single hydrologic events in rivers. J Hydrol. 111(1-4):18.

[YSI] YSI Inc. 2020. EXO user manual. Revision K. Yellow Springs (OH): Xylem, Inc.

Zeileis A, Grothendieck G. 2005. zoo: S3 infrastructure for regular and irregular time series. J Stat Softw. 14(6): 1-27. https://doi.org/10.18637/jss.v014.i06

Zuecco G, Penna D, Borga M, van Meervald HJ. 2016. A versatile index to characterize hysteresis between hydrological variables at the runoff event timescale. Hydrol Process. 30:18.

Appendix A: Additional data quality control and outlier analysis

Quality-checked datasets excluded from C-Q analysis

RLCP datasonde deployment and data quality issues

The RLCP (2021) deployed a datasonde (Proteus Water Quality Probe, Proteus Instruments Ltd., Stoke Prior, UK) in the River Lark approximately 1.5 km downstream of Fornham All Saints, at Mill Farm, between December 2020 and March 2021. The RLCP datasonde measured temperature (°C), ammonium concentration (mg/l), pH, oxidation-reduction potential (mV), turbidity (NTU), conductivity (µS/cm), and tryptophan-like fluorescence (ppb) at 15-minute intervals; dissolved oxygen was not measured. The RLCP datasonde was dislodged by flooding 23 days after deployment and stopped logging data at 11:30 GMT 27 December 2020 (A. Hinchley, RLCP Chairperson, personal communication with the author, October 3, 2022). It was recovered by RLCP volunteers and re-deployed, but the sensors were not calibrated, cleaned, or serviced before it was re-deployed (A. Hinchley, RLCP Chairperson, personal communication with the author, October 3, 2022), and measurements taken by the optical sensors and ISEs appeared, upon visual inspection, to have experienced significant drift and decreased data accuracy. Therefore, solute measurements taken by the RLCP datasonde after 11:30 GMT 27 December 2020 were not considered suitable for analysis. However, temperature measured by the factory-calibrated thermistor was considered reliable for the entire deployment period, because this sensor does not require maintenance and is accurate to ±0.1 °C (PIL 2021, 2022). Ammonium concentration (mg/l) is only accurate to ±5% or 2 mg/l (PIL 2021), which made 99% of the ammonium concentration values not distinguishable from zero. Therefore, the RLCP datasonde was excluded from this C-Q hysteresis analysis.

Initial measurements from the Proteus sonde were taken at 5 min intervals, likely due to configuration issues, so every third measurement was included until regularly spaced 15 min measurements began. The Proteus sonde occasionally logged data at irregular intervals and values not within 3 minutes of the quarter hour were considered missed measurements in the time series and excluded on the basis that these were not sampled close enough to the correct time interval. The completeness of the dataset was first manually examined for gaps, then checked against a date and time sequence generated with RStudio (RCT 2022)

to confirm all missing 15-minute frequency measurements were identified. The data were then checked using the same procedures as outlined for the EA datasonde. An extended gap occurred between 11:30 27 December 2020 and 12:00 02 January 2021 due to the datasonde being dislodged by flooding (A. Hinchley, RLCP Chairperson, personal communication with the author, October 3, 2022).

Additional sources of rainfall data excluded from analysis

An automated personal weather station personal weather station (Vantage Pro2 Plus, Davis Instruments, Hayward, CA, USA) located near Saxham, Bury St. Edmunds, in the upper Lark catchment provided subscription-based access to 15-minute resolution weather measurements, including rainfall. Quality checks according to Blenkinsop et al.'s (2017) methods revealed operational failure of the tipping-bucket rain gauge for most, if not all, of the study period for which data were available. Data from this rain gauge was excluded from analysis because monthly totals were significantly below the amounts indicated by EA for the same months (EA 2021a, 2021d, 2021e, 2021f, 2021h, 2021i, 2021j).

An additional automated weather station located on the Moreton Hall housing estate in Bury St. Edmunds also provided open access to 15-minute rainfall and temperature information via the Met Office Weather Observation Website (MO 2022). The accuracy of the Moreton Hall instrumentation was unknown, as published values were not available and the station owner could not be reached. The accuracy was assumed to be ±1.0 °C, the widest margin of error generally acceptable for automated personal weather stations (Overton 2009). However, this dataset was excluded from analysis after quality checking revealed many repeated values indicating calibration or other operational errors, such as recording daily total precipitation (Blenkinsop et al. 2017). Additionally, examination of the time series revealed gaps and non-agreement of the downloaded and online hosted data sets with respect to the time measurements were recorded.

Air temperature data validation and exclusion from analysis

Initially, several sources of air temperature data were sought for this analysis to model the expected temperature of the River Lark, using Mackey and Berrie's (1991) equation. Observed variation from the modelled temperature was intended for use as a surrogate for storm-related changes in nutrient concentration and delivery. However, this thread of

analysis was abandoned in favor of C-Q hysteresis analysis, due to the latter methodology's promise for indicating dominant nutrient sources and pathways during stormflow.

Air temperature measurements at 15-minute intervals were also available from the personal weather station located near Saxham, in the upper Lark catchment (DI 2021b). The weather station temperature instrumentation is accurate to ±0.3 degrees Celsius (DI 2021a), but no quality assurance checks were completed by the data provider, and only raw measurements were available. Therefore, several checks were implemented to ensure the data were suitable for use in water temperature modelling. Values not within 3 minutes of the quarter hour were considered missed measurements in the time series and excluded on the basis that these were not sampled close enough to the correct interval and did not represent conditions at the intended time. The completeness of the record was first manually examined for gaps, then checked against a date and time sequence generated with RStudio (RCT 2022) to confirm all missing 15-minute frequency measurements were identified.

Ambient temperature measurements from automated weather stations are known to be biased by environmental factors, notably exposure to intense sun or wind (Coney et al. 2022), so differences in the 15-minute temperature record were also checked. Rapid temperature changes were described by Clark et al. (2018) for an exceptionally strong hailstorm that occurred in northern England in 2015. A maximum increase of 1.3°C was observed over 10 minutes, as well as a maximum decrease of 3.2°C over 8 minutes (Clark et al. 2018). The maximum decrease in the Saxham temperature values was 3.9°C over 15 minutes, which is a slower rate of change than described by Clark et al. (2018). However, the maximum increase observed in the Saxham values was 2.2°C over 15 minutes, which exceeds the rate of change documented by Clark et al. (2018), so the data were checked by 5-point moving window modified z-scores to augment the visual inspection of monthly plots. Temperature measurements which changed by more than 1°C as compared to the preceding measurement and had modified z-scores with absolute value ≥2 were flagged for manual review. After manual inspection, these values were determined to be natural inflection points and retained.

Finally, air temperature at the Saxham weather station (DI 2021b) was checked for accuracy via linear regression using the pre-validated average hourly air temperatures measured by Rothamsted Research's Brooms Barn Meteorological Station (2022a). The

Brooms Barn meterological station uses a Campbell Scientific EE181 E+E Relative Humidity and Temperature probe (RR c2022b), which is accurate to ±0.2 degrees at 23°C, with accuracy decreasing by 0.1°C per 20°C of temperature above or below this point (CS 2017). The acceptable threshold to determine agreement between sites was set at $p < 0.01$ and $R^2 > 0.70$. Linear regression found hourly average, minimum, and maximum temperatures at both sites were strongly related ($p < 0.001$ and $R^2 = 0.98$). Thus, the temperature data from the Saxham weather station were considered accurate enough to model river temperature.

Systematic outliers in the EA datasonde dataset

All ammonia, DO, and temperature measurements which were more than two standard deviations from the medians, calculated using a 5-point moving window, were manually reviewed. There were 321 rows of paired ammonia and DO data that were considered true outliers due to having single point measurements which deviated significantly from the pattern of neighboring points and were not natural inflection points. Of the true outliers detected, 277 of the values removed occurred at 00:30, 4:30, 8:30, 12:30, 16:30, or 20:30 GMT. This is 86.3% of the outliers, but only 8.3% of the total ammonia and DO measurements were taken at these times. Table A.1 provides a breakdown of the outliers removed from the dataset at each time. Measurements taken directly before and after the four-hour outlier timestamps were examined to determine if they were also affected by the systematic error. These measurements accounted for only 3.2% of the outliers, so the cause of the systematic error was short-lived.

Table A.1 Occurrence of outliers in the ammonia and DO data produced by the EA datasonde deployed in the River Lark at Fornham All Saints, UK, May to October 2021.

Time	Outliers	Percent of measurements at time
00:30	44	40.4
04:30	50	46.3
08:30	44	40.7
12:30	39	35.4
16:30	53	48.6
20:30	47	43.1

There were 97 temperature measurements which were considered true outliers because they were not true inflection points but were 0.5°C different from their nearest neighboring measurements. Of these outliers, 63.9% occurred at the four-hour intervals previously described. Temperature was overall less affected by the systematic error than ammonia and DO, but outliers also occurred more frequently in the evening or night (see Table A.2).

Table A.2 Occurrence of outliers in the temperature data produced by the EA datasonde deployed in the River Lark at Fornham All Saints, UK, May to October 2021.

Time	Outliers	Percent of measurements at time
00:30	12	8.1
04:30	2	1.4
08:30	2	1.4
12:30	8	5.5
16:30	22	14.6
20:30	16	10.7

Appendix B: Additional storm event concentration-discharge plots

All plots were created in RStudio (RCT 2022) using ggplot2 (Wickham 2016), then arranged using gridExtra (Auguie 2017).

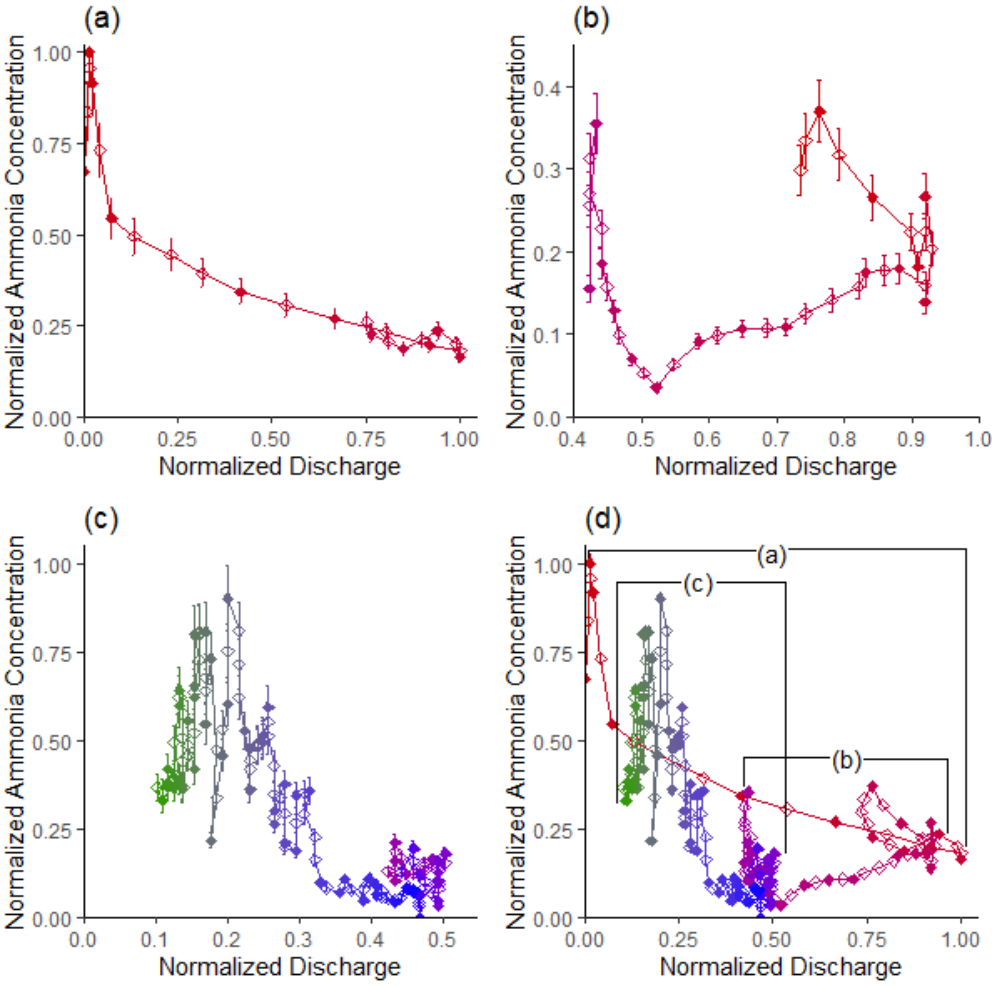

Figure B.1 Normalized concentration-discharge (C-Q) plots for each discharge peak (a-c) in the River Lark at Fornham St. Martin, UK during storm event 1, 04 June 2021 to 06 June 2021. Plots (a-c) show discharge peaks one to three, respectively, and the extent of each is shown in (d). Time is indicated by line/diamond color, from red (start) to green (end). Open diamonds represent times for which discharge measurements were available, but concentration was interpolated. Vertical bars on points in plots (a-c) show measurement error.

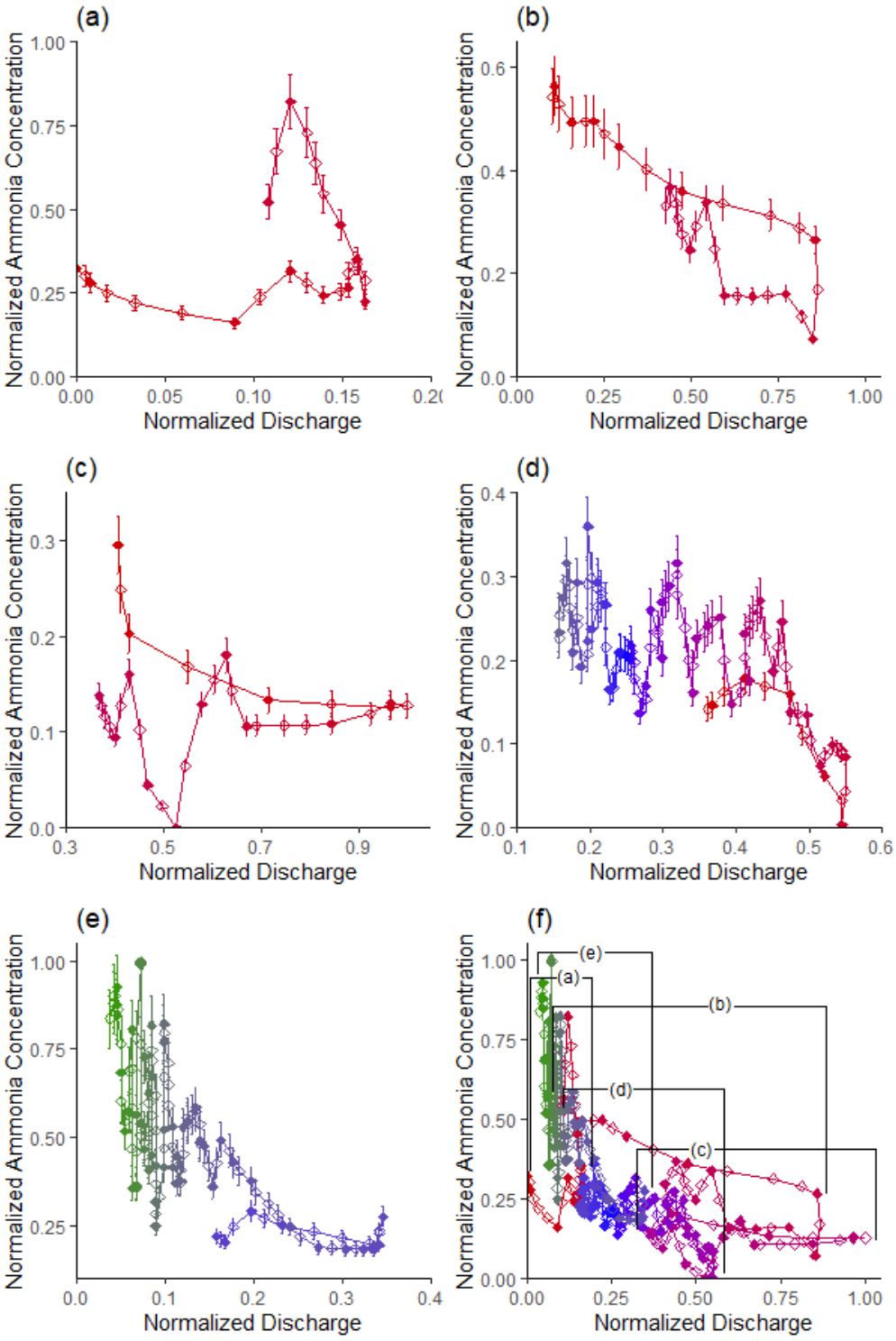

Figure B.2 Normalized concentration-discharge (C-Q) plots for each discharge peak (a-e) in the River Lark at Fornham St. Martin, UK during storm event 2, 18 June 2021 to 21 June 2021. Plots (a-e) show discharge peaks one to five, respectively, and the extent of each is shown in (f). Time is indicated by line/diamond color, from red (start) to green (end). Open diamonds represent times for which discharge measurements were available, but concentration was interpolated. Vertical bars on points in plots (a-e) show measurement error.

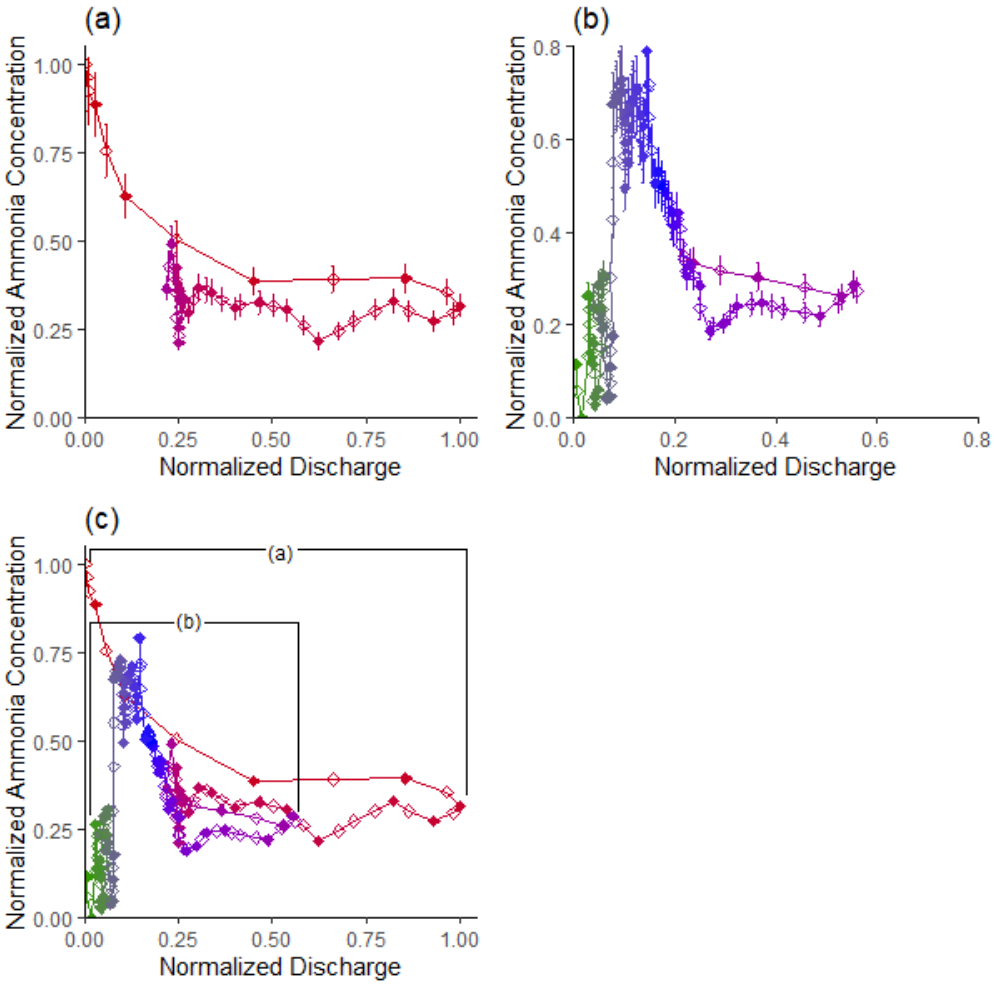

Figure B.3 Normalized concentration-discharge (C-Q) plots for each discharge peak (a-e) in the River Lark at Fornham St. Martin, UK during storm event 5, 05 to 07 July 2021. Plots (a-b) show discharge peaks one and two, respectively, and the extent of each is shown in (c). Time is indicated by line/diamond color, from red (start) to green (end). Open diamonds represent times for which discharge measurements were available, but concentration was interpolated. Vertical bars on points in plots (a-b) show measurement error.

Appendix C: Description of volunteer role at RLCP

My volunteer work with the River Lark Catchment Partnership (RLCP) has provided many opportunities for professional development, especially through interactions with RLCP stakeholders. Since January 2021, I have advised RLCP regarding citizen science (CS) projects, provided GIS support, and recently served as a representative to the UK-wide Catchment Systems Thinking Cooperative (CaSTCo) project. A comprehensive list of my interactions with RLCP and tasks completed as a volunteer is provided in Table C.1 below.

Advising RLCP's CS program has helped me hone my communication and interpretation skills as an environmental science professional through regular participation in RLCP volunteer meetings, including the pollution group. At each meeting, known and potential pollution sources along the Lark and its tributaries are discussed, as well as the possible water quality effects. Future CS water sampling activities are also planned, including regular sampling of the Lark tributaries and targeted sampling to detect and monitor pollution point sources. The RLCP Chairperson has often requested that I present information to the group on relevant topics, especially those related to the STW discharge permit limits I researched for the group. I also developed a draft CS protocol for continuous discharge monitoring of the tributaries of the Lark, which explained the conceptual basis of ungauged streamflow measurement and its application for the tributaries using the pressure transducer method. During volunteer discussions, I was frequently asked to explain environmental science concepts, such as the factors affecting dissolved oxygen content. These interactions with other RLCP volunteers improved my ability to break down complex natural phenomena into terms that can be understood by members of the public.

As an RLCP representative to CaSTCo, I have also engaged with professional scientists and project managers working for the project and other catchment partnerships. CaSTCo is a novel project, sponsored by the UK Rivers Trust and water utility providers, which seeks to bring together catchment partnerships from across the country to standardize CS data collection, sharing, and analysis for improved understanding of challenges to the ecological health of UK rivers (CW c2022). Though the project is in its early stages, I have attended several meetings and voiced concerns about the sustainability of RLCP involvement. The additional resources provided by CaSTCo are a boon to the development of CS in the Lark catchment, but it's essential that RLCP does not over-commit to delivering infeasible data

products. As I have advised RLCP CS water quality sampling activities and am developing the tributaries flow monitoring program, I have a good understanding of what can be accomplished by RLCP volunteers. I have assisted the RLCP Chairperson in communicating this capacity and the overall goals of RLCP CS work to CaSTCo management, to ensure our objectives are aligned. I have also joined the CaSTCo data platforms working group to prepare RLCP for management of increasingly larger volumes of data as the CS program grows. My experiences with GIS work for RLCP have illustrated that data management and sharing is a weakness of the CS program, so I hope to learn what has worked for other catchment partnerships and find a solution that can fit RLCP's needs.

I am very grateful for all the opportunities that volunteering with RLCP has awarded me during my degree program. Advising the RLCP CS program has challenged me to synthesize the concepts I have learned in my coursework to improve and develop sampling plans and ensure volunteers understand the relevance of the measurements that are taken. Furthermore, my role in the CaSTCo project has given me the chance to represent the unique perspective of a non-profit, community-driven organization at the national level and to participate in shaping the future of water quality monitoring in the UK.

Table C.1 Reverse chronological log of interactions with RLCP and tasks completed in a volunteer capacity.

Date	**Task or interaction**
31 Oct 2022	Met with CaSTCo PM from Rivers Trust and several RLCP Trustees to discuss RLCP involvement and progress toward funding.
27 Oct 2022	Created plots of 2017-2022 EA phosphate and ammonia monitoring data for pollution report and sent to Chairperson.
26 Oct 2022	Met with Chairperson and Citizen Science (CS) Manager/ Volunteer Coordinator to discuss continuous flow monitoring of the River Linnet and progress of CaSTCo project.
16 Oct 2022	Corresponded via email with Chairperson in preparation for pollution group meeting about STW discharges in Culford stream catchment.
15 Oct 2022	Created new shapefile for STW discharges and merged several surface water layers to provide most comprehensive coverage for the Lark catchment. Shared files with Chairperson via email.

Table C.1 Continued

Date	Task or interaction
13 Oct 2022	Corresponded via email with Chairperson regarding best GIS layers for ditch mapping.
12 Oct 2022	Met with CaSTCo data platforms working group. Included CaSTCo Project Managers (PMs), PMs and professional scientist volunteers from other catchment partnerships, Rivers Trust representatives, and EA representatives.
08 Oct 2022	Prepared simple Lark catchment maps for RLCP Volunteer Coordinator for volunteer introduction package.
03 Oct 2022	Met with Chairperson, CS Manager/Volunteer Coordinator, and National Trust (NT) Ickworth Estate Ranger to discuss CS opportunities along the Linnet. Toured site to determine potential bridges for deployment of constant flow monitoring equipment. RLCP and NT signed Memorandum of Understanding.
02 Oct 2022	Created maps of stream network and land parcels in Linnet catchment for NT Ickworth CS project planning.
27 Sep 2022	Correspondence with chairperson and volunteers regarding calculation of un-ionized ammonia from total ammonia.
07 Sep 2022	Visited NT Ickworth Estate with Chairperson. Walked along the Linnet to observe the topography of the estate and locate ditches and field drains to understand the predominant runoff sources.
05 Sep 2022	Created vicinity map of NT Ickworth Estate with known streams, drains, and ditches to prepare for site visit and meeting with NT ranger.
01 Sep 2022	Met with CaSTCo Anglian Region project representatives and River Wensum Partnership PM to discuss how RLCP plans to utilize professional mangers allocated for the region, and my role in the project.
26 Aug 2022	Met with Chairperson to discuss CaSTCo collaboration with River Wensum Partnership and my role as liason.
24 Aug 2022	Reviewed draft volunteer coordinator role description shared by River Wensum Partnership CaSTCo PM to provide feedback to Chairperson.

Table C.1 Continued

Date	Task or interaction
23 Aug 2022	Spoke with Chairperson about outcome of first CaSTCo meeting. Discussed plan for RLCP involvement in the project and cooperation with the River Wensum Partnership.
12 Aug 2022	Shared with Chairperson a written protocol for measuring continuous flow in tributaries or ditches.
12 Aug 2022	Shared with Chairperson presentation slides with results of STW effluent BOD vs. Lark DO analysis.
10 Aug 2022	Reviewed and provided feedback on draft CS planning document sent by Chairperson as output of two prior planning meetings.
03 Aug 2022	Attended CS planning meeting with Chairperson, CS Manager/Volunteer Coordinator, and a representative from Suffolk Wildlife Trust to prepare for CaSTCo meeting and plan long term CS objectives. Discussed flow monitoring of tributaries, restoration of tributaries by Anglian Water, potential bathing water designation of Lark, and impact of runoff from new housing development along the Lark.
31 Jul 2022	Reviewed and commented on draft CS meeting agenda per Chairperson's request.
28 Jul 2022	Corresponded via email with RLCP Treasurer to clarify the purpose of CS sampling equipment included in grant proposal
26 Jul 2022	Spoke with RLCP Treasurer to discuss draft response to grant committee second time.
25 Jul 2022	Spoke with RLCP Treasurer to discuss response to grant committee's inquiry for further details regarding tributaries flow measurements included in CS proposal package.
23 Jul 2022	Met with Chairperson to prepare for CaSTCo kickoff meeting. Discussed methods of measuring flow for intermittent discharges to ditches and other ephemeral streams and future partnership with NT Ickworth for CS monitoring of the River Linnet.
12 Jul 2022	Participated in GIS file sharing session with Chairperson and lead GIS analyst volunteer. Discussed RLCP data management.

Table C.1 Continued

Date	Task or interaction
01 Jul 2022	Mapped coordinates for effluent discharge permits previously extracted from EA consents database to determine the actual locations of discharges along Lark and tributaries.
Jun - Jul 2022	Researched methods to quantify discharge in Lark tributaries and farm ditches, and feasibility of continuous monitoring, per Chairperson request.
29 Jun 2022	Met with RLCP Chairperson and CS Manager and a Suffolk Wildlife Trust representative to set short- and medium-term goals for CS in the Lark catchment.
26 Jun 2022	Provided resources via email to CS volunteers explaining different forms of ammonia.
09 Jun 2022	Shared STW discharge permits information extracted from consents database with Chairperson via email.
May - Jun 2022	Compiled spreadsheet containing all discharge permit limits for STWs located within the Lark catchment, not permitted for individual homes. Approximately 70 permits, with multiple determinants.
19 May 2022	Reviewed pollution analysis report and provided feedback via email per Chairperson request.
16 May 2022	Corresponded with Chairperson via email to explain the various forms of nitrogen are measured in water quality testing, and how to calculate ionized and unionized ammonia from total ammonia-N.
12 May 2022	Researched Lark STW effluent permit limits using EA discharge consents database and corresponded via email with Chairperson to share initial results.
11 May 2022	Met with Chairperson to discuss ~40 STW permits received from FOI request and what information can be extracted. Determined further research necessary for phosphate limits.
01 May 2022	Compiled list of all STWs that discharge to the River Lark and tributaries and requested permits from EA which were not included previously.

Table C.1 Continued

Date	Task or interaction
27 Apr 2022	Reviewed draft CS sampling map created by lead GIS volunteer to help determine best data representation. Attended QGIS training with Chairperson and lead volunteer GIS analyst.
26 Apr 2022	Attended tributary CS sampling group meeting led by CS Manager/Volunteer Coordinator. Discussed correct methods to calculate ionized and unionized ammonia from total ammonia-N.
20 Apr 2022	Shared project proposal with Chairperson.
17 Apr 2022	Reviewed draft pollution analysis and CS water quality sampling report produced by chairperson.
04 Apr 2022	Attended pollution group meeting, led by CS Manager/Volunteer Coordinator and Chairperson.
02 Apr 2022	Reviewed 2021 Anglian Water CSO monitoring data to determine which STWs spilled and if any locations were not included.
01 Apr 2022	Requested 2021-2022 effluent sampling data from Anglian Water for all STWs in the Lark catchment.
30 Mar 2022	Attended QGIS training with Chairperson and lead volunteer GIS analyst; met with Chairperson to discuss sewage discharges and CS water sampling in the Lark catchment.
23 Mar 2022	Reviewed results of CS tributaries snapshot water sampling blitz and recommended chairperson expand sampling to include dissolved oxygen.
07 Mar 2022	Attended pollution group meeting, led by CS Manager/Volunteer Coordinator and Chairperson.
March 6, 2022	Analyzed 2020 Fornham STW CSO data, incorporating daily flow volumes and rainfall to provide context to spill occurrences.
06 Mar 2022	Collated and organized all sewage-related data and information into a new topic folder within the RLCP cloud-shared evidence base.
02 Mar 2022	Attended QGIS training with Chairperson and lead volunteer GIS analyst.

Table C.1 Continued

Date	Task or interaction
01 Mar 2022	Requested discharge permits from EA for all STWs within the Lark catchment.
25 Feb 2022	Toured Fornham STW with RLCP Trustees and volunteers and engaged in discussion with Anglian Water representatives about the impact of STW discharges on the River Lark and potential future projects to improve the river's ecological status.
20 Feb 2022	Attended tributaries sampling volunteer training day to assist with best practices for grab sampling, field safety, and maintaining sample integrity.
07 Feb 2022	Corresponded with Chairperson via email regarding the impact of misconnections in the stormwater network and potential detection methods.
07 Feb 2022	Attended pollution group meeting, led by CS Manager/Volunteer Coordinator and Chairperson.
01 Feb 2022	Color-coded EA datasonde spreadsheet values and plotted data per Chairperson request.
07 Dec 2021	Met with Chairperson, Restoration Manager, and representatives from Norfolk Rivers Trust and other local consultancies to discuss EA datasonde report.
05 Dec 2021	Attended RLCP annual meeting to meet other volunteers, RLCP Trustees, and representatives from Rivers Trust and EA. Explained potential project to volunteers.
02 Nov 2021	Met with RLCP Chairperson and a Bury Water Meadows Group Trustee to discuss a potential project incorporating study of datasonde data and/or CSO events in the Lark.